ABSTRACT

Title of Dissertation:	INTEGRATING GENETIC INFORMATION WITH MACROSCALE MODELS OF SPECIES' DISTRIBUTIONS AND PHENOLOGY: A CASE STUDY WITH BALSAM POPLAR (*POPULUS BALSAMIFERA* L.)
	Andrew Vincent Gougherty, Doctor of Philosophy, 2019
Dissertation directed by:	Associate Professor Matthew C. Fitzpatrick University of Maryland Center for Environmental Science

To keep pace with future climate change, forest tree species are often predicted to need to shift their geographic ranges and phenology to minimize exposure to climates they have not experienced in the recent past. While many approaches have been developed to predict range shifts and shifting phenology, most large-scale, spatial techniques do not explicitly account for intraspecific genetic variation. This can be problematic when populations are locally adapted to climate, a common characteristic of plant species, as species-level responses to climate may not be representative of populations. In this dissertation, I use balsam poplar (*Populus balsamifera* L.), a northern North American deciduous tree species, to test a variety of techniques of integrating genetic information with spatial models of balsam poplar's distribution and phenology. First, I tested multiple hypotheses, identified in the literature, for their

ability to predict genetic diversity in balsam poplar. Results show that diversity in balsam poplar was highest in the center of the range and lowest near the range edge – consistent with the 'central-periphery hypothesis.' Second, I tested whether genetically-informed distribution models are more transferable through time, than standard distribution models. Using pollen and fossil records to validate models, I show that standard and genetically-informed distribution models perform similarly through time, but genetically-informed models offer additional insights into where populations may have originated on the landscape during the last glacial maximum. Third, I developed a new approach to predict population's exposure to future climate change. Using spatial models of adaptive genetic differentiation, I show that populations in the eastern portion of balsam poplar's range have the greatest predicted exposure to climate change as they would need to migrate the furthest and will see the greatest disruption in their gene-climate association. Fourth, I assessed whether a genomic prediction of common garden observations of phenology can inform phenology measured on the landscape with remote sensing. I show that the genomic prediction was the most important variable explaining the date of spring onset on the landscape, but was relatively unimportant in predicting the heat sum accumulated at the date of spring onset. I also show that model error was correlated with multiple meteorological variables, including winter temperatures – illustrating the challenges of predicting phenology in changing climates.

INTEGRATING GENETIC INFORMATION WITH MACROSCALE MODELS OF SPECIES' DISTRIBUTIONS AND PHENOLOGY: A CASE STUDY WITH BALSAM POPLAR (*POPULUS BALSAMIFERA* L.)

by

Andrew Vincent Gougherty

Dissertation submitted to the Faculty of the Graduate School of the
University of Maryland, College Park, in partial fulfillment
of the requirements for the degree of
Doctor of Philosophy
2019

Advisory Committee:
Associate Professor Matthew C. Fitzpatrick, Chair
Professor Andrew J. Elmore
Associate Research Professor Katia A.M. Engelhardt
Professor Nathan G. Swenson
Assistant Professor Stephen R. Keller

Preface

This dissertation contains five chapters: an overall introduction, and four research chapters. The four research chapters are written in manuscript form, with tables and figures following each chapter. There is a single reference section at the end of the document for the literature cited throughout the dissertation.

Acknowledgements

First, I'd like to thank my advisor Dr. Matt Fitzpatrick for providing me the guidance, insight, and encouragement that made this dissertation possible. I also thank committee members Drs. Steve Keller and Andrew Elmore for the guidance they've provided since the beginning of my PhD program, and Drs. Nate Swenson and Katia Engelhardt for sharing their time and expertise on my committee. I also thank Dr. Paul Gugger for his time on my committee. I'm also appreciative of Matt Lisk, Steven Guinn, and Dr. Diego Nieto-Lugilde for providing help with data wrangling and coding; as well as the collaborators on various projects conducted during my time as a PhD student, namely Dr. Vikram Chhatre, Dr. Cat Stylinksi, Dr. Anton Kruger and Steve Gougherty – all of whom helped me become a better writer and scholar. I also thank the past and current members of the Fitzpatrick lab who, over the past few years, I am sure enjoyed seeing my weekly update figures as much as I enjoyed creating them.

Finally, I am grateful for my family for their unending support and encouragement, and most of all, my wife Megan, whose patience, love, support, and understanding made each stage in this process even remotely achievable.

Table of Contents

List of Tables

List of Figures

List of Abbreviations

cGDD	Cumulative growing degree days
CPH	Center-periphery hypothesis
DOY	Day of year
GDM	Generalized dissimilarity model
H_{exp}	Expected heterozygosity
ky BP	Thousand years before present
LGM	Last glacial maximum
%P	Percent polymorphic loci
SDM	Species distribution model
SNPs	Single nucleotide polymorphisms

Chapter 1: Overview

Over the next century, temperatures in North America are predicted to increase by over 2^{o}C, while precipitation regimes are predicted to shift regionally, in some areas by more than 10% (Romero-Lankao et al., 2014). This reshuffling of climates is expected to require dramatic responses by organisms, as many are likely to be exposed to climates outside those they have experienced in the recent past. Of particular concern are the effects of climate change on forests and forest trees species, which make up roughly 30% of the Earth's land area, but account for a disproportionate amount of global carbon storage and net primary productivity (Bonan, 2008). Understanding and predicting the effects of climate change on forest trees is one of the first steps to developing strategies to mitigate these effects (Heller & Zavaleta, 2009).

Because of their sensitivities to climate, two of the most often predicted responses to climate change by forest trees, and plants in general, are shifts in phenology and changes in geographic distributions (Chen, Hill, Ohlemuller, Roy, & Thomas, 2011; Fei et al., 2017; Menzel et al., 2006; Schwartz & Reiter, 2000; Walther, Berger, & Sykes, 2005). The magnitude of these responses will have a direct impact on species' vulnerability to climate shifts. In areas where the pace of climate change is rapid, for instance, species may be unable to migrate quickly enough to prevent exposure to maladaptive climates. Similarly, rapid shifts in climate could disrupt the finely-tuned relationship species have with climate to maximize their

growing season, while minimizing exposure to harsh climatic conditions (Cleland, Chuine, Menzel, Mooney, & Schwartz, 2007). To understand species' vulnerability to climate change there is a need to understand how species' phenology and ranges may shift in the future.

While many approaches have been developed to understand the effects of climate change on species' distributions and phenologies, many large scale, spatial approaches do not explicitly account for intraspecific genetic variation. This can be problematic when species have genetic population structure or when populations are locally adapted to climate (a common characteristic of plant species) as a species' response to climate may not adequately represent those of populations. With genomic data becoming increasingly available for model and non-model organisms, and the continued development of approaches to identify loci potentially under selection, there are new opportunities to account for this variability in macroscale models (Schoville et al., 2012; Thomassen et al., 2010) that may offer an improved understanding of how species may respond to climate change.

In this dissertation, I use balsam poplar (*Populus balsamifera* L.) as a study system to test multiple ways of integrating genetic information with macroscale models of balsam poplar's range and phenology. Specifically, I test whether genetically-informed models can improve spatial predictions of phenology and range shifts, and, importantly, whether they can offer additional insights into how species may respond to climate change. Below is a brief description of balsam poplar, and an overview of the four following research chapters.

Balsam poplar

Balsam poplar is a northern deciduous tree species, with one of the largest geographic ranges of any North American tree. Its range spans 30 degrees of latitude - ranging from isolated populations in the US Rocky Mountains to north of the Brooks Range in northern Alaska - and over 100 degrees of longitude - spanning nearly the entire boreal region of North America (Little, 1971). As such, balsam poplar occurs over numerous climatic gradients, which previous work has shown populations are locally adapted for multiple functional traits (Keller et al., 2011; Olson et al., 2013; Soolanayakanahally, Guy, Silim, Drewes, & Schroeder, 2009). Like other *Populus* species, balsam poplar is wind-pollinated, wind-dispersed, and fast to reach reproductive maturity but can also reproduce clonally to form large mono- and poly-clonal stands (Zasada & Phipps, 1990). Balsam poplar is closely related to the model tree species *Populus trichocarpa* - the first tree species to have its genome sequenced (Tuskan et al., 2006). Balsam poplar and *P. trichocarpa* are estimated to have diverged approximately 75 kya, and is one of the few examples of tree speciation during the Pleistocene (Levsen, Tiffin, & Olson, 2012).

Chapter 2

Motivating questions: Where is genetic diversity highest in balsam poplar's range? Do hypotheses representing past climate or current range positions best explain the range-wide pattern of genetic diversity in balsam poplar?

In Chapter 2, I test seven hypotheses for their ability to explain the range-wide pattern of genetic diversity in balsam poplar. These hypotheses have varying levels of support in the literature and represent both the effects of past climate, current climate, and current range positions. Using a combination of spatial and non-spatial models, I show genetic diversity can best be explained by the center-periphery hypothesis, which predicts the highest genetic diversity in the center of the range, and the lowest diversity at the range edge.

Chapter 3

Motivating question: Are distribution models that incorporate genetic population structure more transferable to past climates than standard distribution models?

In Chapter 3, I test whether accounting for genetic population structures improves species distribution models. Using both standard SDMs and genetically-informed SDMs, I project balsam poplars distribution to 22 ky BP and test the relative abilities to distinguish pollen and fossil records from background records. I show that, while genetic population structure does not enhance the transferability of distribution models to different time periods, they offer numerous insights not available from standard distributions, such as potential refugial locations and migration paths.

Chapter 4

Motivating question: Where within balsam poplar's range is population-level exposure to future climate change the greatest?

In Chapter 4, I develop a new technique to predict population's exposure to future climate change using adaptive genomic variation. Using this technique, I predict population's minimum adaptive offsets and migration distances to locations where populations are most preadapted to future climate. I show that populations in the eastern portion of balsam poplar's range have both the greatest predicted genetic exposure to climate change, and the furthest migration distances. This new approach allows for a nuanced understanding of how populations may respond to climate change and has implications for identifying regions where conservation or management could be most effective.

Chapter 5

Motivating questions: Can precise observations of phenology made in common gardens be used to inform land surface phenology? What is the relative role of genetic variation and environment in explaining phenology measured at landscape scales?

In Chapter 5, I assess the importance of accounting for genetic variation when predicting phenology at landscape-scales. Using a genomic prediction of phenology based on observations made in multiple common gardens, paired with meteorological variables, I rank the importance of genetic and meteorological variables in predicting multiple phenological metrics on the landscape. The genomic prediction ranked as the most important variable in predicting the timing of spring onset, but was not important in predicting accumulated heat sums. This Chapter illustrates that observations from common gardens can be used to inform phenology on the

landscape and provides a framework for linking phenotypic traits measured at multiple scales.

Chapter 2: Contemporary range position predicts the range-wide pattern of genetic diversity in balsam poplar (*Populus balsamifera* L.)

Abstract

Understanding patterns of genetic diversity within species' ranges can reveal important insights into effects of past climate on species' biogeography and population dynamics. While numerous biogeographical hypotheses have been proposed in the literature to explain patterns of genetic diversity across species' ranges, they are rarely formally compared and comprehensively tested within the same study. Formally comparing competing hypotheses can lead to a better understanding of the underlying causes and consequences of range dynamics on genetic diversity, including potential vulnerability to future global change. Here, we compare seven hypotheses for their ability to describe the geographic distribution of within-population genetic diversity (expected heterozygosity and percent polymorphic loci) across the expansive geographic range of the boreal forest tree, balsam poplar (*Populus balsamifera* L.). We tested each hypothesis using spatial and non-spatial least-squares regression models to assess the importance of accounting for spatial autocorrelation on model performance. We found both metrics of genetic diversity could best be explained by the current range position and genetic structure of populations within the contemporary range. Population genetic diversity showed a clear gradient of being highest near the range center and declining towards the range

edges. In contrast, historical hypotheses accounting for the effects of past climate (e.g. past climatic suitability, distance from the southern edge) had comparatively little support. Model ranks were similar among spatial and non-spatial models, but residuals of all non-spatial models were significantly auto-correlated, violating the assumption of independence in least-squares regression. Our work adds strong support for the "Central-Periphery Hypothesis" as providing a predictive framework for understanding the forces structuring genetic diversity across species' ranges and illustrates the value of applying a robust comparative model selection framework. Our work also emphasizes the importance of accounting for spatial autocorrelation when comparing biogeographic models of genetic diversity.

Introduction

Understanding the processes shaping the macroscale pattern of genetic variation across species' ranges has been a pervasive goal of population genetics and ecology (Eckert, Samis, & Lougheed, 2008; Petit et al., 2003). Population-level genetic diversity may be shaped by historical and/or contemporary features of a species' biogeography – from past migration and shifts in population size, to recent population dynamics and response to environmental change. Because of the importance of genetic diversity to understanding the past, current, and (potentially) future dynamics of species' ranges, numerous hypotheses have been proposed to explain where populations may be expected to have the highest genetic diversity. These hypotheses often fall into two broad categories: (i) c*ontemporary range*

position – which emphasize the relative position of populations within the contemporary geographic or climatic range and (ii) *past climate effects* – which emphasize the proximity of populations to glacial refugia and effects of migration since the last glacial maximum.

Contemporary range position

Hypotheses that emphasize the position of populations within the contemporary range often posit that genetic diversity is related to the proximity of populations to the center of the range. One of the most commonly tested versions of this hypothesis, the central-periphery hypothesis (CPH; also known as the central-marginal hypothesis), predicts that populations near the geographic (or climatic; Lira-Noriega & Manthey, 2014) center of the range have the greatest genetic diversity, while populations near a range edge have the lowest genetic diversity (Eckert et al., 2008). The CPH is based on an abundant-center view of species' ranges, in which population abundance is expect to be greatest near the geographic or climatic center of the range due to its presumed proximity to the species' environmental optimum (Brown, 1984; although the generality of the abundant-center model has been questioned, see Sagarin & Gaines, 2002). High population abundance near the geographic/climatic center is expected to coincide with high effective population sizes (N_e) and elevated gene flow resulting in low genetic differentiation and high within-population diversity (Kirkpatrick & Barton, 1997). Low abundance at the

range edge is expected to have opposite effects – lower gene flow, greater differentiation, and lower within-population genetic diversity (Bridle & Vines, 2007; Hampe & Petit, 2005). Support for the CPH in the literature is mixed. While one review found that as many as 64.2% of studies that tested the CPH found support in favor of the hypothesis (Eckert et al., 2008), another recent review found support in fewer than 50% of studies (Pironon et al., 2017). In a test of the climatic CPH, Lira-Noriega & Manthey (2014) found that population genetic diversity of 40 species of various taxa could be better explained by distance from species' climatic niche centroid than by the geographic distance from the range center.

Past climate effects

Past climate and demographic history may also shape patterns of contemporary genetic diversity across species' ranges. Most of these hypotheses arise from the concept that, following the last glacial maximum (LGM), species migrated poleward out of glacial refugia to fill their current ranges. Poleward migration is often expected to result in decreasing genetic diversity away from refugial locations, due to repeated founding events along the migration routes (Excoffier, Foll, & Petit, 2009; Hewitt, 2000). The exact geographic pattern of genetic diversity that expansion from low-latitude refugia would generate has spurred numerous hypotheses. In its simplest form, species that have undergone a strictly poleward migration following the LGM are expected to exhibit a latitudinal gradient in genetic diversity (Hampe & Petit,

2005). Not all species, however, migrated strictly poleward following the LGM, and some may have refuged near (or north of) the southernmost glacial extent or in microrefugia (Anderson, Hu, Nelson, Petit, & Paige, 2006; Rull, 2009). Species may have migrated east, west or from multiple directions to fill their current ranges (e.g., Williams, Shuman, Webb, Bartlein, & Leduc, 2004), potentially obscuring a simple latitudinal gradient in genetic diversity. Refugial locations identified using distribution models, have often shown elevated levels of genetic diversity (e.g., Carnaval, Hickerson, Haddad, Rodrigues, & Moritz, 2009; Yannic et al., 2013). Relatedly, landscape age (i.e., time since the landscape was last glaciated) has also been found to be a significant predictor of genetic diversity across species' ranges, where younger landscapes often harbor lower genetic diversity (Stewart et al., 2016). Genetic diversity could also be aligned with neutral population structure, which may have arisen from post-glacial migration or from historic separation of ancestral populations. If, for instance, some populations were historically isolated from others, or if populations were more recently founded, these populations could have lower genetic diversity than older or historically well-connected populations. Despite these past climate hypotheses being based on a similar mechanism (i.e., postglacial migration into areas that have become newly climatically suitable) the patterns of genetic diversity predicted by each hypothesis may differ depending on the species' current and past distributions (e.g. if the current range was glaciated or not during the LGM), migration direction, and dispersal characteristic (e.g. propensity for long distance dispersal).

While genetic diversity within species' ranges may be shaped by both contemporary range dynamics and past climate, their relative roles are rarely formally compared. This has led some authors (e.g., Vucetich & Waite, 2003) to suggest that studies often make uncritical assumptions about the roles of contemporary and past effects on genetic diversity within species' ranges. Furthermore, many studies which formed the basis for the CPH (as discussed in Eckert et al., 2008; Pironon et al., 2017) and other hypotheses, often did not sample species' entire ranges, and rarely accounted for potential effects of spatial autocorrelation in the pattern of genetic diversity. Taken together, failure to test the effects of both past climate and contemporary range positions and account for range-wide spatial autocorrelation can leave an incomplete understanding of species' historic biogeography, current range dynamics, and an erroneous understanding of the drivers of genetic diversity within species ranges.

In this study, we attempt to disentangle historical and contemporary landscape drivers of within-population genetic diversity of balsam poplar (*Populus balsamifera* L.), a northern broad-leaf tree species. Previous work has shown a latitudinal gradient in genetic diversity within balsam poplar, consistent with range expansion from a southern refugia (Breen, Murray, & Olson, 2012; Keller et al., 2010). Here, we extend this work using a larger set of sample populations to test multiple hypotheses representing both contemporary climate/range positions and past climate. Specifically, we compared seven hypotheses for their ability to describe the range-wide pattern of genetic diversity in balsam poplar. These included (i) the geographic

central-periphery hypothesis (CPH), (ii) the climatic CPH, (iii) distance from the southern range edge, (iv) past climatic refugia effects, (v) landscape age, (vi) a model integrating the distance from the southern range edge with the CPH, and (vii) a model reflecting population structure and admixture. We also explored the effects of accounting for spatial autocorrelation on model rankings and coefficient estimates, as this helped to ensure model assumptions are being met, and coefficient estimates are unbiased.

Materials and Methods

Study species

Balsam poplar (*Populus balsamifera* L.) is a wide-ranging boreal tree and the northernmost deciduous tree species in North America (Zasada & Phipps, 1990). Balsam poplar tends to be an early successional species found in mesic environments along floodplains, near streams, and other waterways. It is relatively short-lived (rarely living longer than 200 years), fast-growing, and fast to reach reproductive maturity. Being wind dispersed, balsam poplar is capable of long-distance dispersal and, like other *Populus* species, can reproduce vegetatively to form clonal stands. Like other northern tree species, balsam poplar's current range was nearly entirely glaciated during the LGM, and species distribution models (SDMs) suggest the presence of refugia in the Central Rocky Mountains and possibly north of the ice sheets in Alaska (Breen et al., 2012; Levsen et al., 2012). Genetic studies to date

suggest that if a northern refugium was present, it left no signature in the current pattern of genetic diversity, which suggests expansion from refugia in the south (Breen et al., 2012; Keller et al., 2010). Balsam poplar's large contemporary geographic range, occurrence over broad climatic gradients, and post-glacial migration history make it an exemplary species to test the effects of contemporary and past drivers on genetic diversity.

Genetic diversity

We used allele frequencies from single nucleotide polymorphisms (SNPs) to calculate two within-population metrics of genetic diversity that provide complimentary but distinct information on the genetic diversity within populations: average expected heterozygosity (H_{exp}) and percent polymorphic loci (%P). Expected heterozygosity ($H_{exp} = 2pq$) indicates the relative evenness of allele frequencies at biallelic SNP loci, while %P summarizes the fraction of all variable loci (range-wide) that are polymorphic within a given focal population. Both metrics were calculated by integrating existing (Keller et al., 2010; Fig. 2.1) and new (Chhatre et al., In prep.) population genomic datasets. The Keller et al. (2010) dataset consisted of 412 single nucleotide polymorphisms (SNPs) identified by sequencing an initial discovery panel of 15 individuals (1 per population, sampled throughout the range). These SNPs were then used in targeted Sequenom genotyping assays to genotype 474 individuals across a range-wide collection of 34 populations. Further details on SNP genotyping can be

found in Keller et al. (2010). The new SNP dataset was collected across 437 individuals from 51 additional populations using genotyping by sequencing (GBS) following the Elshire et al. (2011) protocol. Loci were filtered to remove low quality variants (non-biallelic, minGQ < 95, heterozygote excess, site missingness >20%). Full details of GBS library preparation, SNP variant calling, and filtering are described in Chhatre et al. (In prep.).

Because SNPs in the Keller et al. (2010) dataset were identified from an initial discovery panel and therefore reflect an ascertainment bias on the site frequency spectrum (Nielsen, Hubisz, & Clark, 2004), we applied a minor allele frequency (MAF) filter to the GBS SNPs to ensure H_{exp} and %*P* were comparable between the two datasets. Specifically, we filtered out SNPs with an MAF below 0.0333 (1/30) from the GBS dataset, which is equivalent to 1/2N diploid individuals (where N=15) used for SNP discovery in Keller et al. (2010). After filtering, this left 24,087 GBS-SNPs to calculate the diversity metrics. The number of SNPs per chromosome was proportional before and after applying the MAF ($r = 0.966$, $p < 0.01$), as were both diversity metrics (H_{exp}: $r = 0.87$, $p < 0.01$, *%P*: $r = 0.95$, $p < 0.01$).

Landscape variables, climate data & occurrences

We calculated eight landscape variables to use as predictors of genetic diversity (Table 1), including four variables representing balsam poplar's contemporary range and four representing effects of past climate: (i) distance from the geographic range center, (ii) distance from the range edge, (iii) climatic

suitability, (iv) climatic distance from the climatic niche centroid, (v) climatic stability since 22 kya, (vi) climatic variability since 22 kya, (vii) distance from the southern range edge, and (viii) landscape age since the last glaciation.

We used climate data from Lorenz et al. (2016) to parameterize SDMs, and to calculate the climatic niche centroid. This climatic dataset includes seamless and debiased climate simulations from 22 kya to the 21st century in 500-year intervals, downscaled to a resolution of 0.5°. We chose six climate variables (summer and winter mean temperature and precipitation, annual precipitation variability, and average evapotranspiration ratio (actual/potential evapotranspiration)) from the Community Climate System Model to parameterize the models. Variables were chosen because of their potential importance in limiting the range of balsam poplar and lack of strong correlation between variables ($|r| < 0.75$).

Occurrences of balsam poplar were collected from online databases (Gbif.org, 2019), the US and Canadian forest inventory programs (Gillis, Omule, & Brierley, 2005; Woudenberg et al., 2010), and records from the literature (Soolanayakanahally et al., 2009). Occurrences far outside the known North American range of balsam poplar (Little, 1971) were removed. To reduce the spatial and climatic bias of the occurrence records, we thinned the points in both geographic and multi-dimensional climate space, similar to the approach described in Varela et al. (2014). Briefly, first the occurrence points were thinned to one per 0.5°grid cell of the climate data. Next, a principal component analysis (PCA) was conducted on climate data extracted at occurrence points. The first two components of the PCA were then plotted on a grid

with a resolution of 0.2 units, and one occurrence was randomly selected per PCA grid cell. After removing outliers and geographic/environmental thinning, 464 occurrences remained.

Species distribution model

We used SDMs to calculate three of the landscape predictors: current climatic suitability for balsam poplar, and climatic stability and variability since 22 kya. We used an ensemble model to predict balsam poplar's current and past distribution using the BIOMOD2 package (Thuiller, Lafourcade, Engler, & Araújo, 2009) in R. Within the ensemble model, we used six algorithms including generalized linear models, boosted regression trees, generalized additive models, flexible discriminant analysis, multiple adaptive regression splines, and random forest. We used 5-fold cross validation iterated twice to validate models, where occurrence data were split into five subsamples and models were trained with four of the subsamples (80% of the data), and tested with the remaining subsample. Model discrimination ability was tested with true skill statistic (TSS), and the final ensemble prediction was calculated as the TSS-weighted mean of all models with TSS above 0.70. Each fold of each algorithm had a TSS above 0.7 (average: 0.83, sd: 0.04), so each was included in the final ensemble. The model was then projected to each of 45 time periods between current climate and climate at 22 kya, in 500 year intervals (Lorenz et al., 2016). The temporal resolution of the Lorenz data (500 year intervals) allowed for finer

assessment of past climate effects than studies limited to snapshot climate predictions for only the LGM and mid-Holocene.

Climatic stability (*sensu* Ortego, Gugger, & Sork, 2015; Yannic et al., 2013) was calculated as the sum of climatic suitability through time, while variability was calculated as the standard deviation of climatic suitability through time. These metrics provide a measure of how the climatic suitability of balsam poplar has changed over the past 22 ky. Areas that were glaciated during a given time period (based on maps by Dyke, Moore, & Robertson, 2003) were not included in the calculations. We also calculated landscape age, similar to Stewart et al. (2016), using glacial data from Dyke et al. (2003) aligned to the 45 time periods. Shapefiles of glacial extent were rasterized to match the scale, resolution, and projection of the climate data. Landscape age was calculated as the time since the landscape was most recently glaciated.

Geographic and environmental centrality

We calculated three metrics representing the position of populations in balsam poplar's current geographic and environmental ranges: distance from the geographic range edge, distance from the geographic range center, and climatic distance from the climatic niche centroid. Distance from the range edge was calculated by generating an alpha hull around occurrence records and calculating the distance between each population and the nearest edge. Alpha hulls are similar to convex hulls, and are

recommended as a way to decrease the bias and spatial error associated with convex hulls when estimating species' range polygons (Burgman & Fox, 2003). Distance from the geographic range center was calculated as the geographic distance from the centroid of the alpha hull, similar to that done by Lira-Noriega & Manthey (2014) and Dallas et al. (2017). The alpha hull was also used to calculate population distance from the southern edge.

We used Mahalanobis distance as a metric of population distance from the climatic niche centroid. Mahalanobis distance is a measure of the multivariate distance between climate extracted at each population location and the average climate of all balsam poplar occurrences. Mahalanobis distances account for correlation among variables by scaling the distances by the covariance between climate variables. The covariance matrix and average climate were based on the climate at the climatically-thinned balsam poplar locations. Climate variables were the same as those used for the distribution models.

Population structure and admixture

In addition to effects of geographic/climatic centrality, and past climate, we also tested for effects of population structure and admixture among genetic clusters on genetic diversity. For the previously published dataset, we used admixture proportions from Keller et al. (2010). For the new MAF-filtered GBS dataset, we estimated admixture proportions using ADMIXTURE 1.30 (Alexander, Novembre, &

Lange, 2009) and chose K = 3 for consistency with Keller, et al. (2010). The three inferred genetic clusters in the GBS data were spatially congruent with the previous dataset – both showed a distinctive eastern cluster, a large central cluster, and a northern cluster that tended to be well-mixed with the central cluster. Using these admixture proportions, we calculated a population-level index of admixture similar to that done by Ortego et al. (2015). To do so, first we averaged admixture proportions across individuals within populations, and calculated the standard deviation of the average proportions. Next, we rescaled this value between 0 and 1, such that the index was 1.0 when populations were evenly mixed among clusters, and 0 when populations were entirely affiliated with a single cluster. For each population, we also determined which of the three clusters had the highest average admixture proportion.

Models & statistical analyses

We assessed the local and global spatial pattern of H_{exp} and %*P* using Moran's Index (*I*), a measure of spatial autocorrelation, where -1.0 indicates perfect dispersion and 1.0 indicates perfect clustering. Correlograms of Moran's *I* for H_{exp} and %*P* were estimated in 100 km increments. Significance was determined for both the correlograms and global statistic by comparing the observed statistic to 999 random permutations.

Using the eight landscape variables, we compared statistical support for models representing seven hypotheses listed in Table 2.1. For each hypothesis, we

created spatial and non-spatial models to assess the effect of accounting for spatial autocorrelation on model performance. To account for spatial autocorrelation, we used conditional autoregressive (CAR) models, which integrated a weighted estimate of the response variable (here, the metrics of genetic diversity) at neighboring locations, in addition to the explanatory variables, in parameterizing the model (Lichstein, Simons, Shriner, & Franzreb, 2002). Neighborhoods were defined as all populations within 600 km of one another (Fig. 2.1). This distance was chosen as it ensured each population had at least one neighbor, and was the approximate maximum distance of continuous significant positive spatial autocorrelation (see Results). A complementary set of non-spatial ordinary least squares (OLS) regression models were fit and compared to the CAR models. Models were compared using Nagelkerke R^2, Akaike information criterion (AIC) and Akaike weights, which are recommended as a way to compare AIC scores across models (Wagenmakers & Farrell, 2004). Each explanatory variable was scaled to a mean of 0 and a standard deviation of 1, to facilitate the comparison of coefficient estimates (Schielzeth, 2010). All modeling and statistical analyses were performed in R (R Core Team, 2017).

Results

Spatial pattern and autocorrelation

Both metrics of genetic diversity (H_{exp} and %P) were highest near the geographic center of the range and declined towards the latitudinal (southern and

northern) and longitudinal (eastern and western) range edges. Both H_{exp} and %P showed moderate (I = 0.28 and 0.45, respectively) but significant spatial autocorrelation ($p < 0.05$) among the 85 populations, indicating that adjacent populations tended to have more similar levels of genetic diversity than distant neighbors. Correlograms of Moran's I revealed H_{exp} and %P were significantly positively autocorrelated up to ~600 km and at ~2000 km, and significantly negatively correlated around 1000 km and between 3000 – 4000 km (Fig. 2.2b & d). Genetic diversity metrics were significantly correlated among the 85 populations (Pearson's $r = 0.88$, $p < 0.001$).

Spatial models of genetic diversity

The top performing models for H_{exp} and %P were the models of population structure, and the geographic CPH, respectively, and had by far the highest Akaike weights and highest Nagelkerke R^2's (Tables 2.2 & 2.3). Inspection of the coefficients revealed that both diversity metrics were greatest near the range center, and lowest near the range edge (Fig. 2.3). Furthermore, we found that climatic distance from the climatic niche centroid was correlated with distance from the range center ($r = 0.30$, $p < 0.01$) and negatively correlated with distance from the range edge ($r = -0.51$, $p < 0.01$) – indicating that populations near the range center tended to be near the niche centroid, while populations near a range edge tended to be more distant.

In general, the spatial models incorporating past climate had less support than models incorporating current climate/range positions. For both H_{exp} and %*P*, past climate CAR models (i.e., landscape age, distance from the southern edge, past climatic stability) consistently had lower Akaike weights (i.e., all models had weights near zero) and tended to have lower Nagelkerke R^2's compared to models representing contemporary range positions. Coefficient estimates for all variables in the past climate models, other than the intercepts, were not significant ($p > 0.05$).

Non-spatial models of genetic diversity

The rank (based on Akaike weights) of non-spatial OLS models for both H_{exp} and %*P* were similar to that of the spatial models. The top model for both H_{exp} and %*P* was the population structure model and the geographic CPH, respectively (Tables S1 & S2). Coefficient estimates for these models again showed higher diversity near range center, and lower near the range edges. The model integrating distance from the southern range edge and the CPH had the second highest support for %*P* (Akaike weight = 0.15), but like the CAR models, only the coefficient for the distance from the geographic center was significant. Similar to the CAR models, OLS models representing past climate effects (i.e., landscape age, distance from the southern edge, past climate stability) had low support, with Akaike weights near zero.

Residual spatial autocorrelation

Residuals of most models, spatial and non-spatial, were spatially autocorrelated, as quantified by Moran's *I*. Of the CAR models, only four models (population structure models for H_{exp} and %*P*, and geographic and climatic CPH for *%P*) had uncorrelated residuals ($p > 0.05$) (Tables 2 & 3). Residuals of CAR models representing contemporary climate/range positions tended to have lower autocorrelation than past climate models, but all spatial models had relatively low autocorrelation (all < 0.11). In contrast, autocorrelation in OLS models was often nearly as strong as the actual diversity metrics being modelled. This suggests that the assumption of independent residuals is being violated in nearly all the non-spatial models.

Discussion

Quantifying patterns of genetic diversity within species' ranges can reveal important insights into species' biogeography, effects of past climate, and where populations may be best positioned to adapt to future climates. However, because these patterns can arise from multiple historic and contemporary processes, it is important to evaluate the comparative strength of different hypotheses. In this paper, we compared multiple biogeographic hypotheses established in the literature and tested them in a model selection framework using the range-wide patterns of genetic diversity in balsam poplar. We found the greatest support for hypotheses representing

populations' position in the contemporary geographic and climatic range, in particular the center-periphery hypothesis (CPH) and population structure models, whereas we found comparatively little support for hypotheses that included variables for historical climate or distance from potential refugia. Our work illustrates the value of applying statistical model selection among multiple competing biogeographic hypotheses, representing both current and past climate, to better understand the landscape-scale predictors of genetic diversity across species' ranges.

Geographic pattern of diversity

Like studies of other tree species (e.g., Walter & Epperson, 2005), we found genetic diversity in balsam poplar populations was spatially autocorrelated over large distances (here, hundreds of kilometers). Interestingly, the strength of spatial autocorrelation did not simply decay with increased distance, but rather oscillated between (significant) positive and negative autocorrelation over thousands of kilometers, indicating that the autocorrelation spanned multiple spatial scales. This pattern seems to be the result of multiple, discontinuous hotspots of diversity in balsam poplar's sampled range, in particular near the center of the range in Saskatchewan and in populations north of the Great Lakes region. Both the diversity hotspots and positive autocorrelation among nearby populations are likely the result of nearby populations undergoing similar processes (such as gene flow and drift) as well as shared common ancestry. Indeed, individuals from these two regions have

been shown to belong to a large genetic cluster (as identified by admixture analyses; Keller et al., 2010) that coalescent models have shown has a large effective population size (N_e) and is the source of asymmetric migration from the center towards the periphery of the range (Keller et al., 2010).

CPH and the abundant-center model

Diversity in balsam poplar was highest in the center of the range and tended to decline towards the range edge, consistent with the CPH. The CPH is presumed to be driven by population abundance – where high abundance in the center of the range promotes high gene flow and N_e, while low abundance at the range edge results in isolation, reduced gene flow and ultimately low genetic diversity. Because we were unable to directly test if abundance peaked in the center of balsam poplar's range and declined toward the edge, it remains unclear if population abundance is the ultimate driver of genetic diversity within balsam poplar's range. There is reason to suspect, however, that abundance in balsam poplar's range does not have a monotonic decline towards the edge. First, multiple studies have shown that the pattern expected by the abundant center model is rarely observed (Dallas et al., 2017; Sagarin & Gaines, 2002). Dallas et al. (2017), for instance, showed that most North American tree species that the authors assessed (~97%) did not peak in abundance in the center of their ranges, but rather species more often had higher abundance near the range edge than the range center. Furthermore, balsam poplar, specifically, shows considerable

variability in abundance along its range edges. Recent analyses by the US Forest Service (Prasad, Iverson, Peters, & Matthews, 2014), for instance, show relatively high balsam poplar abundance at the range edge in the upper Midwest (e.g., northern Minnesota), lower abundance near the Great Lakes and northeastern US, and very low abundance in the Rocky Mountains. This high spatial variability in abundance suggests that, like other tree species, proximity to a range edge may not be the sole driver of abundance in balsam poplar's range. Hence, other hypotheses may be necessary to explain the high diversity in the center of balsam poplar's range irrespective of abundance.

Other processes could plausibly result in the patterns expected by the CPH. For instance, if migration following the LGM occurred mainly from the center of the (current) range towards the range edges, rather than strictly poleward, diversity could be highest in the center of the range and lowest near the edges. Keller et al. (2010) suggested balsam poplar refuged in the Rocky Mountains during the LGM south of the center of the current range, followed by an expansion of the range eastward and northward following glacial retreat. Bottlenecks and founding events along the migratory paths from the center of the current range toward the edges likely left a gradient in genetic diversity often documented in tree species that have undergone long distance migration (Hewitt, 2000; Petit, Bialozyt, Brewer, Cheddadi, & Comps, 2001). This hypothesized migration history may also explain the population structure observed in balsam poplar, where populations at the periphery of the range tended to belong to genetic clusters (i.e., northern and eastern clusters) that had lower diversity

than the cluster at the center of the range (Tables 2 & 3; Keller et al., 2010), and likely explains the relatively strong support for the population structure model. Although we cannot conclusively determine whether range/climatic marginality or population structure is the ultimate driver of genetic diversity (as population structure is correlated with distance from range centrality), both clearly indicate high diversity in the center of the range (which coincides with a genetic cluster with high N_e), and lower diversity in the range edges (coincident with two other genomic clusters).

The possibility that post-glacial migration left a pattern of genetic diversity similar to that expected by the CPH would be unsurprising given recent work showing that migration following the LGM in North American trees rarely left a latitudinal gradient in genetic diversity, as has often been found for European species (Lumibao, Hoban, & McLachlan, 2017). The lack of distinctive migration barriers in North America (Soltis, Morris, McLachlan, Manos, & Soltis, 2006), combined with a large ice-free area north of the southern ice margin (Brubaker, Anderson, Edwards, & Lozhkin, 2005) may have allowed North American species to fill their current ranges from multiple directions, precluding a monotonic trend in genetic diversity within the range. This is apparent in other *Populus* species, such as *P. trichocarpa* a sister species of balsam poplar, which has been shown to have low diversity in the center of its range (Zhou L., Bawa R., & Holliday J. A., 2014), possibly reflective of refugia north and south of the current range. In contrast, *P. tremuloides* has been shown to have the lowest diversity in the southeastern portion of its range, and a peak near the center of its latitudinal range (Callahan et al., 2013). The similarity to quaking aspen

(*P. tremuloides*) is particularly interesting, as balsam poplar and quaking aspen share similar current ranges, and have co-occurred in the past (evidenced from the North American pollen database) – possibly suggestive that they have undergone similar migratory histories and could be under similar forces shaping their genetic diversity.

Spatial autocorrelation

Our comparison between the CAR and OLS models revealed the importance of accounting for spatial autocorrelation when assessing the drivers of genetic diversity at large spatial scales. Although the model ranks differed only slightly among the spatial and non-spatial models, the residuals of the non-spatial models were comparatively strongly autocorrelated, indicating lack of independence and violation of model assumptions. In fact, for multiple OLS models, residuals were nearly as strongly spatially autocorrelated as the actual diversity metric being modelled. While the spatial models did not completely account for the autocorrelation (many of these models also had significant residuals autocorrelation), residuals of all spatial models were substantially less autocorrelated than the actual diversity metrics.

Although spatial effects are infrequently accounted for when assessing landscape drivers of genetic variability, when model residuals are strongly autocorrelated, spatial models should be used to ensure coefficient estimates are unbiased and OLS assumptions are not violated. Failing to account for spatial relationships of genetic variability can affect the sign and magnitude of model

coefficients and the associated inference (Dormann et al., 2007). Despite spatial models requiring additional steps to be fit (e.g. defining a spatial neighborhood), future studies should account for spatial non-independence, or at least test for (and report) the presence of spatial autocorrelation in model residuals to ensure this assumption is not being violated.

Conclusions

Our analyses indicated that genetic diversity in balsam poplar reflects distances from the geographic range center and edges, consistent with high N_e in the range center and lower N_e toward the range edges. In general, effects of past climate were not well supported, suggesting the main demographic center of the species has migrated into mid-latitudes during range expansion following the LGM, and maintained high diversity there, whereas edge populations show low diversity due to low N_e and/or reduced connectivity. Furthermore, our results point to the benefit of comparing multiple competing hypotheses when assessing the pattern of genetic diversity across species' ranges, as well as the advantage of considering spatial effects to ensure assumptions are not violated and results are not biased.

Tables

Table 2.1. Landscape variables used in models of expected heterozygosity and percent polymorphic loci in balsam poplar.

Model	Variable description	Variable abbreviation
Geographic CPH	Distance from the geographic range edge	geoEdge
	Distance from the geographic range center	geoCenter
Southern edge + CPH	Distance from the geographic range center	geoCenter
	Distance from the southern range edge	southernEdge
Climatic CPH	Current climatic suitability	suitability
	Climatic distance from the climatic range center	climDist
Past climate stability	Climatic stability since LGM	stability
	Climatic variability since LGM	stabilitySD
Landscape age	Landscape age	landAge
Distance from southern edge	Distance from the southern range edge	southernEdge
Population structure/mixing	Admixture index	mix
	Highest average ancestry coefficient	maxCluster

Table 2.2. Summary statistics for conditional autoregressive models of H_{exp} in balsam poplar, ranked by relative support.

Model	Coefficient	Estimate	*p*-value	AIC	AIC weight	Nagelkerke R^2	Moran's I (residuals)	Moran's I *p*-value (residuals)
Population structure/mixing	Intercept	0.208	<0.01	-456.40	0.84	0.39	0.00	0.37
	mix	0.028	0.06					
	maxCluster-Eastern	-0.034	<0.01					
	maxCluster-Northern	-0.007	0.27					
Geographic CPH	Intercept	0.205	<0.01	-451.81	0.08	0.35	0.07	0.03
	geoEdge	0.004	0.11					
	geoCenter	-0.009	<0.01					
Climatic CPH	Intercept	0.208	<0.01	-450.73	0.05	0.34	0.05	0.06
	suitability	0.006	<0.01					
	climDist	-0.007	<0.01					
Southern edge + CPH	Intercept	0.204	<0.01	-449.63	0.03	0.33	0.09	0.01
	geoCenter	-0.011	<0.01					
	southernEdge	-0.001	0.55					
Landscape age	Intercept	0.201	<0.01	-431.12	0.00	0.15	0.10	0.01
	landAge	-0.001	0.72					
Distance from southern edge	Intercept	0.201	<0.01	-431.01	0.00	0.14	0.10	0.01
	southernEdge	2.9E-04	0.91					
Past climate stability	Intercept	0.200	<0.01	-430.64	0.00	0.16	0.11	0.01
	stability	0.002	0.35					
	stabilitySD	-0.002	0.33					

Table 2.3. Summary statistics for conditional autoregressive models of %*P* loci in balsam poplar, ranked by relative support.

Model	Coefficient	Estimate	*p*-value	AIC	AIC weight	Nagelkerke R^2	Moran's I (residuals)	Moran's I *p*-value (residuals)
Geographic CPH	Intercept	0.694	<0.01	-161.44	0.77	0.43	0.04	0.12
	geoEdge	0.037	0.01					
	geoCenter	-0.040	<0.01					
Climatic CPH	Intercept	0.705	<0.01	-158.53	0.18	0.41	0.02	0.19
	suitability	0.038	<0.01					
	climDist	-0.034	<0.01					
Southern edge + CPH	Intercept	0.680	<0.01	-154.76	0.03	0.38	0.06	0.04
	geoCenter	-0.058	<0.01					
	southernEdge	-0.006	0.64					
Population structure/mixing	Intercept	0.716	<0.01	-154.38	0.02	0.39	0.00	0.35
	mix	0.088	0.32					
	maxCluster-Eastern	-0.168	<0.01					
	maxCluster-Northern	-0.056	0.15					
Landscape age	Intercept	0.667	<0.01	-140.95	0.00	0.26	0.08	0.02
	landAge	-0.016	0.16					
Distance from southern edge	Intercept	0.664	<0.01	-139.04	0.00	0.24	0.08	0.02
	southernEdge	0.003	0.85					
Past climate stability	Intercept	0.655	<0.01	-139.73	0.00	0.26	0.09	0.01
	stability	0.003	0.79					
	stabilitySD	-0.021	0.10					

Figures

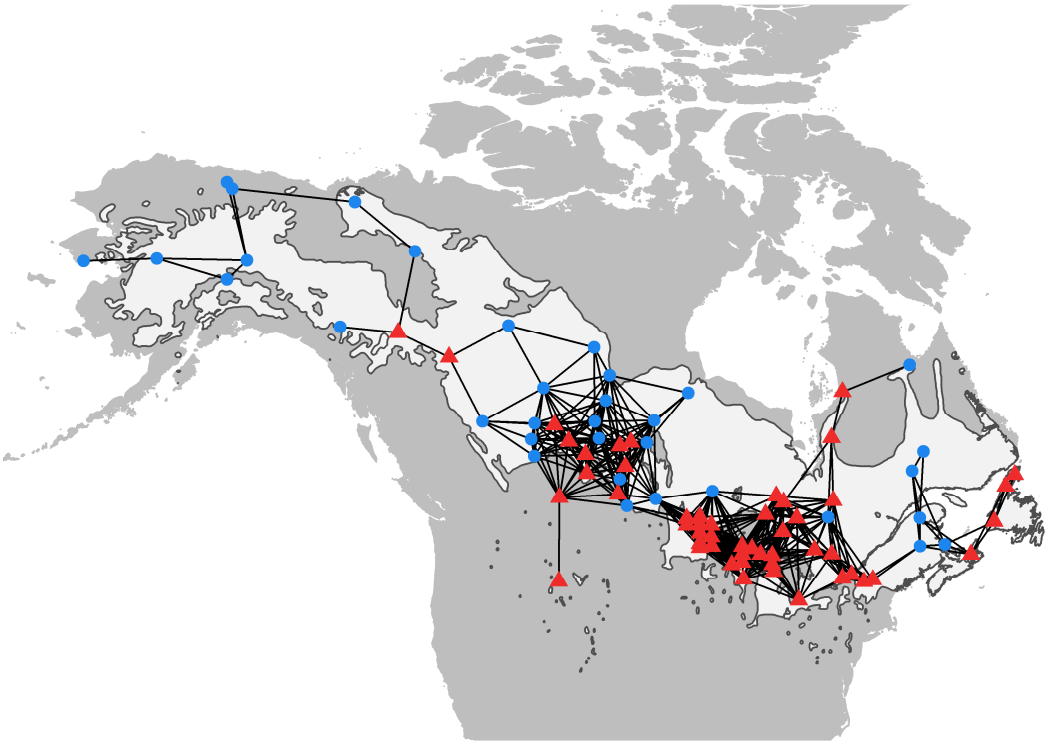

Fig. 2.1. Map showing location of newly sampled populations (red triangles; Chhatre et al., In prep.), populations from Keller et al. (2010) (blue circles), and the neighborhood network used in spatial analyses (black lines; see Methods). Balsam poplar range polygon is shown in white (Little, 1971).

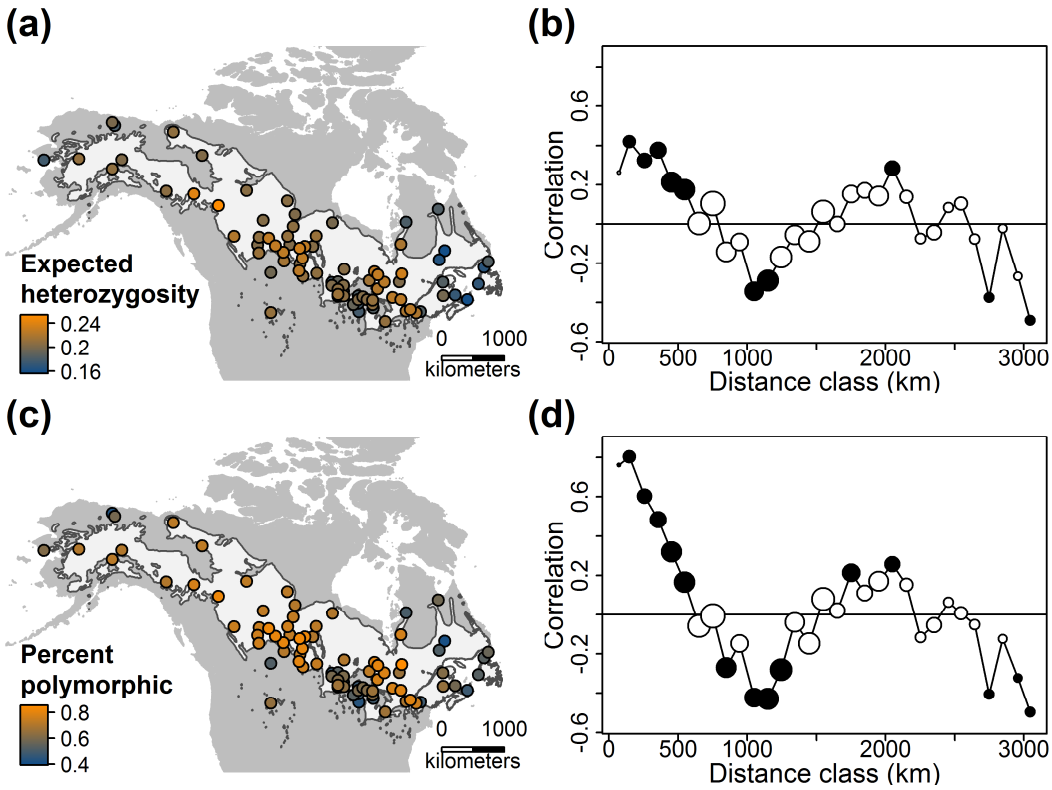

Fig. 2.2. Maps and correlograms of (**a** & **b**) expected heterozygosity and (**c** & **d**) percent polymorphic loci among 85 balsam poplar populations. Circle size in the correlograms are proportional to the number of records used within each distance class, and filled circles indicate significant autocorrelation at particular distance classes (two sided, $p > 0.975$ or $p < 0.025$). Balsam poplar range polygon is shown in white (Little, 1971), in (**a**) and (**c**).

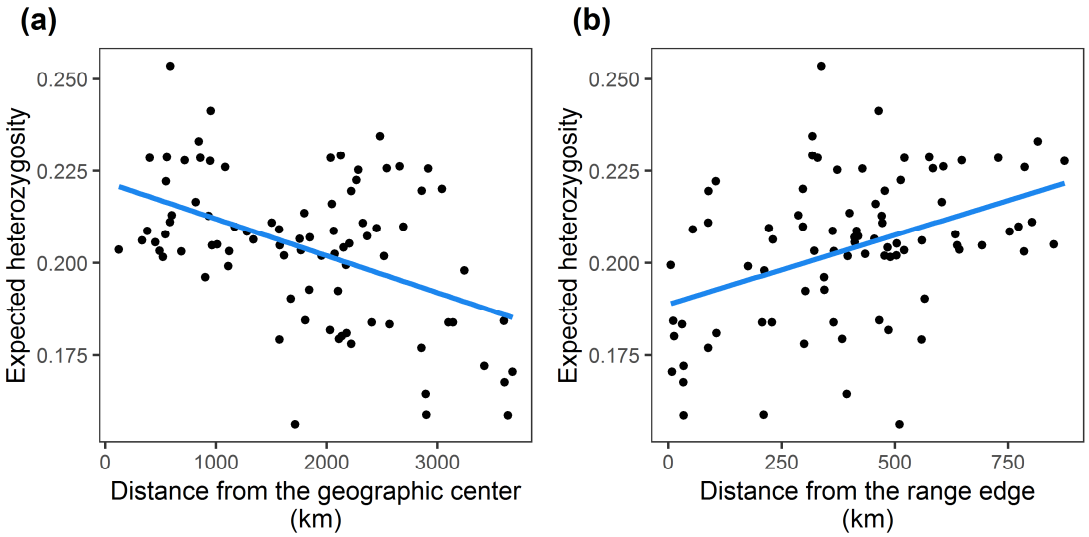

Fig. 2.3. Relationship between balsam poplar expected heterozygosity and (**a**) distance from the geographic range center and (**b**) distance from the range edge. Least-squares regression lines are shown in blue.

Chapter 3: Are genetically-informed distribution models more transferable to past climates than standard distribution models? A case study with balsam poplar (*Populus balsamifera* L.).

Abstract

In response to future climate change, species are often predicted to need to shift their geographic ranges. The typical way to predict range shifts, species distribution models (SDMs), however, assume species are genetically uniform throughout their ranges. While techniques have been developed to account for species' genetic population structure, they have rarely been tested for their ability to be transferred to time periods outside those used in model training. Assessing model transferability through time is especially important as a major goal of SDM studies is to project distributions to future climates, which may be comparably novel to current climates. Here, we used standard and genetically-informed distribution models (gSDMs) to predict the future and past range of balsam poplar and used historic balsam poplar pollen and macrofossil occurrences to compare model transferability. In general, standard and gSDMs performed similarly through time – both predicted an expanding range and a northward shift as glaciers receded from the landscape over the past 22 ky, but a contracting range in future climates. Both standard and gSDMs showed moderate abilities to distinguish balsam poplar pollen/fossils from background samples, but tended to predict lower suitability at pollen/fossil sites during the Pleistocene-Holocene transition. Although gSDMs applied to balsam poplar did not prove more transferable than standard SDMs, they provided numerous insights not

available from standard SDMs, such as the change in suitable area of genetic clusters through time and potential refugial locations. We argue more work should be done to determine which species may benefit most from the gSDM approach and the need to test gSDMs with temporally or spatially independent occurrences, as is often suggested for standard SDMs.

Introduction

Geographic shifts in species' ranges are a commonly predicted biotic response to future climate change (Chen et al., 2011; Fei et al., 2017; Hickling, Roy, Hill, Fox, & Thomas, 2006; Parmesan, 2006; Scheffers et al., 2016) and are expected to have a variety of effects on ecosystems, at multiple organizational levels (Montoya & Raffaelli, 2010; Schweiger, Settele, Kudrna, Klotz, & Kühn, 2008; Walther, 2010). At the species-level, shifting ranges may result in loss of range area, and extirpation of populations at the trailing edge of range expansion. In turn, loss of edge populations could reduce genetic diversity and adaptive capacity within species, especially if trailing edge populations are adapted to marginal environmental conditions within the range and/or harbor unique alleles not found elsewhere in the range (Alsos et al., 2012; Hampe & Petit, 2005). Accurate predictions of species' range shifts, hence, are needed to understand where populations may be most at risk of extirpation and the associated potential loss of genetic diversity.

Species distribution models (SDMs) are among the most common approaches to predict species range shifts (Araújo et al., 2019). SDMs, however, make multiple simplifying assumptions that can affect their performance and biological realism (Elith & Leathwick, 2009; Franklin, 2010; Wiens, Stralberg, Jongsomjit, Howell, & Snyder, 2009). For instance, SDMs typically assume genetic uniformity throughout the range (Fitzpatrick & Keller, 2015; Gotelli & Stanton-Geddes, 2015). The assumption of genetic uniformity can be problematic when species are structured into populations, encompass multiple lineages/subspecies, or when populations are locally adapted to climate – a characteristic of many plant species (Leimu & Fischer, 2008; Savolainen, Lascoux, & Merilä, 2013). The primary approach to accommodating genetic population structure in SDMs is by creating individual models for each biologically-relevant (e.g. genetic, morphological) subunit within a species' range, and combining model predictions into a single composite prediction for the entire species (i.e., here, genetically-informed SDMs or gSDMs). While the gSDM approach has shown promising results when compared to standard species-wide predictions (e.g., Ikeda et al., 2017; Marcer, Méndez-Vigo, Alonso-Blanco, & Picó, 2016; Oney, Reineking, O'Neill, & Kreyling, 2013; Pearman, D'Amen, Graham, Thuiller, & Zimmermann, 2010), it is often unclear if gSDMs are better able to predict responses to climate change, compared to standard SDMs (Peterson, Doak, & Morris, 2019). Assessing how well gSDMs can be transferred to time periods not used in model training is especially important as a major goal of gSDMs studies is to

predict species' range shifts in future climates when climate may be dissimilar from current climate.

While assessing the transferability of models decades into the future may not be possible, past occurrences, such as pollen and fossil records, offer a unique opportunity to test the ability of models fitted at one time to be transferred to another time. If gSDMs have a greater ability to predict the occurrence of pollen and fossils records than standard SDMs, gSDMs may similarly be more reliable in future climates. While future climates may become more novel than past climates (compared to current climate), requiring greater model extrapolation (Fitzpatrick et al., 2018), pairing past climate simulations with pollen/fossil data offer one of the few ways to validate the temporal transferability of SDMs with independent data. Furthermore, projecting gSDMs to past climates can offer numerous insights not available from standard SDMs, such as where different populations originated on the landscape and potential migration routes used to fill the current range. Using past climate simulations in concert with pollen/fossil data and genetic information can, not only help inform model transferability but may also provide inference about how species' ranges have shifted in the past and how past range shifts compare to future range shifts.

In this study we used balsam poplar, a northern North American tree species, to test the transferability of standard and gSDMs to past climates since the last glacial maximum (LGM) and used pollen/fossil records to validate models. Because pollen/fossil records were not used during model calibration, this provides a true test

of the transferability of standard and gSDMs to new time periods. We also used the distribution models to assess how the size of the range has shifted since the LGM, and how it may shift in the future. We show that while gSDMs may not enhance transferability, they can offer numerous insights not available from standard SDMs and should be continued to be developed to enhance their accuracy.

Materials and Methods

Genomic clusters

Recent genetic studies have shown balsam poplar to be structured into three genetic clusters – a distinct cluster in the eastern portion of the range, and a gradient of two clusters in the northern and central parts of the range (Keller et al., 2010; Meirmans, Godbout, Lamothe, Thompson, & Isabel, 2017). To create gSDMs, we used admixture proportions from two SNP datasets (Ch. 2; Chhatre et al., In prep.; Keller et al., 2010), which together covered 85 populations throughout the range of balsam poplar. We used a minor allele frequency filter (described in Ch. 2) to ensure the two datasets were comparable. Populations were assigned the cluster with the highest average admixture coefficient for individuals within the population, resulting in 11, 62, 12 populations in the northern, central, and eastern clusters respectively.

Because each cluster had relatively few populations (i.e., fewer than needed to create robust distribution models), like other studies (e.g., Ikeda et al., 2017; Oney et al., 2013), we supplemented the sampled population locations with occurrences from

multiple sources, including the global biodiversity information facility (Gbif.org, 2019), the US and Canadian Forest Inventory analyses (Gillis et al., 2005; Woudenberg et al., 2010), and recent sampling efforts (Ch. 5). Occurrences were assigned the cluster of the nearest sampled population. Although assigning clusters to unsampled locations introduces some uncertainty into subsequent analyses, because clusters were spatially structured, and admixture coefficients were spatially autocorrelated over hundreds of kilometers (see Results), this approach should provide a reasonable approximation of cluster affiliation at unsampled locations.

Because of strong spatial and climatic bias in the occurrences, we thinned occurrences in both geographic and environmental spaces. To do so, first, one occurrence was selected per grid cell of the climate data (0.5 degree resolution, see below). Next, a principal components analysis was conducted on climate extracted at the remaining occurrence locations. Finally, scores for the first two components were plotted over a 0.2 resolution grid and one occurrence was randomly selected per grid cell. Of the 4173 occurrences collected, 475 were kept after thinning and were used in the subsequent distribution models. Of the 475 occurrences, 149 were assigned to the northern cluster, 274 to the central cluster, and 52 to the eastern cluster.

We used pollen and macrofossil records collected from online databases (www.neotomadb.org; Goring et al., 2015) and the literature (Mann, Groves, Reanier, & Kunz, 2010) to validate models. Although pollen is often identified only to the genus-level, morphological differences in pollen of *Populus* species has allowed some researchers to identify pollen to balsam poplar specifically (as in Brubaker et

al., 2005; Brubaker, Garfinkee, & Edwards, 1983; Cwynar & Spear, 1991; Edwards, Anderson, Garfinkel, & Brubaker, 1985 and various entries in the North American Pollen Database). We used only pollen identified as *Populus balsamifera*, but not *Populus balsamifera*-type or undifferentiated *Populus* pollen in our analyses. Pollen and macrofossils were assigned the nearest time period of the climate layers (±250 years), based on their calibrated dates before present. In total, we used 390 pollen/fossil site-years to validate the distribution models.

We used downscaled and debiased climate data from Lorenz et al. (2016) to hindcast and forecast our distribution models. The distribution models were parameterized with six climate variables that lacked strong correlation ($|r| < 0.75$) with other variables: summer and winter mean temperature and precipitation, annual precipitation variability, and average evapotranspiration ratio (actual/potential evapotranspiration). Distribution models were hindcasted to 22 ky BP in 500-year increments, and projected to four future climates (2030, 2050, 2070, 2090), for two emission scenarios (RCP 4.5 and 8.5), and twelve global circulation models without dispersal limitations. Climate data had a resolution of 0.5 arc degrees.

SDM calibration and validation

We used the BIOMOD2 platform in R to create ensemble distribution models (Thuiller et al., 2009). Specifically, we used six algorithms (generalized linear models, boosted regression trees, generalized additive models, flexible discriminant analysis, multiple adaptive regression splines, and random forest) and two replicates

of five-fold cross validation (where 80% of data is used to train the models, and 20% is used to test the models, iterated 5 times, run twice) for a total of 60 models in each ensemble. Ensemble models were created separately for each genomic cluster (northern, central, and eastern clusters) and for the entire species as whole. Because we lacked true absences for balsam poplar, 1000 pseudo-absence points were selected from across North America, and were selected at least 2° from any occurrence used in model training (Barbet-Massin, Jiguet, Albert, & Thuiller, 2012). Pseudo-absences and presences were given equal weight in each of the models to ensure pseudo-absences did not have an outsized impact when fewer occurrences were used to train cluster models (compared to the species-wide model). Because of a lack of consensus in the best approach to evaluate model discriminatory ability of SDMs and limitations to any single statistic (e.g., sensitivity to prevalence and spatial extent, weighting of omission/commission errors, etc.; Leroy et al., 2018; Lobo, Jiménez-Valverde, & Real, 2008), we used three commonly-used statistics to evaluate predictions of testing data: true skill statistic (TSS; Allouche, Tsoar, & Kadmon, 2006), AUC, and kappa.

We used a committee averaging approach to create the ensemble predictions. To do so, binary predictions (created by maximizing TSS) were averaged across all models with TSS scores above 0.7. The resultant continuous map illustrates the proportion of models that predict the cluster (or species) to be present across the landscape. To create binary maps of the ensemble predictions, we applied a threshold of 0.5 to the committee averaged maps – illustrating areas where at least 50% of models predict presence of the cluster (or species).

To compare the ability of standard SDMs and gSDMs to predict balsam poplar pollen and macrofossils in past climates, we first combined our individual cluster predictions into a single composite prediction. The composite prediction was calculated as the probability of at least one cluster being present across the landscape (Pearman et al., 2010), as given by:

$$P(x) = 1 - \prod_i (1 - P(x_i)), \qquad \text{Equation 3.1.}$$

where $P(x)$ is the probability of at least one cluster being present, and $P(x_i)$ is the probability of *i*'th cluster. Next, climatic suitability was extracted at pollen/macrofossil locations from both the composite prediction of the gSDM, and the standard SDM and from an equivalent number of pseudoabsence points from unglaciated parts of the landscape. Because most time periods had relatively few pollen/macrofossils (*Populus* is often "palynologically silent"; Godwin, 1934; Pedersen et al., 2016), we calculated AUC, TSS, and kappa for the pollen/macrofossils pooled over all time periods. We also assessed model extrapolation directly by assessing the relationship between suitability and climatic novelty at pollen/macrofossil occurrences. This analysis informed whether suitability declined as pollen/fossil occurrences become more climatically distant from the climate used to train models. Climate novelty was calculated using Mahalanobis distance, a scale-invariant multidimensional distance metric. Mahalanobis distance was calculated from the average current North American climate to climate extracted

at pollen and macrofossil sites. Distances were transformed to probabilities using the lower tail of a chi-square distribution – illustrating the probability of climate at pollen/macrofossil sites falling outside current North American climate.

We assessed variable importance for each ensemble distribution model to determine whether clusters responded differently to climatic variables, and whether important variables differed from the species-wide model. To do so, we used variable importance metrics from BIOMOD2. Briefly, variable importance was calculated by testing the correlation between model predictions when a single variable is permuted, and when it is not, and then subtracting the value from 1.0. A high correlation between model predictions when a variable is permuted and when it is not, indicates a variable has a small effect on the model prediction, and hence, is not very important in the model. For each of the 60 models, each variable was permuted ten times, for a total of 600 permutations per variable. Variable importance was averaged over each of the models in the ensemble.

Analyses

We tested for multivariate spatial autocorrelation in admixture coefficients among the 85 populations using the MPMCORRELOGRAM package. Specifically, we quantified the relationship between the geographic distance between population locations and Euclidean distance between populations' admixture proportion. Pearson's correlation was calculated in 100 km bins up to 3000 km (approximately half the maximum distance between populations). Significance was determined using

999 permutations, and a progressive Bonferroni correction to *p*-values. We also tested how well predicted suitability of the three clusters in current climate related to observed admixture at the 85 populations. To do so, we extracted suitability for each cluster model at the population locations and standardized the values to sum to 1 by dividing the suitability for each cluster by the summed suitability (because admixture proportions similarly sum to 1).

To assess past and future range dynamics of the clusters, we assessed how the suitable area of each cluster varied over time. To calculate the area of suitable climate for past predictions, continuous predictions were converted to binary (1/0) maps using the threshold that maximized TSS. Because each time-period included 60 predictions, a map cell was considered suitable if the majority (> 50%) of the binary models found it suitable (i.e., equal to 1.0). We repeated this procedure for future climate predictions, but averaged over the 12 GCMs. Once a composite binary map was calculated, the suitable area was calculated using the 'area' function in the RASTER package in R.

Results

Validation statistics

Each of the ensemble models, whether fit species-wide or to individual genetic clusters, had good ability to discriminate between presences and pseudo-absences in current climate (Fig. 3.1). Across the 60 models in each of the ensembles

(i.e., northern, central, eastern, and species-wide models), average AUC was greater than 0.90, average TSS was above 0.80, and average kappa was above 0.75 for each cluster except the eastern cluster (average kappa = 0.67). There were, however, significant differences in validation statistics across the models. The species-wide model had among the lowest TSS and AUC, but among the highest kappa, compared to each of the three cluster models. The central cluster models were not significantly different from the species-wide models for any of the metrics ($p > 0.05$) and the northern cluster models were not significantly different than the central cluster except for kappa, where the northern cluster had a lower kappa ($p < 0.05$). The eastern cluster, in contrast, had the highest TSS, but the lowest kappa.

Pollen locations and validation

Balsam poplar pollen and macrofossils tended to occur in areas of high predicted climatic suitability for both the gSDM (i.e., combination of northern, central, eastern models) and standard SDM. The occurrence of pollen/macrofossils tended to track the receding ice sheet northward, often very near the southern margin of the glacier. Pollen/fossils extended nearly the entire length of balsam poplar's transcontinental range – from Beringia to the western Great Lakes to Atlantic Canada (Fig. 3.2). Interestingly, there were fossils that were solely suitable for each of the three clusters. AUC scores, calculated by pooling over all time periods, were 0.82 and 0.81, for the gSDM and standard SDM respectively. TSS (gSDM: 0.53, standard: 0.59) and kappa (gSDM: 0.53; standard: 0.59) were each similar between the gSDM

and standard SDM. Despite moderately high validation statistics, pollen/fossil suitability tended to decline between 10 and 15 ky BP, for both the composite and standard predictions. Many pollen/macrofossils between 10-15 ky BP occurred in eastern North America along the southern edge of the receding Laurentide glacier. In contrast, older fossils in Beringia were consistently predicted to have high suitability. The relationship between climatic novelty (quantified by Mahalanobis distance) and pollen/fossil suitability was weak, though significant, for the gSDM (r = -0.16, p < 0.01), and insignificant for the standard SDM (r = -0.04, p = 0.46) – indicating pollen/macrofossils in novel climates tended to have marginally lower gSDM suitability than pollen/macrofossils in more analogous climates.

Predicting admixture

Admixture proportions were autocorrelated across the 85 populations over hundreds of kilometers. Multivariate spatial autocorrelation analyses showed admixture coefficients were positively correlated up to a maximum of 1500 km, and random or negatively correlated at longer distances. SDMs for the three clusters had a good ability to predict cluster affiliation, as well as the relative mixing among clusters within populations. Generally, the climatic suitability of the northern, central, and eastern clusters at population locations was proportional to average admixture coefficients within populations (Fig. 3.3).

Variable importance

Variable importance differed across the cluster and the species-wide models (Fig. 3.4 & 3.5). The most important variables in the species-wide model were each related to temperature, specifically average winter temperature, while variables related to precipitation (summer and winter precipitation and precipitation variability) had relatively low importance. Temperature variables were similarly important to each of the cluster models, in particular average summer temperature. Unlike the other models, however, the eastern cluster had high importance of annual average evapotranspiration ratio, which tended to be amongst the lowest ranking variables in the other models.

Change in suitable area

The availability of climatically suitable area varied among the three genomic clusters through time, but some consistencies did emerge (Fig. 3.6 & 3.7). In general, each cluster increased in area over the past 22 ky. The suitable area available to each cluster at 22 ky BP ranged from 25 – 75% smaller than their current suitable area, while the species as a whole (gSDM and standard SDM) was around 50% smaller than the current range. As the glaciers receded in northern North America, each cluster expanded its range as it migrated northward (or eastward in the case of the northern cluster in Beringia), until eventually filling its contemporary range ~7.5 ky BP (Fig. 3.2). The central cluster exhibited the greatest relative increase in suitable area over the past 22 ky BP, and by 12 ky BP had the greatest absolute available area

among the three clusters. The eastern cluster similarly exhibited a gradual increase in suitable area over the past 22 ky, but maintained among the lowest absolute area from 22 ky BP to present. In contrast, the northern cluster had the greatest absolute suitable area at 22 ky BP, approximately 75% of its current range. The suitable area available to the northern cluster oscillated at the end of the Pleistocene, before steadily increasing to its current range size over the past 10 ky.

Suitable area for each of the clusters was predicted to decline by 2090. The central cluster is predicted to see a modest decrease in suitable area by 2030 (~15%), then maintain a stable range size through the end of the 21st century. Over the coming decades, the central cluster is predicted to gradually shift northward including into Alaska, where it currently has relatively low suitability. In contrast, the eastern cluster is predicted to decline by more than 25% of its current range by 2030, and further decline by the end of the century. The suitable area for the northern cluster followed a distinctly different future trend. By 2030, the northern cluster is predicted to increase in suitable area by nearly 50%, followed by a steady decline through the end of the century, ultimately resulting in a modest (< 5%) net loss in area by 2090. The modest loss in range area is the result of the northernmost parts of North America becoming climatically suitable for the northern cluster by 2030 and a declining northern landmass as the shift northward continues in later decades.

Discussion

In this study, we compared the transferability of gSDMs and standard SDMs to multiple time periods using an independent set of pollen and fossil records to test model performance. In contrast to other studies, we found that predictions from standard and gSDMs were largely consistent through time and gSDMs did not improve model performance in balsam poplar. Despite the lack of improved performance, gSDMs offered numerous insights not available from standard SDMs, such as predicted changes in cluster range size and potential refugial locations during the LGM. Our findings suggest gSDMs can provide useful information about species' past and future range shifts, but could be further improved to enhance transferability.

Model comparison

We found when models were tested with an independent set of occurrences not used to train models, the gSDMs did not perform better than standard SDMs. The lack of substantial improvement with gSDMs stands in contrast to other studies that have sometimes reported a multi-fold improvement in model accuracy with gSDMs, compared to standard SDMs (e.g., Ikeda et al., 2017). Most studies that compare standard and gSDMs, however, limit model training and testing to current climate (Ikeda et al., 2017; Marcer et al., 2016; Oney et al., 2013), and hence do not inform whether gSDMs are more transferable than standard SDMs to time periods outside those used to train models. This is an especially important distinction as a major motivation of integrating SDMs with genetic information, is to improve predictions of

species' range shifts in future climates (Ikeda et al., 2017; Maguire, Shinneman, Potter, & Hipkins, 2018; Oney et al., 2013). Our findings suggest that to fully understand differences in performance of gSDMs and SDMs, model testing should be conducted on independent data, ideally from areas or time periods not used to train models, as is recommended for standard SDM implementations (Araújo et al., 2019). Testing models on occurrences from multiple time periods provides a true test of model transferability and extrapolation to novel climates, which is especially important when predicting to future climates (Fitzpatrick et al., 2018).

There are numerous reasons why the gSDM approach, applied to balsam poplar, may not have improved performance compared to standard SDMs. First, gSDMs assume that clusters are completely differentiated from one another – insofar that each cluster is represented by a separate, independent model. While the assumption of complete differentiation may be adequate for species that are divided into subspecies or strongly differentiated along climatic gradients, complete differentiation may not be biologically realistic when individuals have mixed ancestries, or when populations include individuals from multiple ancestries. In balsam poplar, populations in the western portion of the range tend to be mixed among the central and northern clusters (Keller et al., 2010; Meirmans et al., 2017). Modeling the northern and central clusters separately likely introduces some uncertainty into the models (e.g., potentially affecting parameter estimates or model structure) as the northern and central models may be quantifying a mixed signal, not entirely representative of the hypothetical pure clusters. Furthermore, climate is likely

not the sole factor limiting the distribution of genetic clusters, and climate could be aligned with population structure by coincidence. Geographic isolation, limited dispersal/gene flow (Lecocq, Harpke, Rasmont, & Schweiger, 2019), or historical events (e.g., bottlenecks, founding events, genomic barriers) are also likely to be important factors limiting the distribution of clusters that would not be captured in correlative, climate-based SDMs. While using adaptive variation (versus population structure) to subdivide species' climatic niches could help ensure clusters represent functional climatic differences, current adaptive variation may not be representative of the ancestral differences being assessed here. Despite its limitations, neutral population variation remains among the most common way to split species' climatic niches into multiple subsets (Smith, Godsoe, Rodríguez-Sánchez, Wang, & Warren, 2019).

The gSDM approach, when used to predict past distributions, similarly assumes clusters have existed continuously on the landscape. However, clusters delineated by subdividing the range using neutral allele frequencies may not meet this assumption. For instance, if intraspecific variation arose following the LGM, the projection of individual clusters to earlier time periods (i.e., the LGM) may not be biologically meaningful. This could be the case with balsam poplar, as Keller et al. (2010) found the northern and eastern clusters likely differentiated from the central cluster during the migration northward to fill the current range. In other words, historically, there may have been a different number of clusters, compared to the three there are today. While the genetic population structure may not have been

present during the LGM, the pollen records suggest that the climate space currently occupied by the clusters was consistently occupied by the species, regardless of population structure. For instance, pollen/fossil sites exist in portions of Beringia that were suitable for the northern cluster before this cluster presumably differentiated from the central cluster, potentially violating the assumption that climate space occupied by clusters is temporally stationary. The non-stationarity in the climate space occupied by the clusters could be contributing to a mismatch between the pollen/fossil record and the current population structure that may partially explain why gSDMs do not enhance transferability when projected to past climates.

It remains unclear when it is most advantageous to model clusters as discrete units. Most gSDM studies, including this one, have been done on single species which make it difficult to generalize results, especially since gSDM studies utilize a variety of modeling techniques and validation methods. Some, though not all, gSDM studies that report improved performance over SDMs have been conducted on species with disjunct ranges. In these cases, geographic isolation may more strongly differentiate clusters, and better fulfill the gSDM assumption of complete differentiation. Balsam poplar, in contrast, despite being structured into multiple genetic clusters, has a large continuous range with few impediments to gene flow, which may limit any advantage of separating the range into discrete units. Future work focused on (i) when it is most advantageous to split a species' climatic space into multiple subsets, (ii) the minimum/maximum number of subsets required to best capture the species' entire climatic niche and (iii) whether any functional or

geographic traits affect gSDM performance (as has been done for standard SDMs, e.g., Hanspach, Kühn, Pompe, & Klotz, 2010; Syphard & Franklin, 2010) could help improve the biological realism and, potentially, the performance of the gSDM approach.

Past distribution and refugia

While the gSDMs did not necessarily improve model performance, when paired with pollen/fossil data, gSDMs offer numerous insight into balsam poplar's past range. gSDMs and pollen/macrofossil records suggest that following glacial retreat, balsam poplar's migration northward was broad-fronted. By 13 ky BP suitable climate and pollen/fossil records extended from Beringia, to the center of the current range (Minnesota, Wisconsin), to the easternmost part of the current range in Nova Scotia. gSDMs and pollen/macrofossil records both point to the possibility that balsam poplar filled its range from multiple refugia– specifically in Beringia and south of the Cordilleran and Laurentide ice sheets (Fig. 3.2). The suitable area south of the ice sheets during the LGM was nearly continuous from the Rocky Mountains to the Atlantic Coast and was likely the primary refugium for balsam poplar as each of the three clusters had suitable area in this region. This is consistent with Keller et al. (2010), who suggested a refugium in the Rockies based on a signature of range expansion and the phylogeographic relationship between the three clusters. While genetic studies to date have not detected a signature of a refugia or expansion out of Beringia (Breen et al., 2012; Keller et al., 2010), both SDMs and pollen suggest

balsam poplar was present in Beringia during the LGM. Others have also reported the presence of balsam poplar pollen and fossils in Beringia. Brubaker et al. (2005), for instance, reported *Populus* pollen (the predominant species, they suggest, being balsam poplar) from at least 20 ky BP and an increase in occurrence and abundance of *Populus* pollen after 15 ky BP. They note that the increase in *Populus* pollen abundance is unlikely to be the result of migration from outside Beringia as an ice-free corridor to the southern ice margin had not yet opened. When the ice-free corridor did open, however, our SDMs suggest climate within the corridor was suitable for balsam poplar nearly as soon as it opened (~13 ky BP) and recent work has shown *Populus* species, based on pollen and eDNA data, were likely the dominant tree species in parts of corridor (MacDonald & McLeod, 1996; Pedersen et al., 2016). This lends to the possibility that populations south of the ice sheet came into contact with Beringial populations soon after the ice-free corridor opened. Long and continued contact between populations north and south of the ice sheet could have eroded any distinctive markers that would have been emblematic of a distinctive northern refugium, and could explain the gradient in cluster affiliation throughout the western part of the range.

Future trajectories

Like studies of other North American plant species, we found the range of balsam poplar is predicted to shift northward in future climates (e.g., Iverson, Prasad, & Matthews, 2008; Morin, Viner, & Chuine, 2008; Oney et al., 2013). The largest

increases in suitability tended to occur in the northernmost portions of North America, where, interestingly, recent studies report an expansion of balsam poplar's distribution and an increase in its abundance (Roland, Stehn, Schmidt, & Houseman, 2016). Roland et al. (2016) suggest the expanding distribution and increasing abundance is primarily being driven by warming summer temperatures, which, coincidentally, we found to be the most important climatic driver for the northern cluster. The expansion of balsam poplar along its northern edge is likely facilitated by its ability to rapidly reach reproductive maturity, produce an ample annual seed crop and disperse its seeds long distances. Although we cannot be sure whether balsam poplar will be able to track its suitable climate throughout its range, these findings illustrate balsam poplar's sensitivity to climate change and the need for an accurate understanding of species' range shifts.

Figures

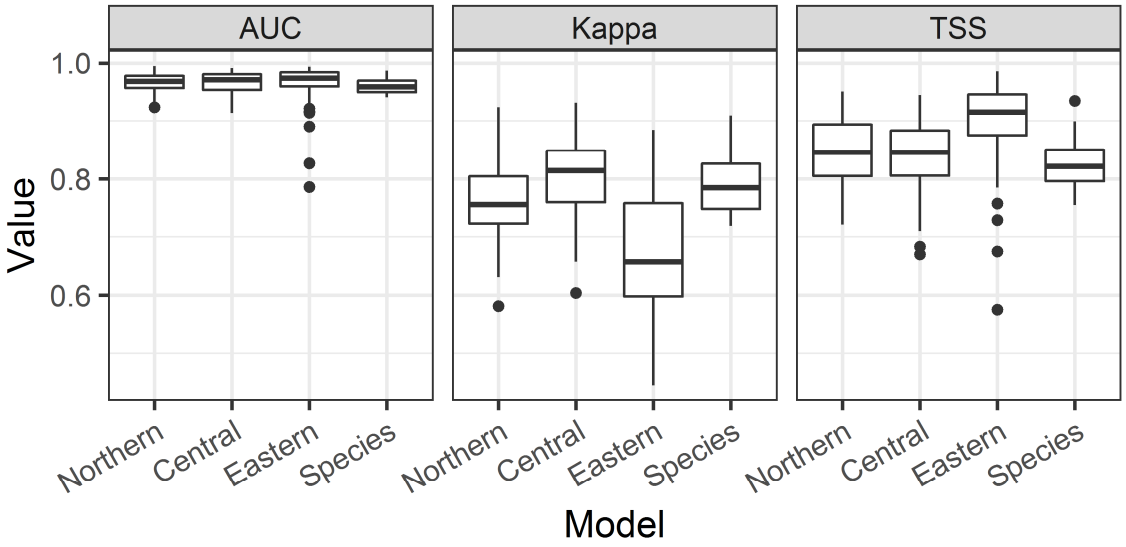

Fig. 3.1. Validation statistics for central, eastern, northern clusters and species-wide ensemble models for balsam poplar (*Populus balsamifera*). Each ensemble includes 10 folds of 6 algorithms.

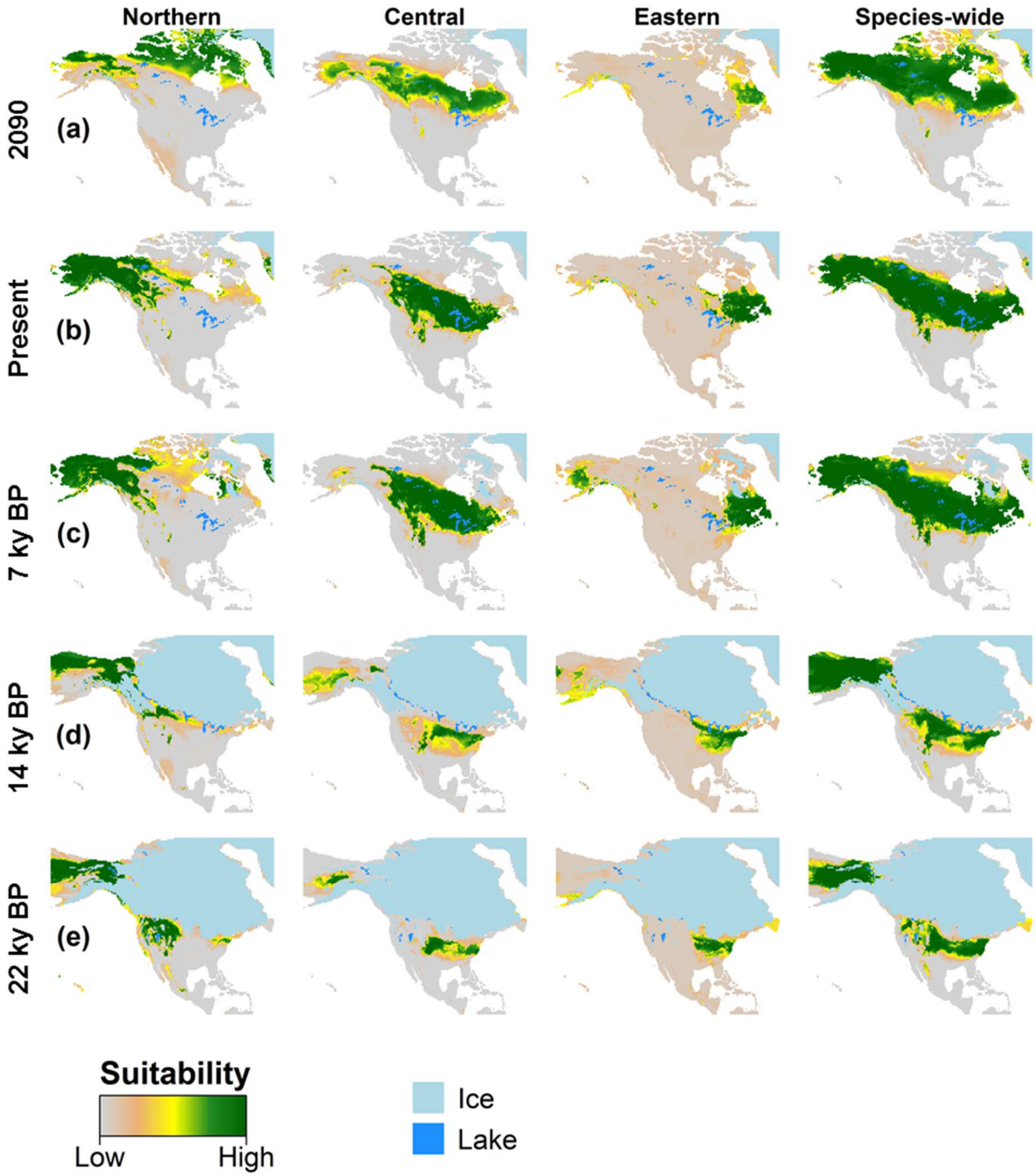

Fig. 3.2. Ensemble predictions for northern, central, and eastern clusters, and species-wide models for balsam poplar (*Populus balsamifera*) for (**a**) 2090, (**b**) current climate, (**c**) 7 ky BP, (**d**) 14 ky BP, and (**e**) 22 ky BP.

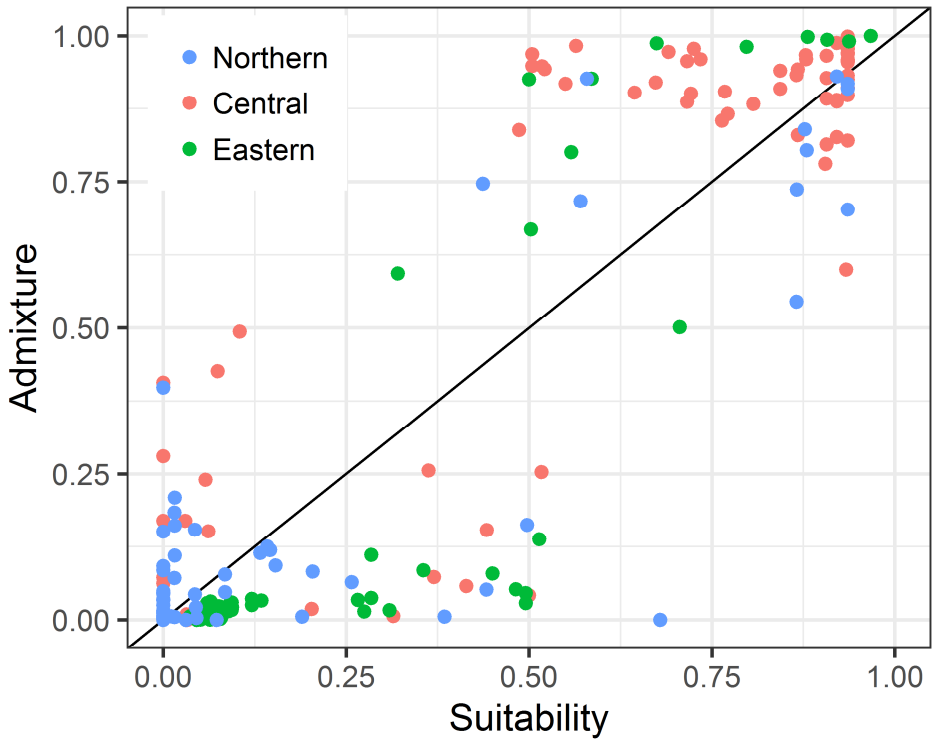

Fig. 3.3. Predicted suitability and average admixture proportions of 85 populations across three genetic clusters.

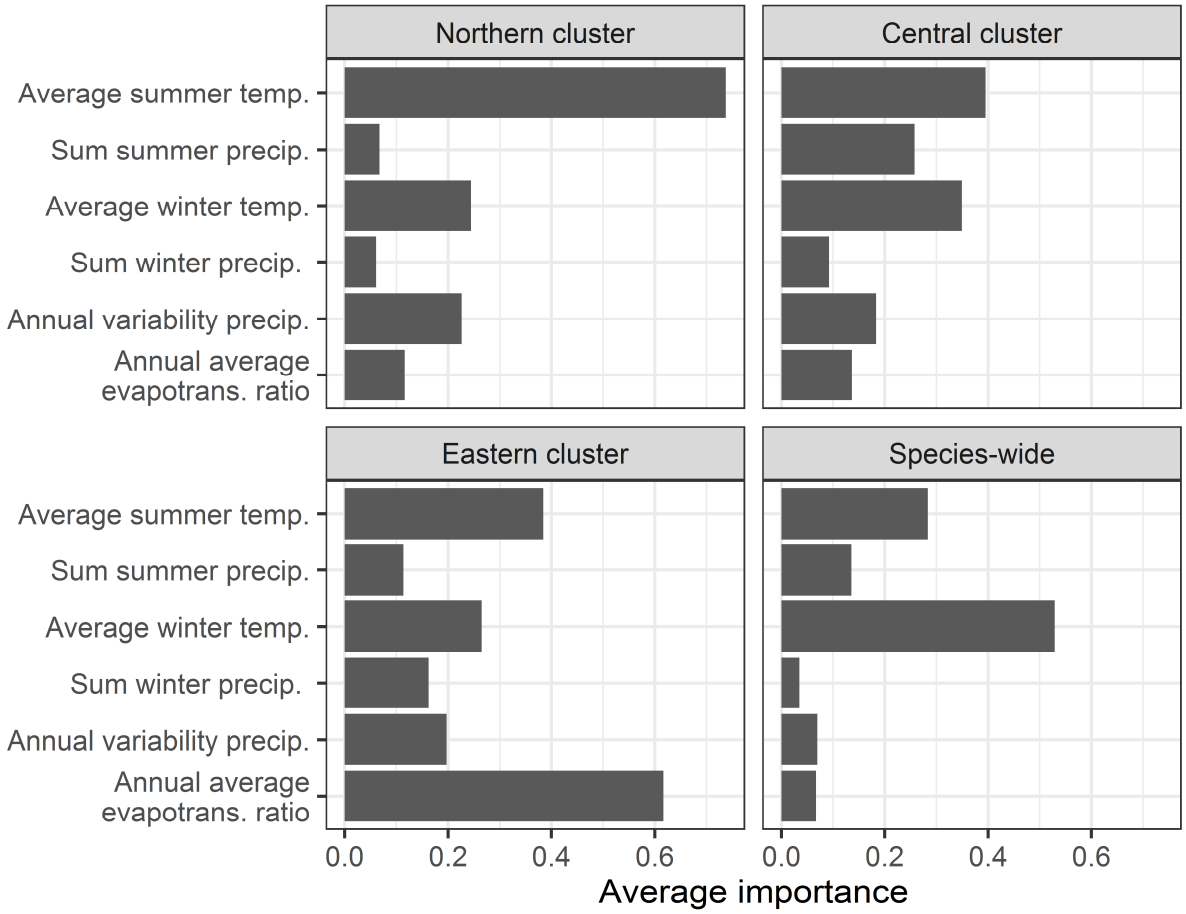

Fig. 3.4. Average variable importance of northern, central, and eastern clusters and species-wide ensembles models for balsam poplar (*Populus balsamifera*).

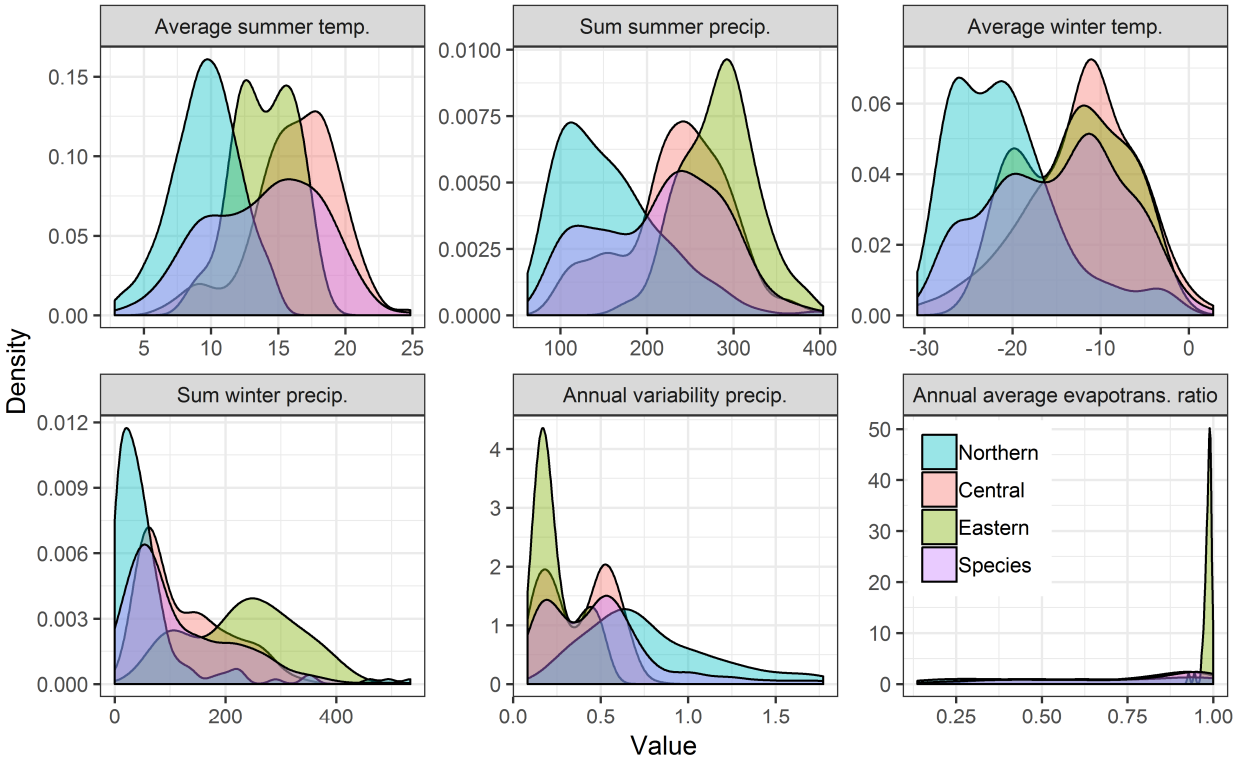

Fig. 3.5. Distribution of occurrences of three balsam poplar (*Populus balsamifera*) clusters and the entire species over six climatic variables used in ensemble distribution models.

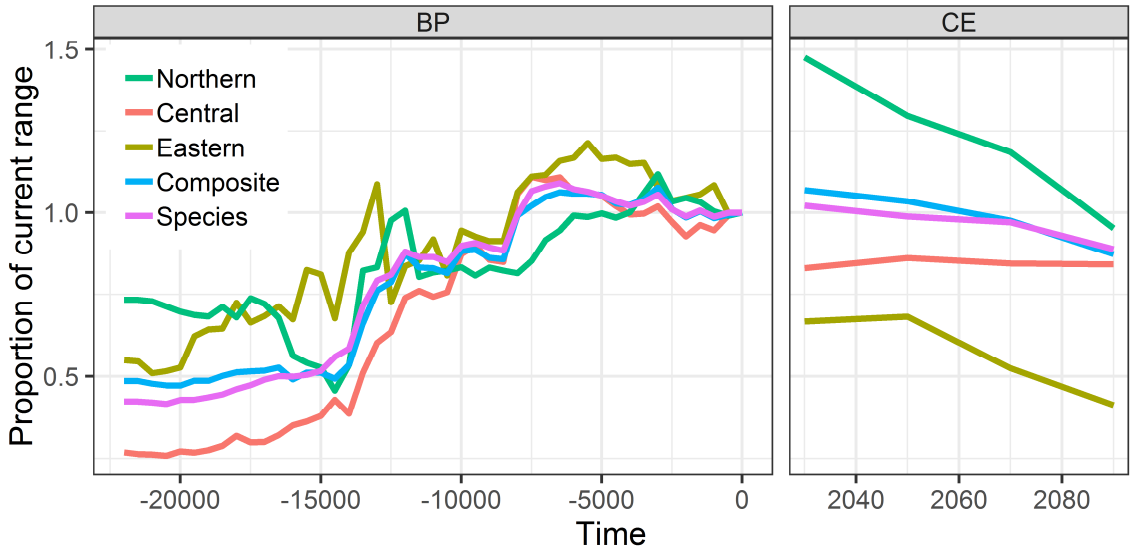

Fig. 3.6. Change in geographic area through time of three balsam poplar (*Populus balsamifera*) individual clusters and the entire species, standardized by the current range area. The area for the entire species was based on two estimates: a single, species-wide model ('Species') and a combination of the three cluster models ('Composite').

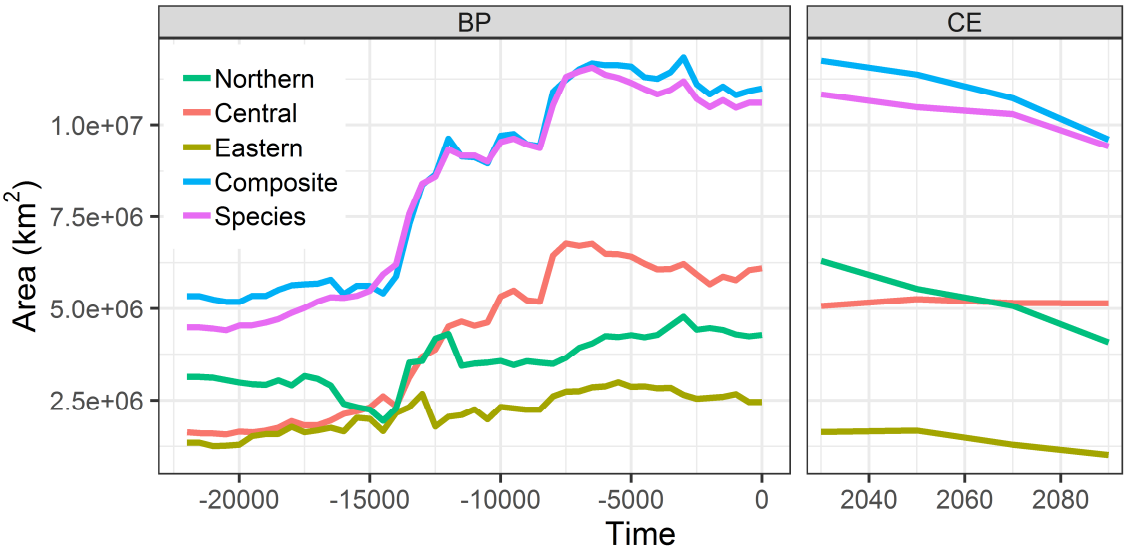

Fig. 3.7. Change in geographic area through time of three balsam poplar (*Populus balsamifera*) individual clusters and the entire species. The area for the entire species was based on two estimates: a single, species-wide model ('Species') and a combination of the three cluster models ('Composite').

Chapter 4: Future climate change will promote novel gene-climate associations in balsam poplar (*Populus balsamifera* L.), a forest tree species

Abstract

A central challenge to predicting climate change effects on biodiversity is integrating information on intraspecific variation, specifically population-level local adaptation to climate. Assessing how climate change could disrupt the gene-climate association of loci involved in climate adaptation can provide a new way of understanding population risk and exposure to climate change. For the wide-ranging boreal tree species, balsam poplar (*Populus balsamifera*), we used models of population-level genetic differentiation to estimate multiple metrics of its genetic exposure to climate change. These metrics included predicted shifts in genetic composition with and without migration, the potential for future novel gene-climate associations, as well as the distance and direction populations would need to migrate to minimize genetic composition change. We found exposure to climate change was greatest in the eastern portion of balsam poplar's range, where future maladaptation peaked, migration distances to sites minimizing maladaptation were greatest, and the emergence of novel gene-climate associations were most likely. Our results suggested a greater likelihood of gene-climate associations disappearing from the landscape when migration distances were limited – consistent with the possibility of migration lessening maladaptation to future climate. Our work helps differentiate different types

of exposure of populations to climate change and the suite of potential strategies that could be used to minimize the risk of extirpation.

Introduction

Future shifts in climate are expected to reshuffle climates globally, with new novel climates (i.e., new combinations or seasonality of temperature and precipitation) emerging, and some current climates disappearing from the landscape (Williams, Jackson, & Kutzbach, 2007). Because climate is a main constraint of most species' ranges, disappearing and novel climates will have a variety of consequences on biodiversity including extinction of endemic species, disappearance of current ecological communities, and the emergence of novel species assemblages (Williams & Jackson, 2007; Williams et al., 2007). Within species, climatically-adapted populations are likely to be particularly vulnerable to disappearing and novel climates. Disappearing climates could cause existing populations to become maladapted to local climate, resulting in local extirpation and disappearance from the landscape in the absence of genetic rescue by migration or adaptation. On the other hand, the emergence of novel climates, which existing genotypes have no prior selection history, could favor the evolution of novel genetic associations through the process of recombination of existing climate-adaptive alleles.

Migration has the potential to lessen the effects of disappearing and novel climates on locally adapted populations. Dispersal to areas where populations are preadapted to climate could limit the risk of extirpation, especially in parts of species'

ranges where climate change is minimal, or where analogous climates are expected to emerge nearby (e.g., upslope in mountains regions). If migration distances are particularly long, however, or the minimum adaptive offset (i.e., predicted disruption of gene-climate association, sensu Fitzpatrick & Keller, 2015) is particularly high, populations may face extirpation regardless of their ability to migrate or adapt. Quantifying the magnitude of maladaptation and the distance populations would need to migrate to minimize maladaptation, has the potential to inform where populations may be most at risk from climate change and where conservation or management efforts may be most effective.

In this paper, we develop a new approach to quantifying population-level exposure to climate change as a function of multiple metrics of population genetic maladaptation to future climate, and migration distances to locations that minimize maladaptation (Fig. 4.1). Using balsam poplar (*Populus balsamifera* L.) as a case study, we show maladaptation to future climates is highly variable throughout the geographic range, whereby some populations may be maladapted to all future North America climates, while others may be preadapted to future climate at or near their current location (i.e., would not need to migrate to minimize maladaptation). We also show that the distance populations would need to migrate to minimize maladaptation varied over multiple orders of magnitude, with the largest migration distances far outpacing balsam poplar's ability to disperse unassisted. Our metrics of genetic maladaptation and migration distances allow for a nuanced understanding of how

different responses to climate change may vary geographically while informing the relative vulnerability of populations to future climate change.

Materials and Methods

Balsam poplar

Balsam poplar is a northern broad-leaved forest tree species that occurs over a large portion of the boreal region of Canada and the northern United States. The expansive range of *P. balsamifera* spans more than 30 degrees of latitude across multiple broad climatic gradients (Little, 1971), with the center of its range in the boreal region of Canada that is expected to see amongst the highest levels of future warming in North America (Romero-Lankao et al., 2014). Trees in the genus *Populus* have emerged as a model system for landscape genomic studies of local adaptation to climate (Fetter, Gugger, & Keller, 2017) and balsam poplar, in particular, has been shown to be locally adapted to climate for numerous functional traits (Keller et al., 2011; Soolanayakanahally et al., 2009).

Generalized dissimilarity models

We used generalized dissimilarity models to map predictions of local adaptation to climate (Fig. 4.S1). Generalized dissimilarity models (GDM; Ferrier, Manion, Elith, & Richardson, 2007) are a type of non-linear matrix regression that accounts for the curvilinear relationship between climatic (and optionally,

geographic) distance and genetic differentiation among populations separated along environmental gradients. We fit GDM to genetic differentiation (F_{ST}) of 33 single nucleotide polymorphisms (SNPs) in the *Populus* flowering time gene network genotyped in 995 individuals from 81 populations from across the range of balsam poplar (Keller, Chhatre, & Fitzpatrick, 2018). Genes in the flowering time network are associated with both reproductive and vegetative plant phenology, by regulating the timing of seasonal growth, dormancy, and reproduction with the permissive growing season. We selected SNPs that had a relationship with environment, identified using Bayenv2 and latent factor mixed models. The environmental variables assessed for a relationship with SNPs included the first 3 components of a principal components analysis (PCA) of 19 bioclimatic variables and elevation, meant to capture the dominant climatic gradients across balsam poplar's range. See Keller et al. (2018) for a full description of how candidate SNPs were identified. We used SNPs showing an association with any of the 3 PCA axes identified across a range-wide sample (see Table 2 in Keller et al., 2018). Based on these 33 climate-associated candidate SNPs, we calculated a multi-locus pairwise F_{ST} among the 81 populations using the 'genet.dist' function in the HIERFSTAT package (Goudet & Jombart, 2015) in R. Any pairwise F_{ST} values less than zero were assigned a value of zero.

GDM was parameterized with six bioclimatic variables that lacked strong correlation ($|r| < 0.75$). These included: summer and winter mean temperature (bio10, bio11) and precipitation (bio18, bio19), isothermality (bio3), and mean diurnal range (bio2) downloaded from the WorldClim dataset (Hijmans, Cameron, Parra, Jones, &

Jarvis, 2005), at a resolution of 10 arc-minutes. We tested for variable importance in the model by permuting each variable 100 times and determining the average decline in deviance explained after permutation. Models were parameterized in current climate (centered on ~1975) and predicted to future climate (centered on 2070) using a composite average of five global circulation models (GCMs; UCAR Community Climate System Model, NOAA Geophysical Fluid Dynamics Laboratory Coupled Physical Model, MET Office Hadley Center Earth System Model, NASA Goddard Institute for Space Studies-E2-R, and the Norwegian Earth System Model). We performed all analyses using two different emission scenarios (RCP 4.5 and 8.5) for 2070. Results and discussion refer to the composite mean of the five RCP 8.5 projections for 2070 unless specifically noted. GDMs were fit using the GDM package (Manion, Lisk, Nieto-Lugilde, Mokany, & Fitzpatrick, 2017) in R.

Genetic exposure metrics

We used GDM to quantify the disruption of adaptive gene-climate associations expected under climate change using three different formulations of 'genetic offset,' which we term: (i) local, (ii) forward, and (iii) reverse genetic offset (Fig. 4.1). Following Fitzpatrick & Keller (2015), local offset (a metric of predicted maladaptation to future climate within a focal site) was calculated by predicting F_{ST} for locally adaptive SNPs between present and future climate at the same location, assuming no migration or gene flow. Forward offset is the minimum expected disruption in the gene-climate association assuming populations have unlimited

dispersal capacity. Forward offset was quantified by first predicting F_{ST} between current climate at each focal grid cell within balsam poplar's current range and all future climate grid cells in North America (exclusive of Mexico). From these predictions, we then identified the future climate grid cell with the minimum predicted F_{ST}, which we term forward F_{STmin} or forward offset. The distance to the location that minimized forward offset represents the minimum migration distance required to minimize maladaptation. High values of forward offset indicate maladaptation to all future North American climates. To assess the sensitivity of forward offset to dispersal constraints, we tested how F_{STmin} varied when migration was limited to five distance classes (50, 10, 250, 500, 1000 km). In addition to geographic distances, we also calculated the initial bearing populations would follow if they were to migrate to the location that minimized forward offset. Distance and bearing were calculated with the 'distGeo' and 'bearing' functions, respectively, in the GEOSPHERE package (Hijmans, 2017) in R.

Reverse offset follows the same idea as forward offset, but is calculated from future climate to current climate. In this case, we first used the GDM (the same model discussed above) to predict F_{ST} between each future climate grid cell within balsam poplar's current range and all current climate grid cells within balsam poplar's current range. From these predictions, we then identified the current climate grid cell with the minimum predicted F_{ST}, which we term reverse F_{STmin} or reverse offset. Reverse offset provides a metric of how novel the future gene-climate association is predicted to be at a given site, relative to existing gene-climate associations present at any

location throughout balsam poplar's range under current climate. As such, high values of reverse offset indicate "genetic novelty" as there is no analogous gene-climate association found anywhere in the current landscape. Note that for reverse offset we only considered pixels within balsam poplar's current range at both times periods to ensure future novelty in gene-climate associations was quantified only with respect to locations where balsam poplar currently occurs (i.e., within the current range) as opposed to the entirety of North America.

To simultaneously visualize local, forward, and reverse offset, we mapped these three metrics as the red, green, and blue bands of an RGB image, respectively. Because values of local offset were systematically higher than forward or reverse offset, we rescaled values within each band to their quantiles before plotting. This ensured the full range of colors were possible in the RGB images, and is analogous to a histogram equalization performed on each band. We also tested for correlation between local, forward, reverse offsets and distances. We used a spatially-corrected Pearson's correlation coefficient to quantify these relationships. The spatial correlations were implemented with the SPATIALPACK package (Vallejos, Osorio, & Bevilacqua, 2018) in R, after projecting latitude/longitude coordinates to an equidistant projection (Azimuthal equidistant).

Results and Discussion

Model fitting

GDM explained 65.2% of the deviance in F_{ST}. Variable permutation revealed that winter precipitation was the most important variable in the model. Isothermality and summer temperature were of secondary importance, while summer precipitation, mean diurnal range, and winter temperature were least important. All variables were significant ($p < 0.01$) except winter temperature ($p = 0.16$). Variable importance was positively associated with the magnitude of predicted F_{ST} along the respective climatic gradients. For instance, the greatest predicted differentiation occurred over the gradients in winter precipitation, isothermality and summer temperature gradients, while predicted differentiation was low for the winter temperature gradient.

Local, forward, and reverse offset

Local genetic offset was moderately high throughout the range of balsam poplar (mean $F_{ST} = 0.07$) and peaked in the eastern portion of the range in Atlantic Canada and northern parts of the range in Alaska and the Yukon Territory. The spatial pattern of forward offset was largely consistent with local offset ($r = 0.74$, $p < 0.01$), but was considerably lower – consistent with the potential for migration to dampen the disruption of genetic climate adaptation. Like local offset, forward offset was lowest in the center of the range in central Canada, and increased eastward and northward. Reverse offset (i.e., future novelty) was highest in the extreme eastern

portion of the range and in northern areas in the Northwest Territories, suggesting these areas were most likely to experience selection under future climates for gene-climate associations that are not well-represented by current gene-climate associations across the landscape.

While the predicted patterns of local, forward, and reverse offset were highly variable in different parts of the range, some generalities did emerge (Fig. 4.2, 4.S2, 4.S4). For instance, all three metrics were low in the center of the range, indicating populations in this region are predicted to have the lowest overall exposure to future climate change because they (i) have low offset in their current location (i.e., with no migration), (ii) have low offset in other portions of North America (i.e., are preadapted to future climate somewhere in North America; low forward offset), and (iii) existing populations elsewhere in the range are preadapted to future climate in the center of the range (i.e., low reverse offset). In contrast, exposure was highest in the eastern part of the range and sporadically in the northern part of the range, where all three metrics of genetic offset peaked. That is, based on our knowledge of adaptive gene-climate associations, there are no existing balsam poplar populations that are predicted to be preadapted to the future climates expected to develop in this region, including local populations and populations from elsewhere in the range. While other parts of the range had various combinations of high local offset and high forward or reverse offset, only in the eastern part of the range were all three metrics consistently high, revealing a high likelihood of climate maladaptation in this region with little

opportunity for migration to mitigate impacts. As such, we would expect extirpations of balsam poplar populations to be most likely in these portions of the range.

Migration distances and direction

Interestingly, migration distances (i.e., distances to the location of forward offset) were only weakly correlated with forward offset ($r = 0.14$, $p = 0.25$) – implying that, across populations, longer distances were not linked to higher forward offset. Distances to forward offset peaked in the eastern portion of the range, where they exceeded 5000 km (Fig. 4.3a). Locations minimizing forward offset for many of the cells in the northeastern portion of the range were in mountainous areas in the western half of North America – indicating populations in the easternmost portion of the range would need to migrate across nearly the entire North American continent to minimize forward offset. The shortest distances to forward offset, in contrast, occurred along the southern range edge, and sporadically in the northern portion of the range, often near mountainous areas. Very few locations (<1%) had distances of zero, suggesting that populations in nearly all parts of the range would need to migrate some distance to reach the location they are most preadapted to in the future, barring allele frequency change *in situ*. Limiting the search distance for forward offset revealed a negative relationship between forward offset and distance (Figs. 4.4, 4.S5, 4.S6), suggestive of a tradeoff between migration distances and forward offset. Forward offset decreased considerably when the search distance was expanded from 0 to 500 km (mean decrease in forward offset across all cells: 53.9%), while the

decline in forward offset between distances of 500 and 1000 km was considerably lower (mean decrease: 14.9%), indicating a declining benefit of lowering forward offset as search distances increased. The relative range-wide pattern of forward offset was similar across search distances but the magnitude differed (Figs. 4.S5, 4.S6).

While most range-shift projections from species-level bioclimatic models suggest a poleward trajectory, our results suggest that if populations migrate towards the location that minimizes forward offset, range shifts may be considerably more complex. For example, while most (82.8%) locations in balsam poplar's range had an overall northward trajectory (i.e., the location with minimized forward offset was at a higher latitude than the source pixel), we found considerable variability along the southernmost range edge (Fig. 4.3b). In these southern edge populations, the migration trajectory was sporadically westward, eastward, and even southward. The variability in direction was most apparent in the upper Great Lakes region where directionality varied over short distances. Recent observational studies have shown similar variability when populations are aggregated over entire species (Fei et al., 2017; VanDerWal et al., 2013). Fei et al. (2017), for instance, showed that over the past 30 years, eastern North American tree species have more often shown a westward shift in abundance than a poleward shift. The authors propose this is due to shifting precipitation regimes and moisture availability increasing suitability for eastern tree species in the center of North America. Precipitation was also important in our GDM, and may be causing a similar effect in our predictions. The lack of a strict poleward shift in observational studies could partially be due to local adaptation

of populations that, when aggregated across an entire species, translates into species-level variability in migration direction.

Advances

Impacts of climate change on populations will be mediated by the spatial pattern and magnitude of climate change and the ability of populations to adapt or migrate in response. Our study quantifies these varied responses by developing a spatially-explicit understanding of the relative roles of local maladaptation, minimum migration distances, and gene-climate novelty on population-level exposure to climate change. In doing so, we attempt to shed new light on several major unresolved questions concerning how climate change will affect populations within a species' range, specifically: (i) where will climate change cause the greatest mismatch between locally adapted populations and climate?, and (ii) which existing populations may be most preadapted or maladapted to future climates? By simultaneously calculating multiple metrics of maladaptation and migration distances, our approach provides insight into the tradeoff between *in situ* selection versus migration, and helps elucidate where within the range each may be most effective at reducing the genetic offset under future climates. It is important to emphasize that our approach makes no attempt to assess the ability of populations to adapt or migrate, or predict mean fitness and evolutionary response over multiple generations (Shaw, 2018). Nevertheless, our approach provides intuitive metrics of population-level exposure to climate change

that may serve as a useful baseline for understanding where populations may be most at risk from climate change.

Interestingly, contrary to some theoretical work (e.g., Hampe & Petit, 2005), exposure to climate change was not greatest along the trailing (southern) edge of balsam poplar's range, but rather at the longitudinal extremes of the range. This is likely partially due to the importance of precipitation in driving differentiation of SNPs we investigated. Changes in winter precipitation, the most important variable in our model, is predicted to be greatest in the eastern and northernmost parts of the range in areas similarly predicted to have high future offset. In the center of the range, and along much of the southern edge, climate shifts are predicted to be relatively modest compared to the eastern portion of the range, leading to relatively lower offset in these areas. These findings are consistent with recent work that has suggested that accounting for local adaptation could yield results contrary to the leading-/trailing-edge paradigm of species' range shifts (i.e., as ranges shift poleward, trailing edge populations are most vulnerable to climate change as they will be the first to experience temperatures outside the species' climatic niche; Peterson et al., 2019). Indeed, other modelling studies have shown accounting for local adaptation can yield unexpected range shifts that are not strictly poleward (Atkins & Travis, 2010). Similarly, numerous empirical studies have reported that range shifts in response to recent climate change are rarely uniformly poleward (Chen et al., 2011; Fei et al., 2017; Groom, 2013; VanDerWal et al., 2013), and may be in multiple directions, including southward. Together, our results point to the possibility that explicitly

considering the gene-climate association of multiple loci across multiple climatic gradients could yield a considerably more complex view of population's responses to climate change than is often implied by a simple shift poleward shifts often predicted by species distribution models.

Limitations and extensions

There are a number of limitations to our approach of predicting population exposure to climate change. First, the offset metrics implicitly assume that the current pattern of genetic differentiation across space is representative of genetic change through time (i.e., space for time substitution). Although the offset metrics have not yet been empirically validated, selecting loci with an *apriori* relationship with climate (Keller et al., 2018), and related to a temporally/spatially variable trait (i.e., phenology), should help ensure we are modelling a robust, reliable gene-climate signal. Second, we used a correlative model (GDM) that does not account for the genetic forces (i.e., selection, gene flow, etc.) that will shape the future pattern of genetic variation. Nor do the models account for potential plastic responses to climate change, or population's ability to persist in variable climates (i.e., interannual climatic variability) – both of which likely contribute to an overestimation of offset metrics. Finally, our models emphasize only abiotic adaptation. While this may be suitable for SNPs related to phenology, populations are also likely to experience unique biotic interactions in future climates (e.g., such as encountering new competitors or new

pest regimes). Hence, it is important to emphasize that the exposure metrics calculated here, are only relevant to the specific SNPs used in our study.

Our approach to mapping forward and reverse offset could be expanded in numerous ways. For instance, the way we identified F_{STmin} in future climates assumes populations would follow a straight-line distance and direction to track the location that minimizes future genetic offset. Unless F_{STmin} is nearby, however, most populations will be unlikely to reach the location of forward offset given dispersal constraints and migration barriers (Carroll, Parks, Dobrowski, & Roberts, 2018; McGuire, Lawler, McRae, Nuñez, & Theobald, 2016). Thus, when considering realistic dispersal constraints, forward offset is likely to be higher than our unlimited migration scenario suggests, as illustrated when the search distance for forward offset was limited (Fig. 4.4). Using the forward offset as a landscape metric of resistance to movement in a dispersal simulation could produce more realistic estimates of F_{STmin}, without relying on discrete distance classes.

Finally, our analyses were conducted on loci in balsam poplar associated with phenology, which have a well-studied physiological and phenotypic relationship with climate that is established to be locally adaptive in balsam poplar (Keller et al., 2011), and will be an important trait in future climates (Richardson et al., 2013). Our approach, however, is generalizable to any number of loci identified in genome scans for selection as having a robust adaptive association with climate. Additional insights could be gained by assessing the pattern of forward and reverse offset predicted based on loci associated with other climatically-adaptive traits (e.g. heat and drought

tolerance, growth rates, etc.). Assessing loci associated with different traits could help elucidate the variable impacts climate change may have on different parts of the genome, and could inform whether populations are likely to be preadapted to a single location on the landscape, or more likely, whether genomic regions underlying different functional traits will be preadapted to different locations within the future landscape.

Conclusion

Population's responses to climate change are likely to be complex, requiring a combination of migration and adaptation to avoid extirpation (Aitken, Yeaman, Holliday, Wang, & Curtis-McLane, 2008; Alberto et al., 2013; Davis & Shaw, 2001). When we attempt to account for this complexity, we found a rich assortment of responses to climate change across the range. In balsam poplar, we found the eastern portion of the range had the highest local, forward and reverse offsets and longest migration distances – indicating eastern populations may have the greatest exposure to climate change compared to the rest of the range and may face the greatest risk of future extirpation. More broadly, our work shows that, just as some climates and biological communities may disappear from the future landscape, and novel ones may emerge in their place (Williams & Jackson, 2007), the same is true for gene-climate associations in climatically adapted tree populations. The concepts of forward and reverse genetic offset provide a new way to consider population-level risk to future

climate change that accounts for local adaptation and goes beyond the constraints of species-level predictions.

Figures

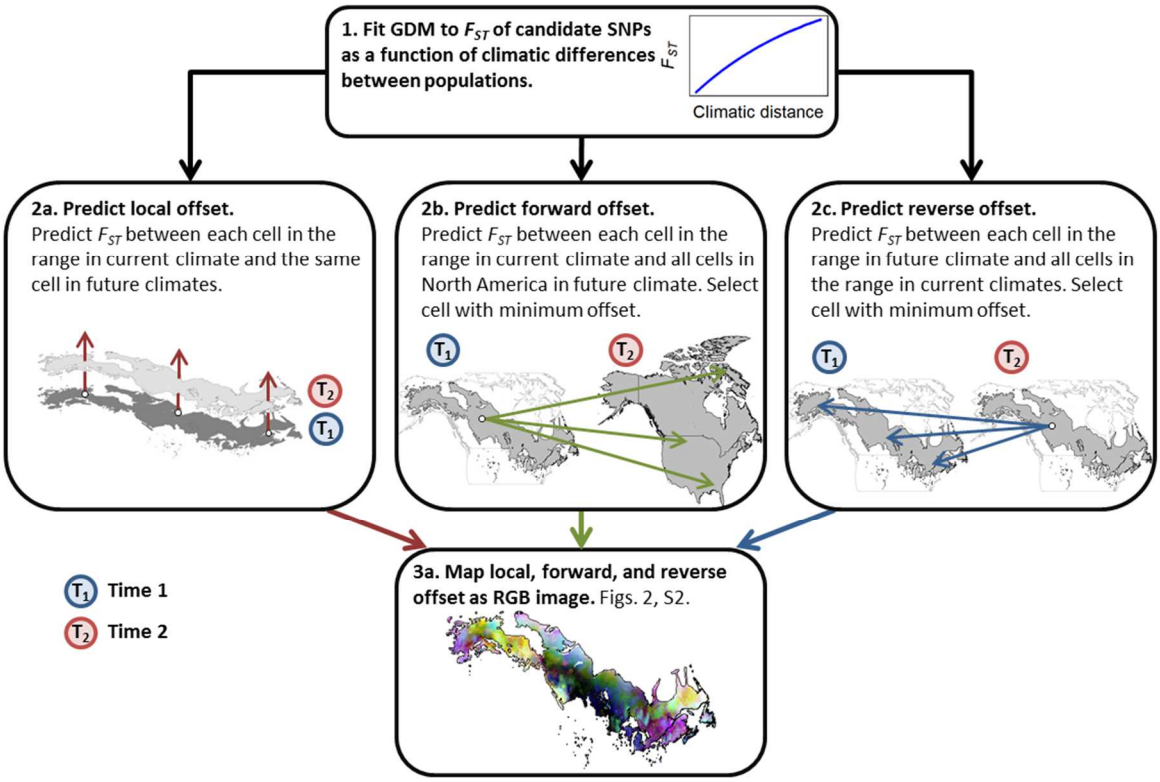

Fig. 4.1. Schematic of how local, forward and reverse offset were calculated and mapped. (**1**) After fitting a generalized dissimilarity model to F_{ST} of climatically-adaptive SNPs, the model is used to predict (**2a**) local, (**2b**) forward, and (**2c**) reverse offset. Local offset is calculated following Fitzpatrick & Keller (2015). Forward offset is calculated by predicting F_{ST} between each cell in the range in current climate and all cells in North America in future climate and selecting the minimum value. Reverse offset is calculated by predicting F_{ST} between each cell in the range in future climate and all cells in the range in current climate and selecting the minimum value. Gray polygons are balsam poplar's range (Little, 1971).

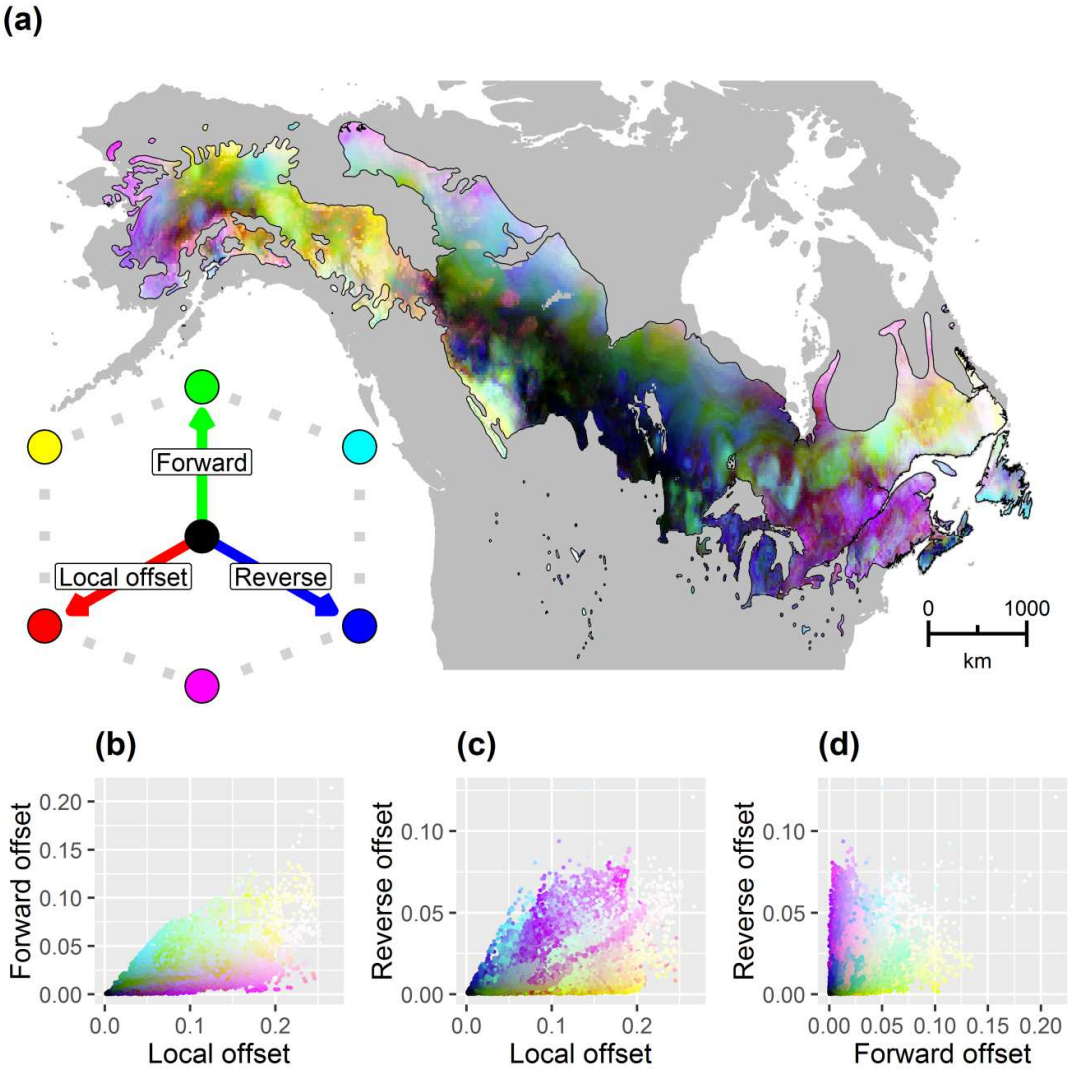

Fig. 4.2. Red-green-blue map of local (red), forward (green), and reverse (blue) offset throughout the range of balsam poplar for 2070 and RCP 8.5. Brighter cells (closer to white) have relatively high values along each of the three axes indicating greater predicted exposure to climate change, while darker cells (closer to black) have relatively lower values, indicating lower exposure to climate change. (**b-d**) Bivariate scattergrams of (**a**). All units are F_{ST}, but forward and reverse offsets are minimized F_{ST}.

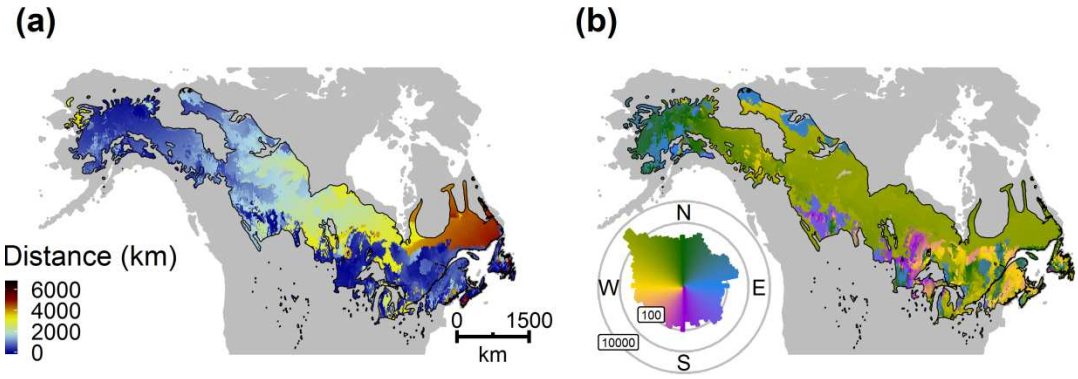

Fig. 4.3. (a) Distance and **(b)** initial bearing to the location that minimizes future offset for balsam poplar in 2070 and RCP 8.5. Polar histogram in (**b**) shows the $\log_{10}$ number of cells in each bearing bin.

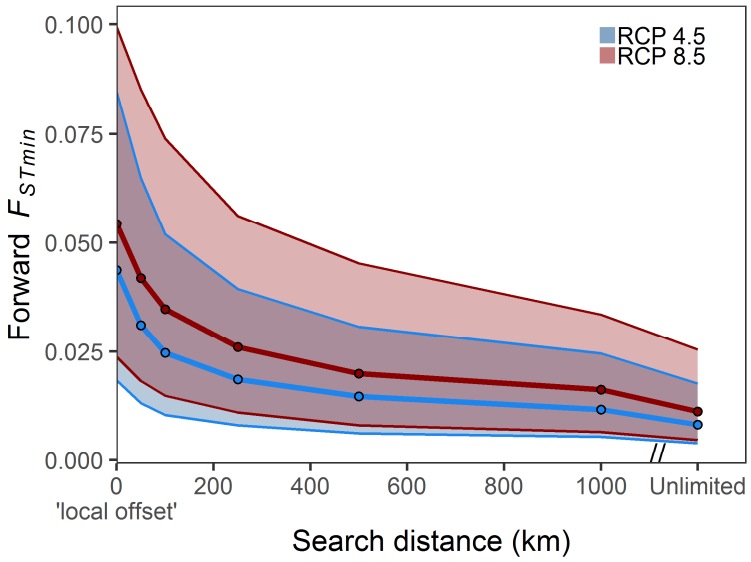

Fig. 4.4. Relationship between search distance and minimized forward offset (F_{STmin}) for 2070. Bands extend between the 25th and 75th percentiles, and points are median values. See also **Fig. 4.S5 & 4.S6.**

Supplemental figures

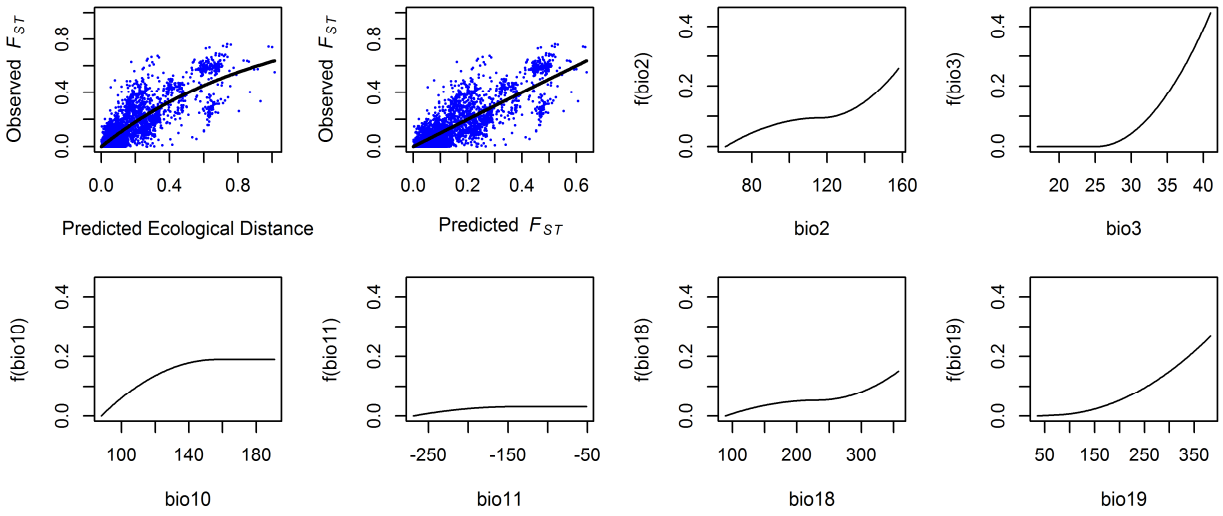

Fig. 4.S1. Generalized dissimilarity model (GDM) fit and climatic response plots. GDM was fit to F_{ST} of 33 SNPs in the *Populus* flowering time network across 81 range-wide balsam poplar populations (bio2: mean diurnal range; bio3: isothermality; bio10: mean summer temperature; bio11: mean winter temperature; bio18: summer precipitation; bio19: winter precipitation).

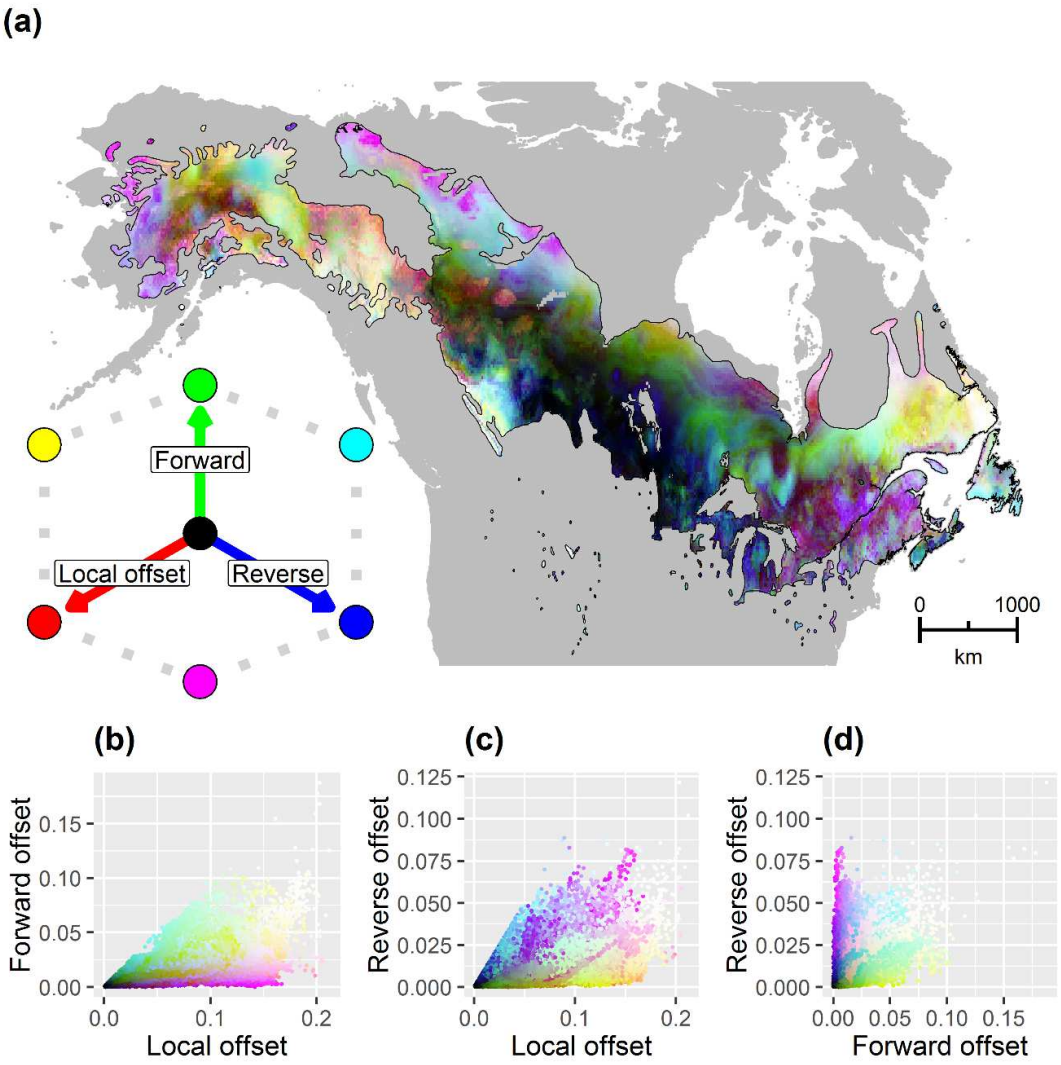

Fig. 4.S2. Red-green-blue map of local (red), forward (green), and reverse (blue) offset throughout the range of balsam poplar for 2070 and RCP 4.5. Brighter colors (closer to white) have relatively high values along each of the three axes indicating greater predicted exposure to climate change, while darker colors (closer to black) have relatively lower values, indicating lower exposure to climate change. (**b**-**d**) Bivariate scattergrams of (**a**). All units are F_{ST}, but migration and novelty offsets are minimized F_{ST}.

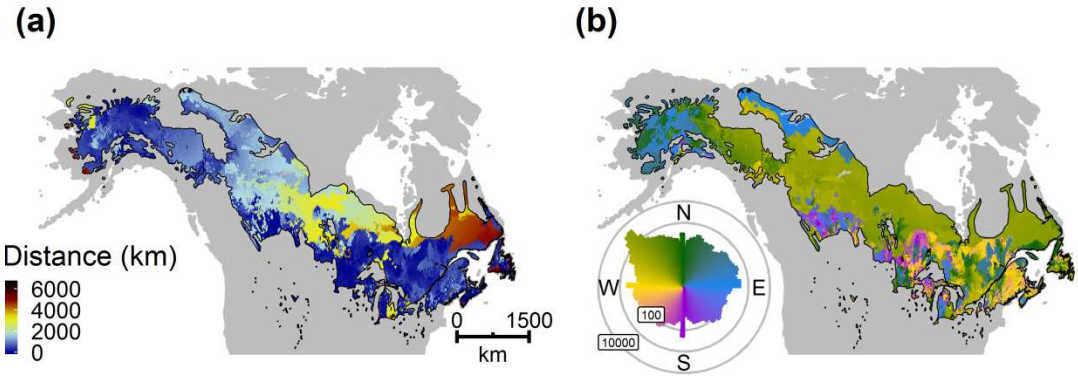

Fig. 4.S3. (**a**) Distance and (**b**) initial bearing to the location that minimizes future offset for balsam poplar in 2070 and RCP 4.5. Polar histogram in (**b**) shows the $\log_{10}$ number of cells in each bearing bin.

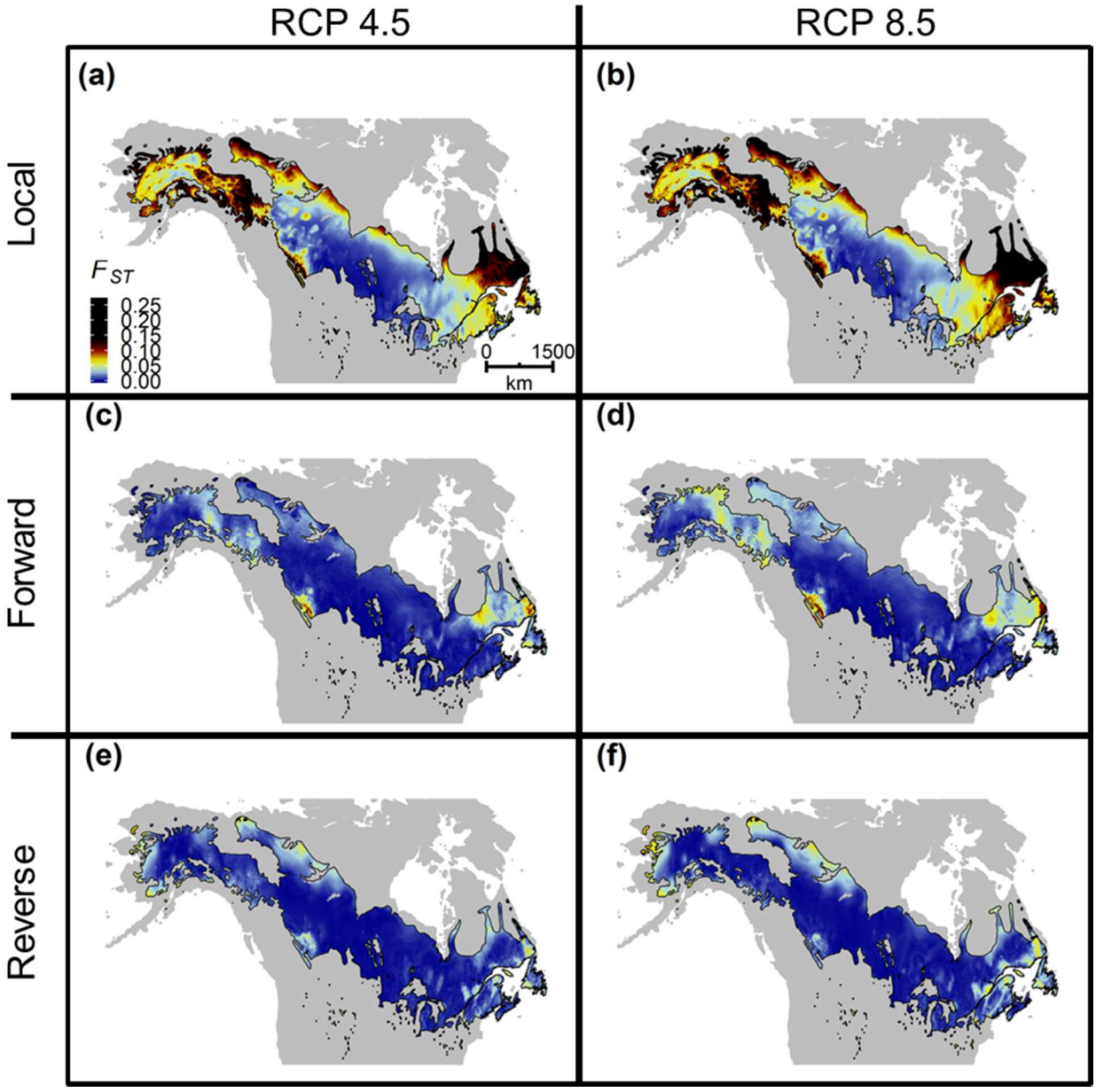

Fig. 4.S4. (**a** & **b**) Local genomic offset, (**c** & **d**) forward offset, and (**e** & **f**) reverse offset for RCP 4.5 (first column; **a**, **c**, **e**) and RCP 8.5 (second column; **b**, **d**, **f**) for 2070. Note the non-linear color scale. **a**, **c**, **e** are plotted as an RGB image in **Fig. 4.S2**, and **b**, **d**, **f** are plotted in **Fig. 4.1**.

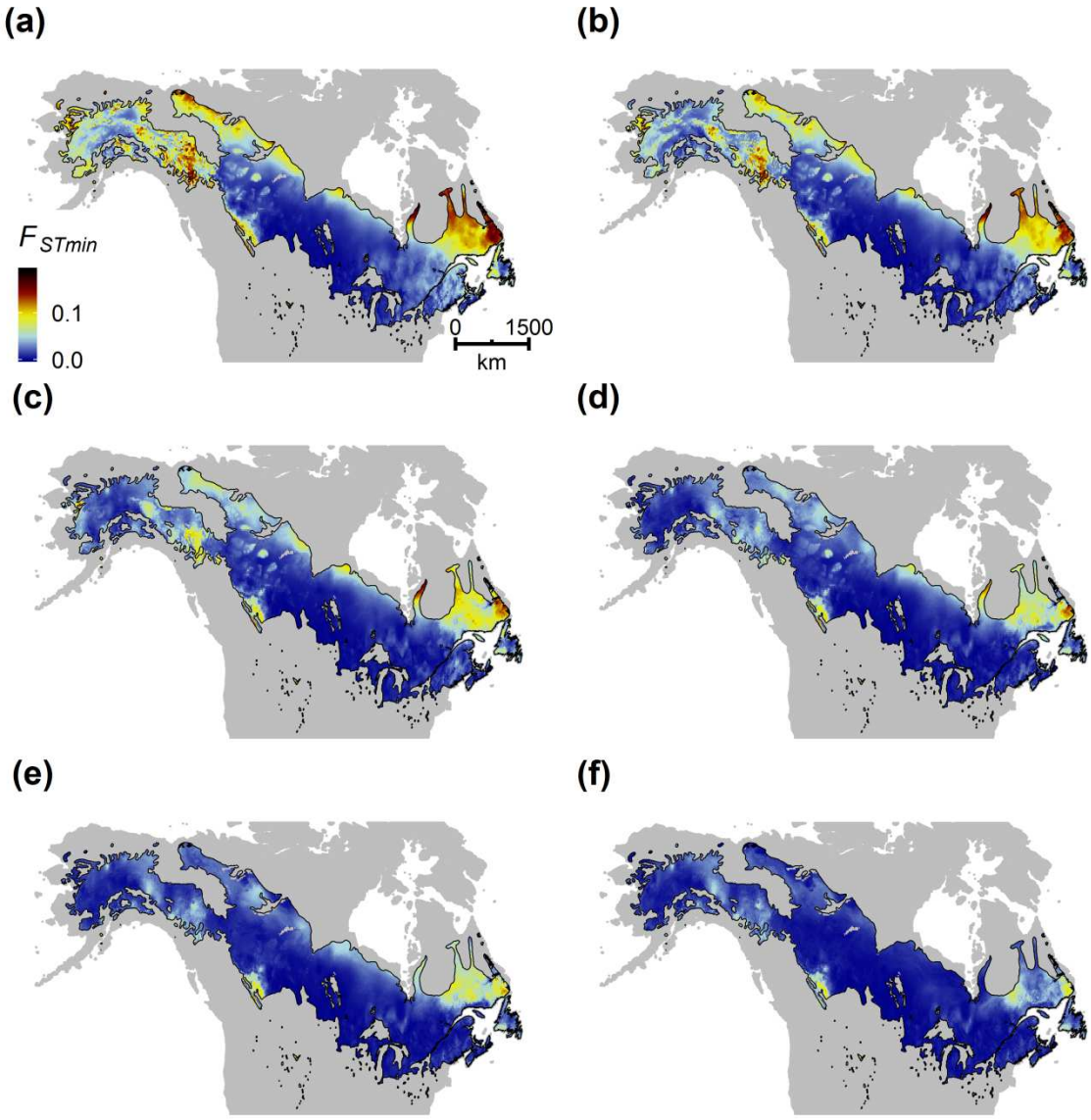

Fig. 4.S5. Effect of search distance on forward F_{STmin} for RCP 4.5 in 2070. Distance classes included (**a**) 50 km, (**b**) 100 km, (**c**) 250 km, (**d**) 500 km, (**e**) 1000 km, and (**f**) unlimited. See also **Fig. 4.3**.

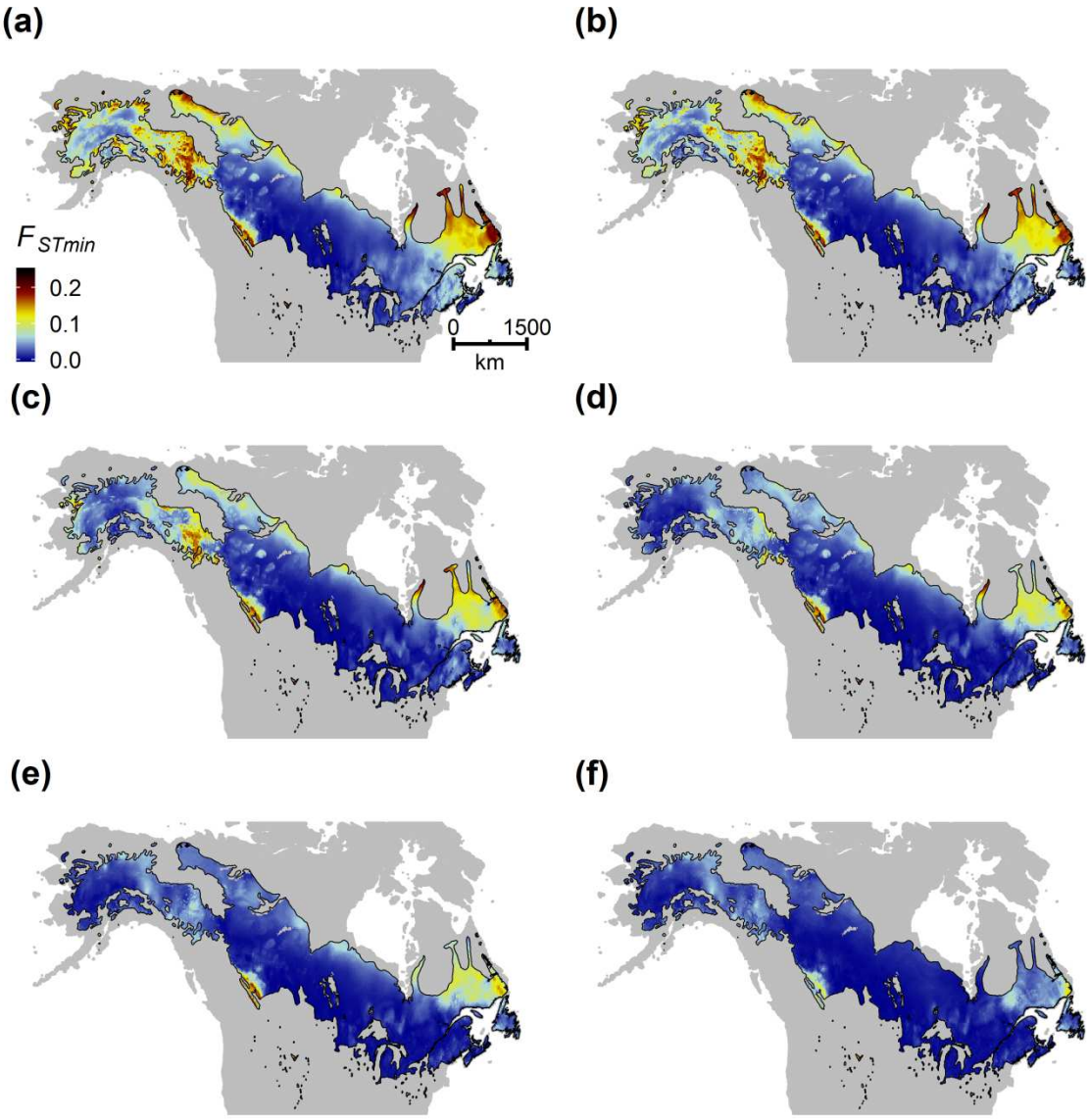

Fig. 4.S6. Effect of search distance on forward F_{STmin} for RCP 8.5 in 2070. Distance classes included (**a**) 50 km, (**b**) 100 km, (**c**) 250 km, (**d**) 500 km, (**e**) 1000 km, and (**f**) unlimited. See also **Fig. 4.3**.

Chapter 5: Integrating genomics, common garden experiments, and remote sensing to understand the phenology of balsam poplar (*Populus balsamifera* L.) at landscape scales

Abstract

The study of plant phenology encompasses multiple disciples that together use techniques that span taxonomic, spatial, and temporal scales. While important insights have been learned at each scale, it is often unclear how well the insights from one scale can inform our understanding of phenology at a different scale. Here, we test the extent which genotype information can be combined with common garden observations of phenology to predict phenology observed at landscape scales using remote sensing. To do so, we combine a genomic prediction of phenology observed in common gardens with meteorological variables to model two metrics of land surface phenology – the day of year of spring onset (DOY), and the number of growing degree days accumulated before spring onset (cGDD). We show that the genomic prediction based on phenology observed in common gardens was the strongest predictor of DOY and outranked all meteorological variables, but was amongst the least important predictors of cGDD. Although both the DOY and cGDD models did well predicting spatial and temporal patterns of phenology withheld during training, model error was correlated with multiple meteorological variables. Our work shows that common garden experiments can inform phenology at landscape

scales, but there remain considerable uncertainty about the ability to forecast phenology to future climates.

Introduction

Phenology, the study of repeated life history events, has received increased attention in recent decades as it is one of the key biological indicators of recent climate change (Parmesan & Yohe, 2003; Tang et al., 2016). A signal of advancing spring has already been detected in long-term, historic records and contemporary observations at a range of scales (Ahas, Aasa, Menzel, Fedotova, & Scheifinger, 2002; Menzel et al., 2006; Schwartz, Ahas, & Aasa, 2006). Shifts in phenology are expected to have consequences across ecosystems from disrupting species' interactions (Memmott, Craze, Waser, & Price, 2007; Rafferty & Ives, 2011) to affecting global nutrient cycles (Piao, Friedlingstein, Ciais, Viovy, & Demarty, 2007). Understanding how plant phenology will shift in future climates will be crucial to understanding how natural systems may be altered by climate change.

While phenology has well-documented genetic and environmental components, the relative roles of each are often uncertain, especially at broad spatial scales. Most broad-scale studies do not explicitly account for genetic variability or local adaptation, and those that do often yield mixed results regarding its importance. Chuine et al. (2000), for instance, found little difference in climatic requirements among populations of nine European tree species, and suggested that considering local adaptation is not crucial to modelling phenological responses to global change.

Vitasse et al. (2009) found similar results when comparing phenology of three woody species across an elevational gradient. Others, however, have found a strong signal of local adaptation in phenology, particularly when phenology is observed in common gardens. Multiple studies, for instance, have reported differences in the amount of cooling or thermal forcing required for bud flush among populations of various tree species when individuals are grown in identical meteorological conditions (Morin, Roy, Sonié, & Chuine, 2010; Myking & Heide, 1995; Olson et al., 2013; Zohner & Renner, 2014), suggesting accounting for local adaptation or genetic differences could be important to understanding the drivers of phenology.

In contrast to the genetic influence on phenology, climatic influences are often more clear. In temperate regions, where moisture is not limiting, temperature is typically a dominant driver of phenology. Whether assessed at the scale of individual plants or forest patches (i.e., satellite pixels), the accumulation of chilling during the winter and heat during the winter/early spring are often strongly tied to the timing of bud flush and leaf emergence (Hunter & Lechowicz, 1992). Although precipitation often plays a lesser role in temperate regions, numerous studies have found preseason precipitation to have an influence on spring phenology (Fu, Piao, et al., 2014; Lambert, Miller□Rushing, & Inouye, 2010; Yun et al., 2018). While the general effects of temperature and precipitation on phenology have been well documented, the temporal range at which meteorological variables influence phenology is often uncertain. Temperature and precipitation in the weeks or months immediately preceding bud flush is often identified as important, but experimental work has

suggested that seasonal temperatures during the previous year can have residual effects on the timing of phenological events in tree species (Fu, Campioli, et al., 2014). This is consistent with other observational work that has shown lag effects of temperature up to two years (Mulder, Iles, & Rockwell, 2017).

Because phenological shifts will be an important biotic response to global change and will affect natural systems at multiple temporal, spatial, and taxonomic scales, the study of its drivers spans multiple disparate disciplines (Pau et al., 2011; Wolkovich, Cook, & Davies, 2014). While previous work has shown that phenology metrics are often correlated across scales (e.g., individual plants vs. near surface cameras vs. satellites; Fisher & Mustard, 2007; Graham, Riordan, Yuen, Estrin, & Rundel, 2010; Liang, Schwartz, & Fei, 2011; Melaas, Friedl, & Zhu, 2013), it is often unclear if the climatic/genetic drivers of phenology are consistent across scales, or if insights from one scale can be used to inform the understanding of phenology at other scales. Linking understandings that span scales has been an elusive but central goal to understanding phenological shifts.

In this paper, we attempt to bridge scales by using observations of phenology across multiple common gardens to predict phenology observed on the landscape using remote sensing. Using balsam poplar (*Populus balsamifera*) as a case study, we modelled phenology in common gardens using genotypic, and genotype × environment information and then combined this genomic prediction with a variety of meteorological metrics to model phenology on the landscape across nearly the entire range of balsam poplar. Using this approach, we addressed multiple questions: (i) do

phenology metrics observed in common gardens match phenology measured on the landscape using remote sensing?, (ii) is accounting for genomics important in modelling land surface phenology?, and (iii) what is the importance of temperature and precipitation at various seasonal lags in driving phenology?

Materials and Methods

Common garden information and genomic prediction

To estimate the contribution of genetic variation to phenology measured on the landscape, we first fit a genomic model to phenology observations made in common gardens. We then used this model to predict phenology of genotyped individuals sampled throughout the range ("landscape samples" below), that were not observed in the common gardens. We used this genomic prediction, in concert with meteorological variables, to predict land surface phenology derived from remote sensing. Using this approach, we sought to determine the extent to which common garden observations of phenology could be used to predict landscape metrics of phenology, and to determine the relative importance of genomic and meteorological variables to land surface phenology.

We used phenology observations of bud flush from three common gardens to train genomic models. Bud flush observations were made in Fairbanks, Alaska (in 2010), Indian Head, Saskatchewan (2010, 2015) (Olson et al., 2013), and in Burlington, Vermont (2015, 2016, 2017), on 869 individual plants whose origins

spanned the entire range of balsam poplar. Bud flush observations across the six garden-years were made two or three times a week during the beginning of the growing season. Observations from Fairbanks and Indian Head (2010) are previously reported in Olson et al. (2013).

To produce the genomic predictions of phenology, we fit mixed effects models where cumulative growing degree days (cGDD) before spring bud flush (of individuals in the common gardens) was used as the response, and individual genotype were included as random effects. Genomic prediction models were fit using the Bayesian approach implemented in the BGGE package (Granato et al., 2018). For model training, we used 2061 bud flush observations for 869 individuals across all six garden-years, as well as genotypic data for each individual at 291 single nucleotide polymorphisms (SNPs). These 291 SNPs were derived from re-sequencing 27 candidate genes in the *Populus* flowering time (FT) pathway (Keller, Levsen, Olson, & Tiffin, 2012; Olson et al., 2013; Palacio-Lopez, Keller, & Molofsky, 2018). We compared three multi-environment genomic prediction models (multi-environment main genotypic effect model, MM; multi-environment single variance genotype x environment deviation model, MDs; and multi-environment, environment-specific variance genotype x environment deviation model, MDe) and an additional set of models with a random intercept of genotype-specific reaction norms (MMl, MDsl and MDel) (Cuevas et al., 2018; Granato et al., 2018; Sousa et al., 2017). We compared models fit with two different covariance functions (i.e., genomic best linear unbiased prediction (GBLUP) and non-linear Gaussian kernel).

To assess model accuracy, we performed a bootstrap analysis where 80% of individuals were used to train the models, and 20% were used to test models. We ran this bootstrap analysis for 1000 iterations for each model and compared the resulting distributions of R^2 values for the linear relationship between observed and predicted cGDD of individuals withheld for testing. In this initial testing, the MDs model fit using a Gaussian kernel was the best, as it produced predictions of cGDD that were closest to common garden observations. For this reason, we used the MDs to generate predictions of cGDD to bud flush for 1478 genotypes collected throughout the range of balsam poplar. All 1478 landscape samples had been genotyped at a set of 198,859 genome-wide SNPs, but only 460 of these individuals had been genotyped at the 291 FT pathway SNPs used to train the model. Therefore, we used the program Beagle (Version 4.1) to phase haplotypes for these 460 individuals and then to impute genotypes at the FT pathway SNPs for the remaining 1018 landscape samples using the phased haplotypes as a reference (B. L. Browning & Browning, 2016; S. R. Browning & Browning, 2007). We then used the MDs genomic prediction model to predict cGDD to bud flush for all 1478 landscape samples.

For each landscape sample, the genomic model generated six predictions of cGDD, one for each of the six garden-years used to train the model. Because we sought to use just one genomic prediction per individual per year in the landscape model, we took a weighted mean of the six genomic predictions, where weights were based on how meteorologically-similar sample sites on the landscape were to the common gardens in years phenology observations were made. To calculate weights,

we first conducted a principal components analysis (PCA) on meteorological variables (seasonal temperature and precipitation, winter snow water equivalent, elevation, cumulative chilling days, and rate of cGDD increase, described below) at all landscape sample sites in all years. Next, we projected the same meteorological variables from garden-years into the same PCA space and calculated a multidimensional Euclidean distance between garden-years and sample sites, which served as our measure of meteorological similarity between each site and the gardens. We used the first nine axes of the PCA to calculate the distance as these captured >95% of the total variation. The inverse of Euclidean distances were used as weights in the weighted mean. Ultimately this process helped ensure that the genomic prediction was representative of the similarity between weather at the common gardens and at sample sites on the landscape.

Land surface phenology

To quantify land surface phenology, we applied the approach described by Elmore et al. (2012) to 250m-resolution remote sensing data from the Moderate Resolution Imaging Spectroradiometer (MODIS). Briefly, this involved fitting a seven parameter dual logistic curve to normalized difference vegetation index (NDVI) extracted at forested MODIS pixels around each of our landscape sample points. Relevant NDVI observations were identified by searching increasing focal distances from the sample location for forested pixels until at least three were

identified. Forest pixels were defined using the 2010 land cover map generated by the North American Land Change Monitoring System (Latifovic et al., 2016). Limiting phenology model-fitting to NDVI extracted at forested pixels has been shown to improve the relationship between satellite-derived phenology and ground observations of phenology of forest trees (Elmore, Stylinski, & Pradhan, 2016). The seven parameter model is defined as:

$$NDVI_t = m_1 + (m_2 - m_7 \cdot t) \cdot \left(\frac{1}{1+ e^{(m_3 - t)/ m_4}} - \frac{1}{1+ e^{(m_5 - t)/ m_6}}\right), \quad \text{Eq. 5.1}$$

where $NDVI_t$ is NDVI on day of year t, m_1 is the baseline NDVI during the winter, m_2 is the difference between the spring and winter NDVI, m_3 and m_4 control the shape of the spring logistic curve, m_5 and m_6 control the shape of the autumn logistic curve, and m_7 controls the slope of the curve during the summer (Elmore et al., 2012). We fit the phenology model to MODIS data from 2000 to 2016.

We used both the m_3 parameter (i.e., date of spring onset, 'DOY' below) and the number of growing degree days (cGDD) accumulated to DOY as phenology metrics. While the m_3 parameter is expected to vary year to year within a site, cGDD should exhibit less interannual variation as it represents the heat sum required for leaf emergence. cGDD is often recommended as a more biologically meaningful phenology metric compared to phenology metrics referenced to a DOY, including for satellite-derived phenology (de Beurs & Henebry, 2010). cGDD was calculated as the

cumulative average temperature of days with an average temperature above 0℃. cGDD was calculated from the Jan. 1 until the date of m_3. cGDD was calculated from daily temperature data from the Daymet dataset (see below; Thornton et al., 2017).

Because phenology metrics from MODIS represent an aggregate signal of all plants within a pixel, we transformed phenology metrics to better represent balsam poplar phenology. To do so, we used ground observations of balsam poplar phenology to model the relationship between balsam poplar phenology and the m_3 parameter, and used the regression equation to transform m_3 at all sample sites to represent balsam poplar. Ground observations of balsam poplar leaf emergence were downloaded from the National Phenology Network. We filtered the phenology data using similar approaches described by Elmore et al. (2016), where observations that were not preceded by observation within 7 days were removed (to ensure trees were being monitored regularly), as were out-of-season observations, i.e., if leaf emergence was observed before day-of-year 60 or after 180. Filtering citizen science data in this way has been shown to improve the relationship between ground observations (NPN) and MODIS-derived phenology. We then quantified the relationship between NPN observations of leaf emergence (n=18) and MODIS phenology using linear regression. Finally, we used the regression equation to transform the m_3 parameter to represent balsam poplar at all sample sites. After transforming MODIS spring onset date, we recalculated cGDD to the transformed date, and used this as a response in our models. Because this was a simple linear transformation of DOY, it does not

affect subsequent models of DOY, but cGDD will shift by the number of growing degree days accumulated between the transformed and untransformed DOY.

Meteorological variables

We calculated 12 meteorological variables to model phenology on the landscape. These included seasonal mean temperatures, sum of seasonal precipitation, the rate of cGDD increase, cumulative chilling degree days (cCDD), elevation, and winter snow water equivalent. Each of these variables were calculated from daily meteorological data from the Daymet database (Thornton et al., 2017). Daymet contains interpolated daily minimum/maximum temperature, precipitation, and snow water equivalent, among other variables, for all of North America at 1 km x 1 km spatial resolution. We accessed the Daymet database using the R package DAYMETR, to batch download daily weather data for all sample locations (Hufkens, Basler, Milliman, Melaas, & Richardson, 2018).

Mean temperature and precipitation sums were calculated over meteorological seasons (three month periods, where the month of the solstice or equinox is included as the starting month of the season), the year preceding leaf emergence. Mean seasonal temperature was calculated as the mean daily temperature ($(T_{max} + T_{min})/ 2$), while precipitation was summed over the entire season. The rate of cGDD increase was calculated from Jan. 1 (the same starting time as cGDD used in predictions) through the end of spring. The rate was calculated by fitting an exponential curve to cGDD over time:

$$cGDD = \exp(a + bt) \quad , \qquad \text{Eq. 5.2}$$

where *t* is day of year, using an iterative nonlinear least-squares algorithm. We used the estimated '*b*' coefficient as an estimate of how fast growing degree days accumulated the year cGDD was calculated.

Chilling was calculated following Kramer (1994). Unlike cGDD, cumulative chilling degree days (cCDD) accumulates individual days (or portion of days) rather than degrees, in relation to how close the average temperature is to the 'optimum':

$$D_{chil} = \begin{cases} 0 & T \leq T_{min} \\ \dfrac{T - T_{min}}{T_{opt} - T_{min}} & T_{min} < T \leq T_{opt} \\ \dfrac{T - T_{max}}{T_{opt} - T_{max}} & T_{opt} < T < T_{max} \\ 0 & T \geq T_{max} \end{cases} \quad , \qquad \text{Eq. 5.3}$$

where D_{chil} is the number of chilling days accumulated in a single day, T_{min} is -3.4, T_{max} is 10.4, and T_{opt} is 3.5. Accumulated chilling days was calculated at the cumulative sum of D_{chil} over the autumn and winter the year before cGDD was observed. Average winter snow equivalent was calculated as the average snow-water equivalent during the winter, with units of kg/m^2.

Moran eigenvector maps

Because sampling sites were non-randomly distributed across the range of balsam poplar, and residuals of non-spatial models tended to be spatially autocorrelated, we used Moran Eigenvector Maps (MEMs) to account for residual spatial variation (Legendre & Legendre, 1998). MEM analysis decomposes a spatial distance matrix into orthogonal eigenfunctions, which can be used as predictors in models. We used the first 10 eigenvectors with positive eigenvalues (which represent positive spatial autocorrelation) as predictors in the models. We used the maximum distance of a minimum spanning tree to define the spatial network.

Statistical models

We used random forest to create two models, one using DOY as the response variable, and another using cGDD as the response. In both models, we used the same meteorological variables, the genomic prediction, and MEMs as predictors. Random forest is a non-parametric, machine learning algorithm that builds many regression trees using random subsets of the training data. We used 1000 trees in the forest, and implemented the model with the RANGER package (Wright & Ziegler, 2017). We quantified the importance of each variable in the model by assessing the increase in mean square error when variables were permuted. A large increase in mean square error indicates larger importance of a particular variable in the model compared to a

permuted variable resulting in a small increase in error. We also assessed the relationship between phenology metrics (DOY and cGDD) and predictor variables using partial dependence plots (Greenwell, 2017), which help to visualize the marginal effects of each predictor variable on the response. We tested for spatial autocorrelation in the model residuals for each year using correlograms in the NCF package (Bjornstad, 2018).

Residual variation

To test how well the model could predict observations withheld from model calibration, we used a variation of 'leave-one-out' cross validation. Rather than omitting single data points, we left out individual years, and individual cells of a spatial grid overlaying the sample sites. To test temporal predictions, we omitted all observations for a given year and tested how well the model could predict cGDD and DOY in the omitted year. To test the spatial predictions, we overlaid a 5^{o} x 5^{o} grid on the landscape, and then built the model using all but one grid cell. We then tested how well the model could predict DOY and cGDD in the omitted grid cell. This spatial and temporal leave-one-out procedure tests whether the signal in the data is robust enough to predict observations withheld during calibration, and implicitly tests the spatial and temporal autocorrelation in the data. We used root mean square error (RMSE) to quantify residual model error. In a further attempt to understand model performance, we tested whether RMSE in withheld years was correlated with any of the meteorological variables we used in our models.

Results

Relationship between NPN and MODIS spring onset

The relationship between NPN observations of balsam poplar leaf emergence and MODIS-derived spring onset was moderately strong ($r = 0.56$, $p = 0.01$). On average, ground observations of balsam poplar phenology occurred after the MODIS spring onset, although the regression line converged with the 1:1 line at later phenological dates (i.e., there were greater differences between MODIS spring onset and NPN observations at earlier phenological dates). We used the following regression equation to transform MODIS phenology to better represent ground observations of balsam poplar: $y = 44.7961 + 0.6825 * m_3$. On average, this resulted in a 3.8 day shift in m_3 across all samples and years.

General patterns of DOY and cGDD

In general, across years, DOY (i.e., the day greenness increased most rapidly, quantified by the m_3 model coefficient of the phenology model, Eq. 5.1) was consistently later at higher latitudes and higher elevations compared to lower latitudes/elevations. The relationship between cGDD and latitude/elevation, however, was more complex. In most years, cGDD declined with latitude - indicating that sites at higher latitudes required fewer GDD to reach the date of spring onset than did sites

at lower latitudes. In 2016, however, the trend was weakly positive ($r = 0.08$, $p = 0.01$). The relationship between cGDD and elevation was more variable - the relationship was negative in five years (2000, 2002, 2008, 2010, 2011) and positive in the remaining years (2001, 2003 - 2007, 2009, 2012 - 2016).

Variable importance and directionality

Random forest models for DOY and cGDD both showed a very strong ability to explain out-of-bag variation (i.e., data withheld during construction of individual trees within the forest; out-of-bag $R^2 = 0.99, 0.93$, respectively). The most important variables to DOY and cGDD, however, were considerably different. For DOY, the genomic prediction was the most important variable, followed by fall temperature, elevation, the rate of cGDD increase, and summer temperature (Fig. 5.1a). Precipitation variables tended to have low importance, although spring precipitation was the sixth most important variable explaining DOY. In general, seasonal temperature variables had a negative relationship with DOY - indicating that, as expected, cooler sites tended to have a later spring onset than warmer sites (Fig. 5.S1). Interestingly, the relationship between DOY and precipitation switched during the course of the previous season - specifically, spring and summer precipitation had a negative relationship with DOY, while fall and winter precipitation had positive relationships. MEMs tended to have relatively high importance in explaining DOY, with many MEMs outranking the top meteorological variables.

Across all 24 predictor variables, the most important variable explaining cGDD was year, followed closely by the rate of GDD increase (Fig. 5.1b). While the relationship between cGDD and year was non-monotonic (i.e., varied year to year), the relationship with rate of GDD increase was clearly negative (Fig. 5.S2). A negative relationship between cGDD and rate of GDD increase indicates that sites that accumulate GDD more slowly tend to accumulate more overall growing degree days than sites that accumulate GDD more rapidly. Precipitation variables also tended to be important in explaining cGDD, with summer, fall, and winter precipitation representing three of the top five variables. Temperature variables tended to be lower ranked, as were the genomic prediction and elevation. In contrast to variable importance for DOY, the MEMs tended to have low importance. In general, the relationship between cGDD and meteorological variables tended to be in the opposite direction of the relationship with DOY. For instance, seasonal temperature variables tended to have positive relationships with cGDD, while temperature was negatively related to DOY.

Residual variation

Models of both DOY and cGDD showed similar abilities to predict variation across space and time. In general, when individual 5^{o} grid cells were omitted from model training, RMSE tended to be highest in high elevation areas in the Rocky Mountains, and in the northern parts of the range in Alaska (Fig. 5.2) regardless of the response variable. This is likely due to high variability in DOY/cGDD over short

distances, which the models failed to predict when similar observations were withheld during model training. RMSE tended to be lowest in grid cells in the center of the range in the Great Lakes region, which had the greatest density of samples, and highest in topographically variable areas.

There were no clear temporal trends in residual error when individual years were omitted from model training, although models of both DOY and cGDD had local peaks of RMSE in 2002 and 2010 indicating models did relatively poorly predicting phenology in these years when they were omitted from training (Fig. 5.3). Models for DOY also had a peak in RMSE in 2015. RMSE of omitted years was correlated with numerous meteorological variables. RMSE of cGDD and DOY were both negatively correlated with winter precipitation and snow - indicating greater error in years with less snow. Even more revealing, RMSE of cGDD was positively correlated with winter temperature ($r = 0.543$, $p = 0.02$), suggesting greater error following warmer winters (Fig. 5.4).

Pattern in residuals

Within individual years, residual spatial autocorrelation for both DOY and cGDD tended to be low, suggesting much of the spatial variation was being accounted for in the full model. When random forest models were fit to residuals (as opposed to phenology metrics), there were few clearly important variables. For residuals of both cGDD and DOY, year was notably more important than other

variables, potentially indicating the importance of other variables that vary year-to-year, but not accounted for amongst our predictors. The rate of growing degree day increase was also important in explaining the residuals of DOY.

Discussion

Our approach shows that fine-scale, precise measures of phenology gathered from multiple common gardens in multiple years can be combined with genomic information to inform land surface phenology. When combined with meteorological information from the year preceding bud flush, much of the spatial and temporal variability in DOY and cGDD could be explained, signifying both the importance of pre-season weather to phenology and the contribution of genetic variability. This work provides a framework for linking precise phenotypic trait measurements in common gardens to landscape-scale patterns.

Use of common garden information and genomic prediction

The genomic prediction varied in its ability to explain cGDD and DOY. Curiously, the genomic prediction of cGDD was more important in explaining landscape DOY than cGDD. This is especially peculiar as the genomic prediction and cGDD were in the same units, and calculated from the same meteorological data set. There are multiple reasons why cGDD modelled from common garden data may have been a better predictor of DOY than cGDD. First, DOY on the landscape reflects the

combined effect of photoperiod and thermal forcing. Although we did not account for photoperiod in our model, recent studies have found photoperiod to be important to phenology of many tree species (e.g., Flynn & Wolkovich, 2018).If the genomic prediction also captured the effects of photoperiod (i.e., by accounting for GxE effects across the multiple gardens) it could have a better relationship with DOY than cGDD. cGDD on the landscape may also be affected by an interaction with photoperiod (Fu et al., 2019; Zohner & Renner, 2015) but this was not directly accounted for in our models, which may be contributing a mismatch between cGDD on the landscape and the genomic prediction. Both landscape cGDD and the genomic prediction were negatively correlated with DOY, suggesting both have similar broad-scale trends with DOY, but are only weakly correlated with one another ($r = 0.06$, $p < 0.01$). This suggests there may be additional factors affecting cGDD either in the gardens or on the landscape that is not fully being accounted for in our models.

Perhaps the most obvious explanation for a lack of correlation between the genomic prediction and cGDD was that cGDD on the landscape is estimated using remote sensing of forest stands and therefore was not strictly representative of balsam poplar. Although we applied a transformation to DOY (and by extension cGDD) to better represent balsam poplar, the resolution of MODIS pixels necessarily meant that the phenology signal represents a mixture of numerous plant species and vegetation types. Variability in balsam poplar abundance and plant community composition across the range likely alters the relative contribution of balsam poplar to the MODIS phenology signal. Furthermore, the actual phenological stage that was measured

differed in the common garden and on the landscape. In the common gardens, observations were made of bud flush of individual plants, while on the landscape the phenology metric was the date greenness increased most rapidly. While previous studies would suggest remote sensing metrics and ground measures of phenology of individual plants are correlated (Elmore et al., 2016; Fisher & Mustard, 2007; Liang et al., 2011), it is unclear whether cGDD scales in a similar way. We attempted to address the fact that balsam poplar bud flush likely occurred before the date of greenness increase by using an earlier, alternative satellite-derived phenology metric (i.e., 'onset of greenness increase' - the date greenness just begins to increase within a pixel), but this date often occurred before any growing degree days had accumulated on the landscape. This further illustrates that even after transforming the MODIS-derived phenology metrics to better represent balsam poplar, the satellite-derived metrics remain an aggregate signal that may not be entirely representative of balsam poplar.

Our results also indicated that landscape cGDD was strongly influenced by the rate at which GDDs accumulated. If this is also true at local scales, cGDD in the garden and on the landscape could become decoupled if GDD accumulated more rapidly (or slowly) in the common gardens than on the landscape. For instance, if cGDD accumulated rapidly in a year phenology observations were made in a garden (i.e., years GP models were trained), it could effectively eliminate the differences between genotypes if all genotypes reached their thermal requirements within several days. Of the six common garden-years, three had increase rates faster or slower than

~90% of all increase rates (i.e., were in the 0.11, 0.10 and 0.93 quantiles of an empirical distribution of all increase rates). The discrepancy between the rate of increase in the garden versus that on the landscape could have contributed to the lack of a relationship between cGDD in the garden and on the landscape, resulting in low importance of the genomic prediction to cGDD.

Importance of temperature and precipitation

The importance of temperature to both cGDD and DOY largely matched previous studies. DOY tended to be earlier in warmer sites, while a greater number of GDD accumulated in warmer sites. Earlier DOY at warmer sites is likely due to plants accumulating their cooling and heat requirements earlier in the season, allowing buds to flush earlier and make use of a longer growing season (Zhang, Friedl, Schaaf, & Strahler, 2004). Conversely, we found that warmer sites also tended to accumulate more GDD than cooler sites - in other words, trees in warmer sites needed more GDD to flush buds than trees in cooler sites. This was apparent in the decline of cGDD with latitude, which was interrupted only by sites in mid-latitude, high elevation areas. Similar relationships have been observed at both satellite and local plant population scales (Fu, Piao, et al., 2014). The positive relationship between cGDD and temperature is likely due to plants in cooler regions having lower heat requirements than those in warmer, southern locations. In cool climates, lower heat requirements are likely an adaptation to cooler springs which may not accumulate as many GDD as lower latitude, warmer springs. A shorter growing

season at high latitudes/elevations likely also contributes to plants at high latitude/elevation sites requiring fewer GDD to flush buds. The latitudinal gradient in landscape cGDD largely matched previous common garden studies of balsam poplar that have shown genotypes from high latitudes tended to require fewer GDD than lower latitude genotypes to flush buds (Olson et al., 2013).

While the relationship between cGDD and temperature was expected based on previous studies, the importance of precipitation to cGDD was somewhat surprising as precipitation is rarely considered an important driver of phenology in non-water limited climates (Polgar & Primack, 2011). Several studies, however, have reported similar relationships between precipitation and cGDD. Yun et al. (2018), using satellite imagery, found winter precipitation to be a major driver of cGDD in Northern Hemisphere boreal forests. They suggest that in years or sites with heavy snowfall, snow may persist longer into the spring, reducing spring temperatures (due to increased albedo effects and decreased absorption of solar radiation), which slows the accumulation of GDD before bud flush in the spring. This is consistent with the possibility of cooler winter temperatures reducing thermal requirements (Fu et al., 2015), and which we also detected in our data ($r = 0.585$, $p < 0.01$). It is worth noting that others have found the opposite relationship between cGDD and the previous winter's precipitation. Fu et al. (2014), also using satellite imagery, found a positive relationship between winter precipitation and cGDD in northern portions of the Northern Hemisphere. They suggest the positive relationship between cGDD and

snow may be due to GDD accumulating before snow has melted and begins contributing to plant's thermal requirements.

Residual model variation

Although models did well overall in predicting cGDD and DOY in years and areas that were omitted from model training, RMSE was correlated with numerous meteorological variables. Perhaps most noteworthy was the positive relationship between winter temperature and RMSE, which suggests that, on average, models do more poorly when predicting phenology following warmer winters. In boreal regions, such as those occupied by balsam poplar, winter temperatures are expected to increase in coming decades - raising concerns about our ability to reliably predict phenology in future climates. Although we do not know the specific mechanism behind the increasing error following warmer winters, there are multiple possibilities. One possibility is that during warm winters, trees fail to reach their chilling requirements, which may alter the thermal requirements for bud flush the following year. Numerous studies, for instance, have suggested that additional GDD can compensate for a lack of winter chilling in trees (Fu, Campioli, Deckmyn, & Janssens, 2013; Guo et al., 2014; Murray, Cannell, & Smith, 1989). If the roles of meteorological variables are non-stationary over space or time (e.g., if chilling plays a greater or lesser role to different genotypes, regions or years) residual error could be correlated along meteorological gradients. Effect of non-stationary meteorological variables could also partially explain the annual variability of cGDD requirements

within sites, which, for numerous tree species, has been reported to have increased over time (Fu et al., 2015), presumably due to reducing chilling. Alternatively, cGDD or DOY can be affected by an interaction between winter temperature and photoperiod. Following cool winters, photoperiod can have a larger influence on leaf emergence than during warmer winters and not directly accounting for photoperiod could obscure this relationship. Ultimately, the finding of a relationship between meteorological variables and model residuals raises concerns about our ability to accurately forecast phenological responses based on a current understanding of the drivers of phenology (Carter et al., 2017; Isabelle Chuine et al., 2016), and highlights the complexity in predicting phenological shifts.

Conclusions

In this study, we tested the relative importance of temperature, precipitation, and genetic variation to predicting multiple metrics of phenology on the landscape. We found the genomic prediction to be amongst the most important variables explaining day-of-year on the landscape, but was not important in explaining cGDD. While models did well predicting phenology withheld from model training, error was correlated with multiple meteorological variables, illustrating the challenges of predicting phenological responses in shifting climates.

Figures

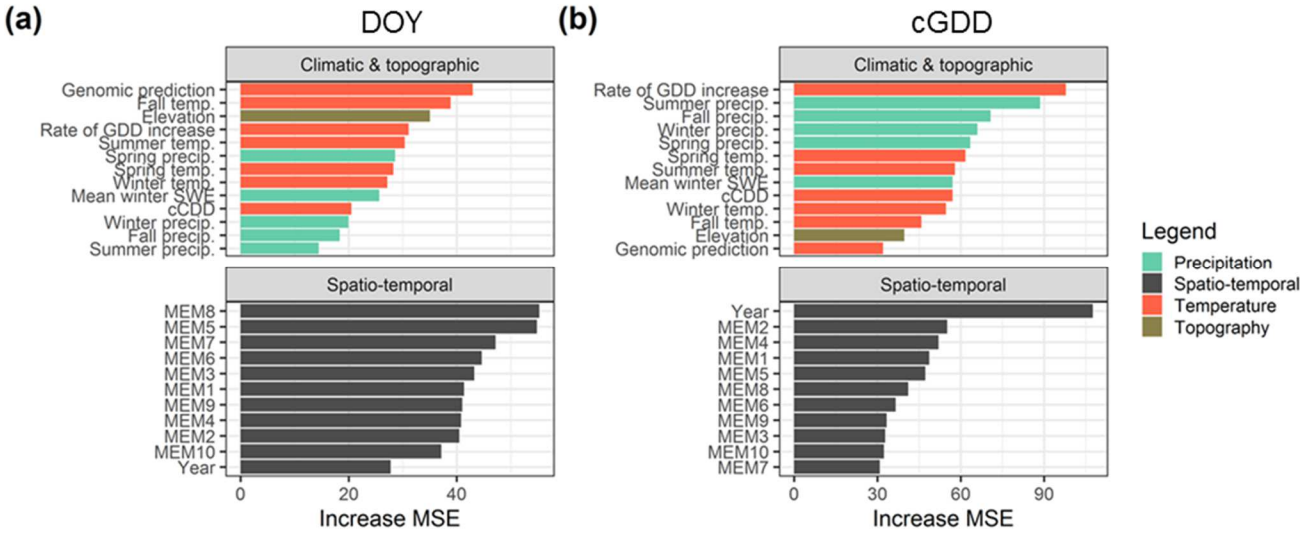

Fig. 5.1. Variable importance (increase in mean square error) from random forest models for (a) day of year (DOY), and (b) cumulative growing degree days (cGDD). MEMs are Moran Eigenvector Maps.

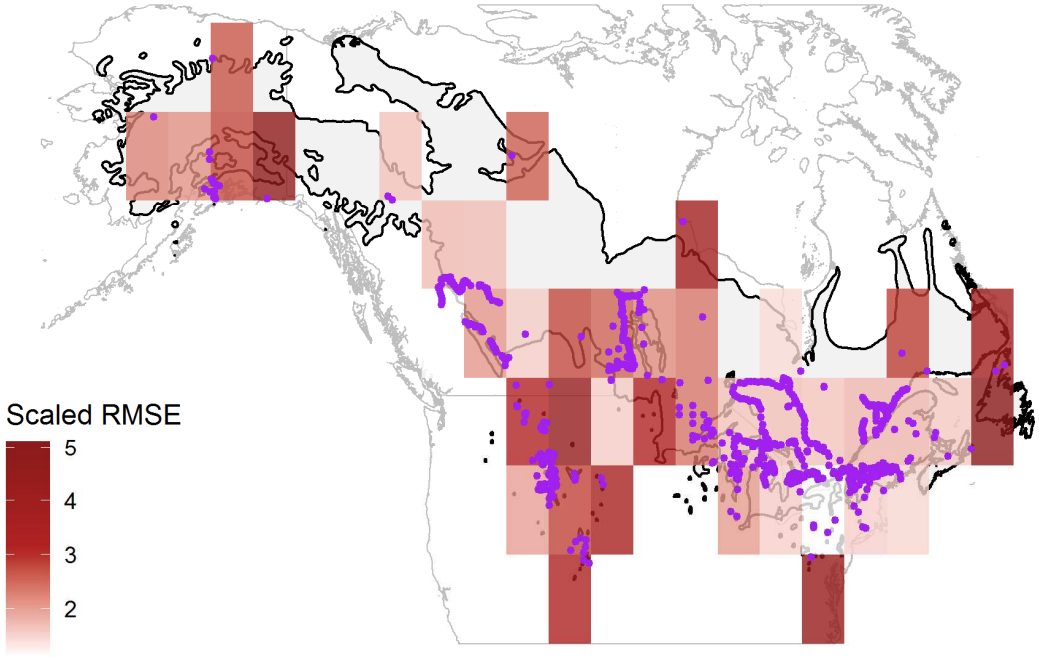

Fig. 5.2. Scaled root mean square error for models of cumulative growing degree days when points from individual cells are left out of model training. The polygon is balsam poplar's range, and purple points are the location of landscape samples.

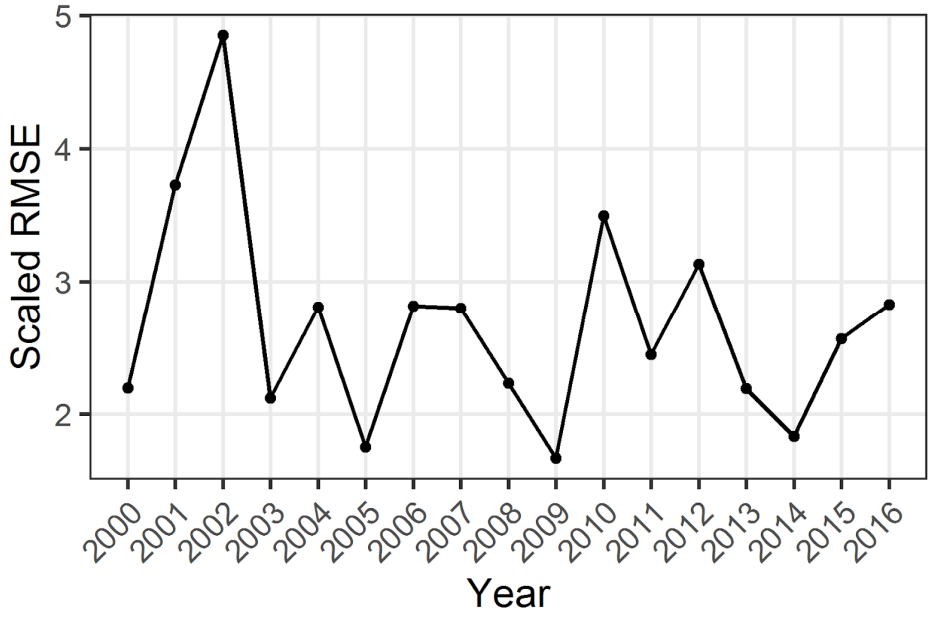

Fig. 5.3. Scaled root mean square error of cumulative growing degree days when data from individual years were withheld from model training.

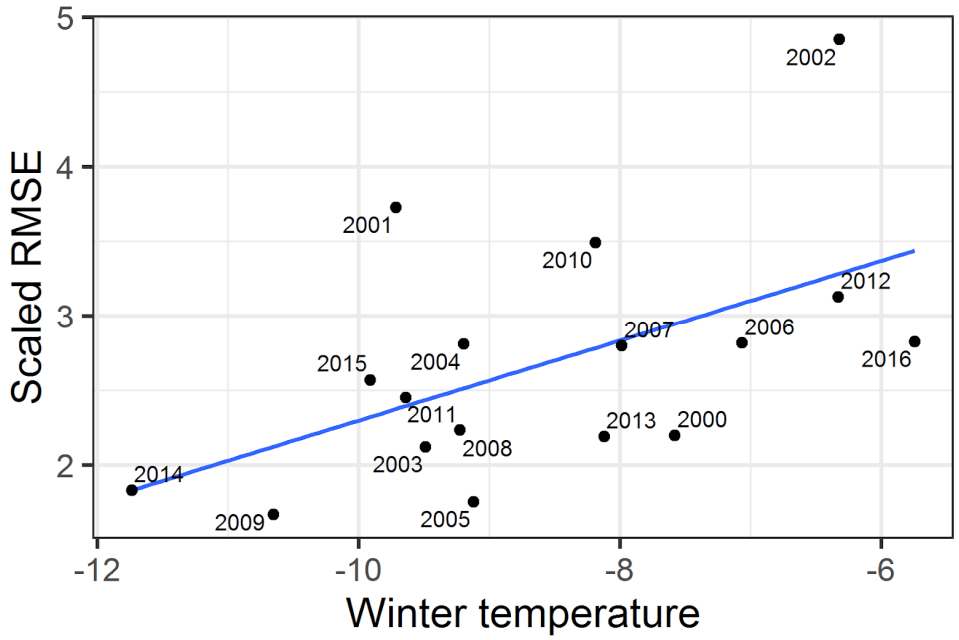

Fig. 5.4. Relationship between scaled root mean square error for cumulative growing degree days (cGDD) and average winter temperatures. In general, models have greater error predicting cGDD following warmer winters.

Supplemental figures

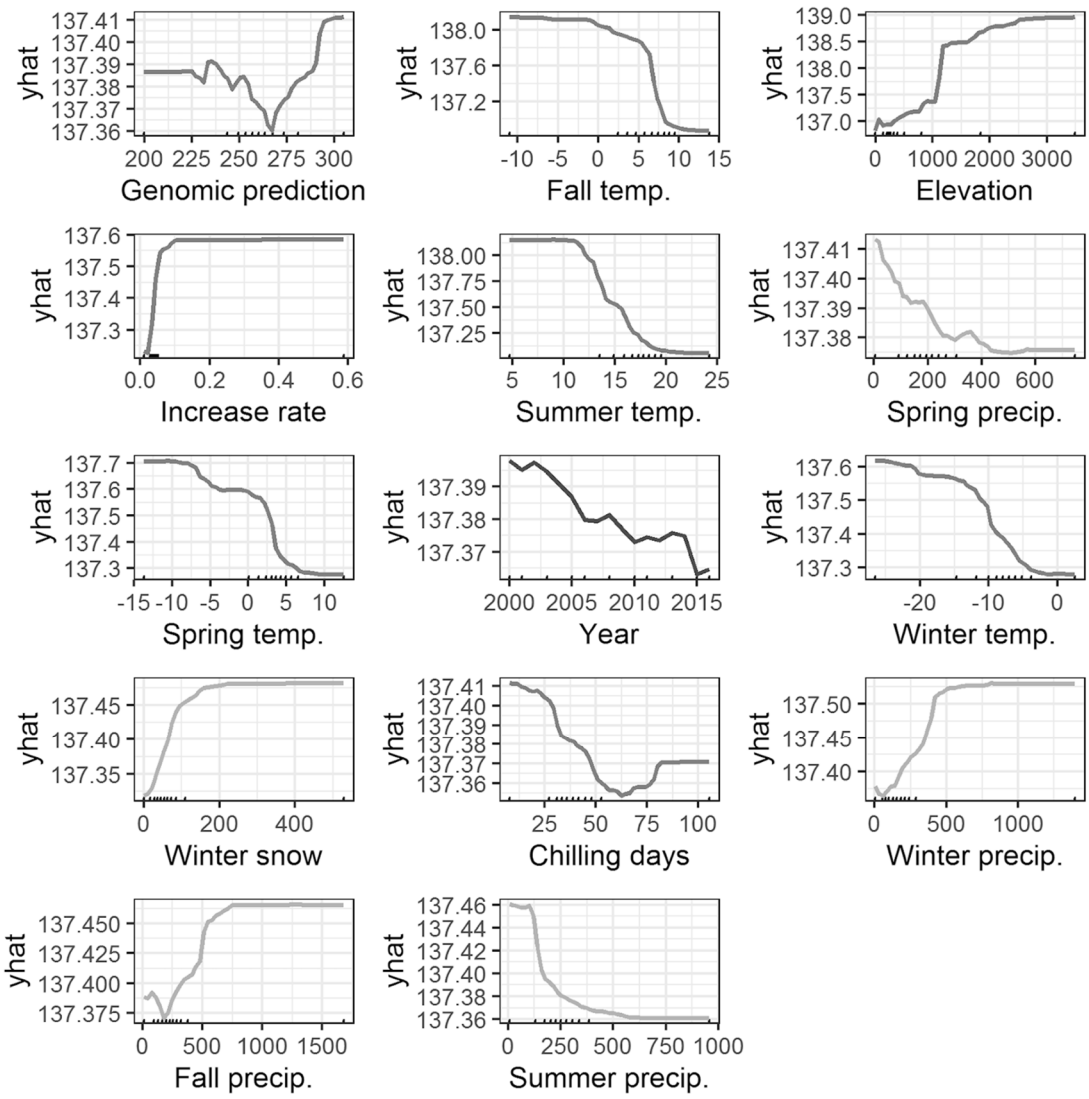

Fig. 5.S1. Partial dependence plots for variables in the random forest model for day of year. Plots are in order of variable importance (**Fig. 5.1a**).

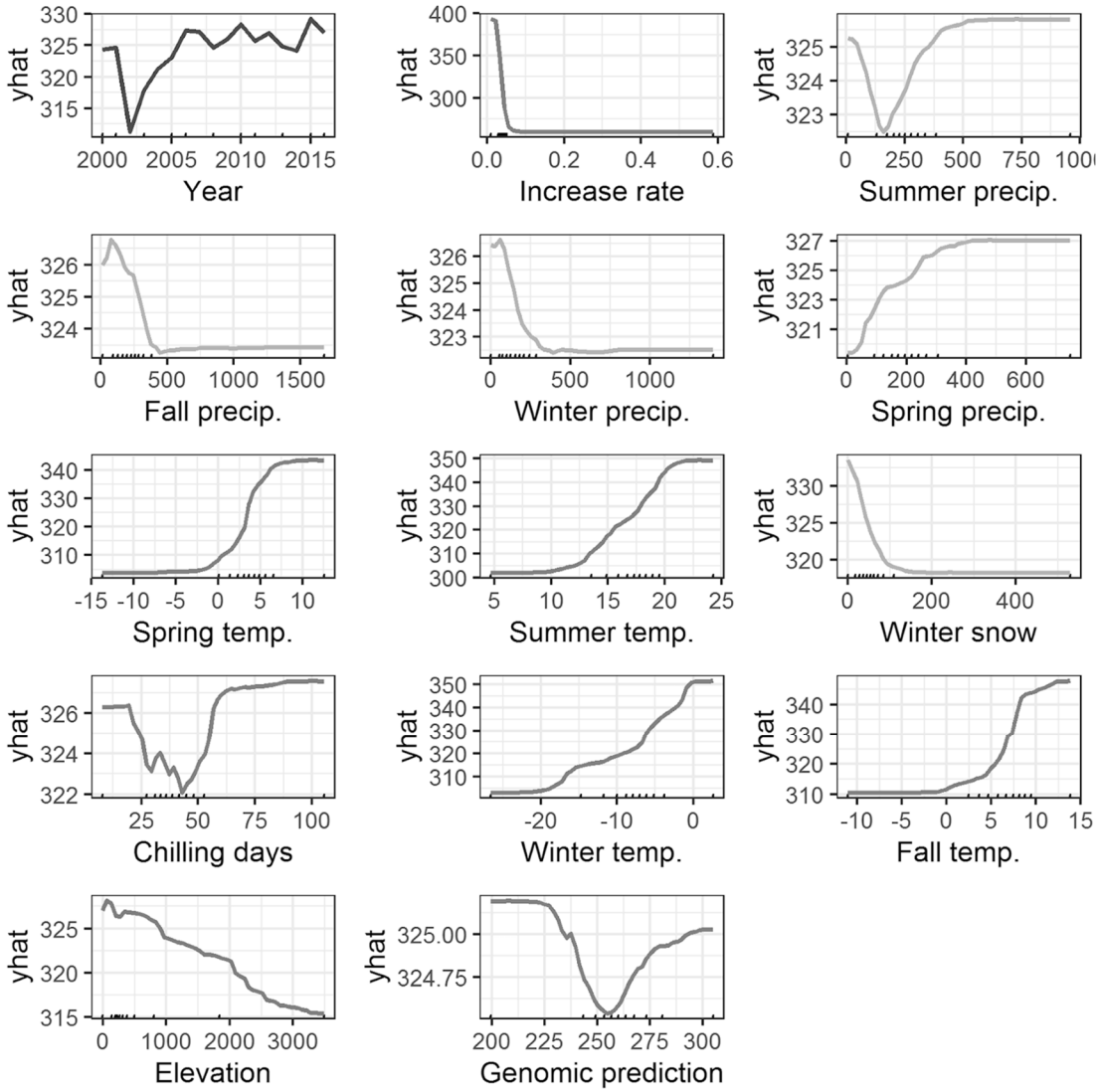

Fig. 5.S2. Partial dependence plots for variables in the random forest model for cumulative growing degree days. Plots are in order of variable importance (**Fig. 5.1b**).

Bibliography

Ahas, R., Aasa, A., Menzel, A., Fedotova, V. G., & Scheifinger, H. (2002). Changes in European spring phenology. *International Journal of Climatology*, *22*(14), 1727–1738. https://doi.org/10.1002/joc.818

Aitken, S. N., Yeaman, S., Holliday, J. A., Wang, T., & Curtis-McLane, S. (2008). Adaptation, migration or extirpation: climate change outcomes for tree populations. *Evolutionary Applications*, *1*(1), 95–111. https://doi.org/10.1111/j.1752-4571.2007.00013.x

Alberto, F. J., Aitken, S. N., Alía, R., González-Martínez, S. C., Hänninen, H., Kremer, A., … Savolainen, O. (2013). Potential for evolutionary responses to climate change - evidence from tree populations. *Global Change Biology*, *19*(6), 1645–1661. https://doi.org/10.1111/gcb.12181

Alexander, D. H., Novembre, J., & Lange, K. (2009). Fast model-based estimation of ancestry in unrelated individuals. *Genome Research*, *19*, 1655–1664. https://doi.org/10.1101/gr.094052.109

Allouche, O., Tsoar, A., & Kadmon, R. (2006). Assessing the accuracy of species distribution models: prevalence, kappa and the true skill statistic (TSS): Assessing the accuracy of distribution models. *Journal of Applied Ecology*, *43*(6), 1223–1232. https://doi.org/10.1111/j.1365-2664.2006.01214.x

Alsos, I. G., Ehrich, D., Thuiller, W., Eidesen, P. B., Tribsch, A., Schonswetter, P., … Brochmann, C. (2012). Genetic consequences of climate change for northern

plants. *Proceedings of the Royal Society B: Biological Sciences*, *279*(1735), 2042–2051. https://doi.org/10.1098/rspb.2011.2363

Anderson, L. L., Hu, F. S., Nelson, D. M., Petit, R. J., & Paige, K. N. (2006). Ice-age endurance: DNA evidence of a white spruce refugium in Alaska. *Proceedings of the National Academy of Sciences*, *103*(33), 12447–12450.

Araújo, M. B., Anderson, R. P., Barbosa, A. M., Beale, C. M., Dormann, C. F., Early, R., … Rahbek, C. (2019). Standards for distribution models in biodiversity assessments. *Science Advances*, *5*(1), eaat4858. https://doi.org/10.1126/sciadv.aat4858

Atkins, K. E., & Travis, J. M. J. (2010). Local adaptation and the evolution of species' ranges under climate change. *Journal of Theoretical Biology*, *266*(3), 449–457. https://doi.org/10.1016/j.jtbi.2010.07.014

Barbet-Massin, M., Jiguet, F., Albert, C. H., & Thuiller, W. (2012). Selecting pseudo-absences for species distribution models: how, where and how many?: How to use pseudo-absences in niche modelling? *Methods in Ecology and Evolution*, *3*(2), 327–338. https://doi.org/10.1111/j.2041-210X.2011.00172.x

Bjornstad, O. N. (2018). ncf: Spatial Covariance Functions (Version 1.2-6). Retrieved from https://CRAN.R-project.org/package=ncf

Bonan, G. B. (2008). Forests and climate change: forcings, feedbacks, and the climate benefits of forests. *Science*, *320*(5882), 1444–1449.

Breen, A. L., Murray, D. F., & Olson, M. S. (2012). Genetic consequences of glacial survival: the late Quaternary history of balsam poplar (*Populus balsamifera*

L.) in North America: Genetic consequences of glacial survival. *Journal of Biogeography*, *39*(5), 918–928. https://doi.org/10.1111/j.1365-2699.2011.02657.x

Bridle, J. R., & Vines, T. H. (2007). Limits to evolution at range margins: when and why does adaptation fail? *Trends in Ecology & Evolution*, *22*(3), 140–147. https://doi.org/10.1016/j.tree.2006.11.002

Brown, J. H. (1984). On the relationship between abundance and distribution of species. *The American Naturalist*, *124*(2), 255–279.

Browning, B. L., & Browning, S. R. (2016). Genotype imputation with millions of reference samples. *The American Journal of Human Genetics*, *98*(1), 116–126. https://doi.org/10.1016/j.ajhg.2015.11.020

Browning, S. R., & Browning, B. L. (2007). Rapid and accurate haplotype phasing and missing-data inference for whole-genome association studies by use of localized haplotype clustering. *The American Journal of Human Genetics*, *81*(5), 1084–1097. https://doi.org/10.1086/521987

Brubaker, L. B., Anderson, P. M., Edwards, M. E., & Lozhkin, A. V. (2005). Beringia as a glacial refugium for boreal trees and shrubs: new perspectives from mapped pollen data. *Journal of Biogeography*, *32*(5), 833–848. https://doi.org/10.1111/j.1365-2699.2004.01203.x

Brubaker, L. B., Garfinkee, H. L., & Edwards, M. E. (1983). A late Wisconsin and Holocene vegetation history from the central brooks range: Implications for

Alaskan palaeoecology. *Quaternary Research*, *20*(2), 194–214. https://doi.org/10.1016/0033-5894(83)90077-7

Burgman, M. A., & Fox, J. C. (2003). Bias in species range estimates from minimum convex polygons: implications for conservation and options for improved planning. *Animal Conservation Forum*, *6*(1), 19–28. https://doi.org/10.1017/S1367943003003044

Callahan, C. M., Rowe, C. A., Ryel, R. J., Shaw, J. D., Madritch, M. D., & Mock, K. E. (2013). Continental-scale assessment of genetic diversity and population structure in quaking aspen (*Populus tremuloides*). *Journal of Biogeography*, *40*(9), 1780–1791. https://doi.org/10.1111/jbi.12115

Carnaval, A. C., Hickerson, M. J., Haddad, C. F. B., Rodrigues, M. T., & Moritz, C. (2009). Stability predicts genetic diversity in the Brazilian Atlantic forest hotspot. *Science*, *323*(5915), 785–789. https://doi.org/10.1126/science.1166955

Carroll, C., Parks, S. A., Dobrowski, S. Z., & Roberts, D. R. (2018). Climatic, topographic, and anthropogenic factors determine connectivity between current and future climate analogs in North America. *Global Change Biology*, *24*(11), 5318–5331. https://doi.org/10.1111/gcb.14373

Carter, J. M., Orive, M. E., Gerhart, L. M., Stern, J. H., Marchin, R. M., Nagel, J., & Ward, J. K. (2017). Warmest extreme year in U.S. history alters thermal requirements for tree phenology. *Oecologia*, *183*(4), 1197–1210. https://doi.org/10.1007/s00442-017-3838-z

Chen, I.-C., Hill, J. K., Ohlemuller, R., Roy, D. B., & Thomas, C. D. (2011). Rapid range shifts of species associated with high levels of climate warming. *Science*, *333*(6045), 1024–1026. https://doi.org/10.1126/science.1206432

Chhatre, V. E., Fetter, K. C., Gougherty, A. V., Fitzpatrick, M. C., Soolanayakanahally, R. Y., & Keller, S. R. (In prep.). Range-wide distribution of locally adaptive standing genetic variation in balsam poplar, *Populus balsamifera* L. *NA*.

Chuine, I., Belmonte, J., & Mignot, A. (2000). A modelling analysis of the genetic variation of phenology between tree populations. *Journal of Ecology*, *88*(4), 561–570. https://doi.org/10.1046/j.1365-2745.2000.00468.x

Chuine, Isabelle, Bonhomme, M., Legave, J.-M., Cortázar-Atauri, I. G. de, Charrier, G., Lacointe, A., & Améglio, T. (2016). Can phenological models predict tree phenology accurately in the future? The unrevealed hurdle of endodormancy break. *Global Change Biology*, *22*(10), 3444–3460. https://doi.org/10.1111/gcb.13383

Cleland, E., Chuine, I., Menzel, A., Mooney, H., & Schwartz, M. (2007). Shifting plant phenology in response to global change. *Trends in Ecology & Evolution*, *22*(7), 357–365. https://doi.org/10.1016/j.tree.2007.04.003

Cuevas, J., Granato, I., Fritsche-Neto, R., Montesinos-Lopez, O. A., Burgueño, J., Sousa, M. B. e, & Crossa, J. (2018). Genomic-enabled prediction kernel models with random intercepts for multi-environment trials. *G3: Genes, Genomes, Genetics*, *8*(4), 1347–1365. https://doi.org/10.1534/g3.117.300454

Cwynar, L. C., & Spear, R. W. (1991). Reversion of Forest to Tundra in the Central Yukon. *Ecology*, *72*(1), 202–212. https://doi.org/10.2307/1938915

Dallas, T., Decker, R. R., & Hastings, A. (2017). Species are not most abundant in the centre of their geographic range or climatic niche. *Ecology Letters*, *20*(12), 1526–1533. https://doi.org/10.1111/ele.12860

Davis, M. B., & Shaw, R. G. (2001). Range Shifts and Adaptive Responses to Quaternary Climate Change. *Science*, *292*(5517), 673–679. https://doi.org/10.1126/science.292.5517.673

de Beurs, K. M., & Henebry, G. M. (2010). Spatio-Temporal Statistical Methods for Modelling Land Surface Phenology. In I. L. Hudson & M. R. Keatley (Eds.), *Phenological Research: Methods for Environmental and Climate Change Analysis* (pp. 177–208). https://doi.org/10.1007/978-90-481-3335-2_9

Dormann, C., McPherson, J., Araújo, M., Bivand, R., Bolliger, J., Carl, G., … Wilson, R. (2007). Methods to account for spatial autocorrelation in the analysis of species distributional data: a review. *Ecography*, *30*(5), 609–628. https://doi.org/10.1111/j.2007.0906-7590.05171.x

Dyke, A. S., Moore, A., & Robertson, L. (2003). Deglaciation of North America. Thirty-two maps at 1:70000000 scale with accompanying digital chronological database and one poster (in two sheets) with full map series. *Geol. Surv. Can. Tech. Rep. Open File 1574.*

Eckert, C. G., Samis, K. E., & Lougheed, S. C. (2008). Genetic variation across species' geographical ranges: the central–marginal hypothesis and beyond.

Molecular Ecology, *17*(5), 1170–1188. https://doi.org/10.1111/j.1365-294X.2007.03659.x

Edwards, M. E., Anderson, P. M., Garfinkel, H. L., & Brubaker, L. B. (1985). Late Wisconsin and Holocene vegetational history of the Upper Koyukuk region, Brooks Range, AK. *Canadian Journal of Botany*, *63*(3), 616–626. https://doi.org/10.1139/b85-077

Elith, J., & Leathwick, J. R. (2009). Species Distribution Models: Ecological Explanation and Prediction Across Space and Time. *Annual Review of Ecology, Evolution, and Systematics*, *40*(1), 677–697. https://doi.org/10.1146/annurev.ecolsys.110308.120159

Elmore, A. J., Guinn, S. M., Minsley, B. J., & Richardson, A. D. (2012). Landscape controls on the timing of spring, autumn, and growing season length in mid-Atlantic forests. *Global Change Biology*, *18*(2), 656–674. https://doi.org/10.1111/j.1365-2486.2011.02521.x

Elmore, A. J., Stylinski, C., & Pradhan, K. (2016). Synergistic use of citizen science and remote sensing for continental-scale measurements of forest tree phenology. *Remote Sensing*, *8*(6), 502. https://doi.org/10.3390/rs8060502

Elshire, R. J., Glaubitz, J. C., Sun, Q., Poland, J. A., Kawamoto, K., Buckler, E. S., & Mitchell, S. E. (2011). A Robust, Simple Genotyping-by-Sequencing (GBS) Approach for High Diversity Species. *PLOS ONE*, *6*(5), e19379. https://doi.org/10.1371/journal.pone.0019379

Excoffier, L., Foll, M., & Petit, R. J. (2009). Genetic consequences of range expansions. *Annual Review of Ecology, Evolution, and Systematics*, *40*(1), 481–501. https://doi.org/10.1146/annurev.ecolsys.39.110707.173414

Fei, S., Desprez, J. M., Potter, K. M., Jo, I., Knott, J. A., & Oswalt, C. M. (2017). Divergence of species responses to climate change. *Science Advances*, *3*(5), e1603055.

Ferrier, S., Manion, G., Elith, J., & Richardson, K. (2007). Using generalized dissimilarity modelling to analyse and predict patterns of beta diversity in regional biodiversity assessment. *Diversity and Distributions*, *13*(3), 252–264. https://doi.org/10.1111/j.1472-4642.2007.00341.x

Fetter, K. C., Gugger, P. F., & Keller, S. R. (2017). Landscape Genomics of Angiosperm Trees: From Historic Roots to Discovering New Branches of Adaptive Evolution. In A. Groover & Q. Cronk (Eds.), *Comparative and Evolutionary Genomics of Angiosperm Trees* (pp. 303–333). https://doi.org/10.1007/7397_2016_19

Fisher, J. I., & Mustard, J. F. (2007). Cross-scalar satellite phenology from ground, Landsat, and MODIS data. *Remote Sensing of Environment*, *109*(3), 261–273. https://doi.org/10.1016/j.rse.2007.01.004

Fitzpatrick, M. C., Blois, J. L., Williams, J. W., Nieto-Lugilde, D., Maguire, K. C., & Lorenz, D. J. (2018). How will climate novelty influence ecological forecasts? Using the Quaternary to assess future reliability. *Global Change Biology*, *24*(8), 3575–3586. https://doi.org/10.1111/gcb.14138

Fitzpatrick, M. C., & Keller, S. R. (2015). Ecological genomics meets community-level modelling of biodiversity: mapping the genomic landscape of current and future environmental adaptation. *Ecology Letters*, *18*(1), 1–16. https://doi.org/10.1111/ele.12376

Flynn, D. F. B., & Wolkovich, E. M. (2018). Temperature and photoperiod drive spring phenology across all species in a temperate forest community. *New Phytologist*, *219*(4), 1353–1362. https://doi.org/10.1111/nph.15232

Franklin, J. (2010). *Mapping Species Distributions: Spatial Inference and Prediction*. Cambridge University Press.

Fu, Y. H., Campioli, M., Deckmyn, G., & Janssens, I. A. (2013). Sensitivity of leaf unfolding to experimental warming in three temperate tree species. *Agricultural and Forest Meteorology*, *181*, 125–132. https://doi.org/10.1016/j.agrformet.2013.07.016

Fu, Y. H., Campioli, M., Vitasse, Y., Boeck, H. J. D., Berge, J. V. den, AbdElgawad, H., … Janssens, I. A. (2014). Variation in leaf flushing date influences autumnal senescence and next year's flushing date in two temperate tree species. *Proceedings of the National Academy of Sciences*, *111*(20), 7355–7360. https://doi.org/10.1073/pnas.1321727111

Fu, Y. H., Piao, S., Vitasse, Y., Zhao, H., Boeck, H. J. D., Liu, Q., … Janssens, I. A. (2015). Increased heat requirement for leaf flushing in temperate woody species over 1980–2012: effects of chilling, precipitation and insolation. *Global Change Biology*, *21*(7), 2687–2697. https://doi.org/10.1111/gcb.12863

Fu, Y. H., Piao, S., Zhao, H., Jeong, S.-J., Wang, X., Vitasse, Y., … Janssens, I. A. (2014). Unexpected role of winter precipitation in determining heat requirement for spring vegetation green-up at northern middle and high latitudes. *Global Change Biology*, *20*(12), 3743–3755. https://doi.org/10.1111/gcb.12610

Fu, Y. H., Zhang, X., Piao, S., Hao, F., Geng, X., Vitasse, Y., … Janssens, I. A. (2019). Daylength helps temperate deciduous trees to leaf-out at the optimal time. *Global Change Biology*, *25*(7), 2410–2418. https://doi.org/10.1111/gcb.14633

Gbif.org. (2019). *GBIF Occurrence Download* [Data set]. https://doi.org/10.15468/dl.0wxmwg

Gillis, M. D., Omule, A. Y., & Brierley, T. (2005). Monitoring Canada's forests: The National Forest Inventory. *The Forestry Chronicle*, *81*(2), 214–221. https://doi.org/10.5558/tfc81214-2

Godwin, H. (1934). Pollen Analysis. an Outline of the Problems and Potentialities of the Method. *New Phytologist*, *33*(4), 278–305. https://doi.org/10.1111/j.1469-8137.1934.tb06815.x

Goring, S., Dawson, A., Simpson, G. L., Ram, K., Graham, R. W., Grimm, E. C., & Williams, J. W. (2015). neotoma: A Programmatic Interface to the Neotoma Paleoecological Database. *Open Quaternary*, *1*. https://doi.org/10.5334/oq.ab

Gotelli, N. J., & Stanton-Geddes, J. (2015). Climate change, genetic markers and species distribution modelling. *Journal of Biogeography*, *42*(9), 1577–1585. https://doi.org/10.1111/jbi.12562

Goudet, J., & Jombart, T. (2015). hierfstat: Estimation and Tests of Hierarchical F-Statistics (Version 0.04-22). Retrieved from https://cran.r-project.org/web/packages/hierfstat/index.html

Graham, E. A., Riordan, E. C., Yuen, E. M., Estrin, D., & Rundel, P. W. (2010). Public Internet-connected cameras used as a cross-continental ground-based plant phenology monitoring system. *Global Change Biology*, *16*, 3014–3023. https://doi.org/10.1111/j.1365-2486.2010.02164.x

Granato, I., Cuevas, J., Luna-Vázquez, F., Crossa, J., Montesinos-López, O., Burgueño, J., & Fritsche-Neto, R. (2018). BGGE: A new package for genomic-enabled prediction incorporating genotype × environment interaction models. *G3: Genes, Genomes, Genetics*, *8*(9), 3039–3047. https://doi.org/10.1534/g3.118.200435

Greenwell, B. M. (2017). *pdp: An R Package for Constructing Partial Dependence Plots*. *9*, 16.

Groom, Q. J. (2013). Some poleward movement of British native vascular plants is occurring, but the fingerprint of climate change is not evident. *PeerJ*, *1*, e77. https://doi.org/10.7717/peerj.77

Guo, L., Dai, J., Ranjitkar, S., Yu, H., Xu, J., & Luedeling, E. (2014). Chilling and heat requirements for flowering in temperate fruit trees. *International Journal*

of Biometeorology, *58*(6), 1195–1206. https://doi.org/10.1007/s00484-013-0714-3

Hampe, A., & Petit, R. J. (2005). Conserving biodiversity under climate change: the rear edge matters: Rear edges and climate change. *Ecology Letters*, *8*(5), 461–467. https://doi.org/10.1111/j.1461-0248.2005.00739.x

Hanspach, J., Kühn, I., Pompe, S., & Klotz, S. (2010). Predictive performance of plant species distribution models depends on species traits. *Perspectives in Plant Ecology, Evolution and Systematics*, *12*(3), 219–225. https://doi.org/10.1016/j.ppees.2010.04.002

Heller, N. E., & Zavaleta, E. S. (2009). Biodiversity management in the face of climate change: A review of 22 years of recommendations. *Biological Conservation*, *142*(1), 14–32. https://doi.org/10.1016/j.biocon.2008.10.006

Hewitt, G. (2000). The genetic legacy of the Quaternary ice ages. *Nature*, *405*(6789), 907–913.

Hickling, R., Roy, D. B., Hill, J. K., Fox, R., & Thomas, C. D. (2006). The distributions of a wide range of taxonomic groups are expanding polewards. *Global Change Biology*, *12*(3), 450–455. https://doi.org/10.1111/j.1365-2486.2006.01116.x

Hijmans, R. J. (2017). geosphere: Spherical Trigonometry (Version 1.5-7). Retrieved from https://CRAN.R-project.org/package=geosphere

Hijmans, R. J., Cameron, S. E., Parra, J. L., Jones, P. G., & Jarvis, A. (2005). Very high resolution interpolated climate surfaces for global land areas.

International Journal of Climatology, *25*(15), 1965–1978. https://doi.org/10.1002/joc.1276

Hufkens, K., Basler, D., Milliman, T., Melaas, E. K., & Richardson, A. D. (2018). An integrated phenology modelling framework in R. *Methods in Ecology and Evolution*, *9*(5), 1276–1285. https://doi.org/10.1111/2041-210X.12970

Hunter, A. F., & Lechowicz, M. J. (1992). Predicting the Timing of Budburst in Temperate Trees. *Journal of Applied Ecology*, *29*(3), 597–604. https://doi.org/10.2307/2404467

Ikeda, D. H., Max, T. L., Allan, G. J., Lau, M. K., Shuster, S. M., & Whitham, T. G. (2017). Genetically informed ecological niche models improve climate change predictions. *Global Change Biology*, *23*(1), 164–176. https://doi.org/10.1111/gcb.13470

Iverson, L., Prasad, A., & Matthews, S. (2008). Modeling potential climate change impacts on the trees of the northeastern United States. *Mitigation and Adaptation Strategies for Global Change*, *13*(5–6), 487–516. https://doi.org/10.1007/s11027-007-9129-y

Keller, S. R., Chhatre, V. E., & Fitzpatrick, M. C. (2018). Influence of Range Position on Locally Adaptive Gene–Environment Associations in Populus Flowering Time Genes. *Journal of Heredity*, *109*(1), 47–58. https://doi.org/10.1093/jhered/esx098

Keller, S. R., Levsen, N., Olson, M. S., & Tiffin, P. (2012). Local adaptation in the flowering-time gene network of balsam poplar, *Populus balsamifera* L.

Molecular Biology and Evolution, *29*(10), 3143–3152. https://doi.org/10.1093/molbev/mss121

Keller, S. R., Olson, M. S., Silim, S., Schroeder, W., & Tiffin, P. (2010). Genomic diversity, population structure, and migration following rapid range expansion in the Balsam Poplar, *Populus balsamifera*. *Molecular Ecology*, *19*(6), 1212–1226. https://doi.org/10.1111/j.1365-294X.2010.04546.x

Keller, S. R., Soolanayakanahally, R. Y., Guy, R. D., Silim, S. N., Olson, M. S., & Tiffin, P. (2011). Climate-driven local adaptation of ecophysiology and phenology in balsam poplar, *Populus balsamifera* L. (Salicaceae). *American Journal of Botany*, *98*(1), 99–108. https://doi.org/10.3732/ajb.1000317

Kirkpatrick, M., & Barton, N. H. (1997). Evolution of a Species' Range. *The American Naturalist*, *150*(1), 1–23. https://doi.org/10.1086/286054

Kramer, K. (1994). Selecting a model to predict the onset of growth of *Fagus sylvatica*. *Journal of Applied Ecology*, *31*(1), 172–181. https://doi.org/10.2307/2404609

Lambert, A. M., Miller-Rushing, A. J., & Inouye, D. W. (2010). Changes in snowmelt date and summer precipitation affect the flowering phenology of Erythronium grandiflorum (glacier lily; Liliaceae). *American Journal of Botany*, *97*(9), 1431–1437. https://doi.org/10.3732/ajb.1000095

Latifovic, R., Homer, C., Ressl, R., Pouliot, D., Hossain, S. N., Colditz, R. R., … Victoria, A. (2016). North American land-change monitoring system. In *Remote sensing of land use and land cover* (pp. 322–343). CRC Press.

Lecocq, T., Harpke, A., Rasmont, P., & Schweiger, O. (2019). Integrating intraspecific differentiation in species distribution models: Consequences on projections of current and future climatically suitable areas of species. *Diversity and Distributions*, *25*(7), 1088–1100. https://doi.org/10.1111/ddi.12916

Legendre, P., & Legendre, L. F. J. (1998). *Numerical Ecology*. Elsevier.

Leimu, R., & Fischer, M. (2008). A Meta-Analysis of Local Adaptation in Plants. *PLOS ONE*, *3*(12), e4010. https://doi.org/10.1371/journal.pone.0004010

Leroy, B., Delsol, R., Hugueny, B., Meynard, C. N., Barhoumi, C., Barbet-Massin, M., & Bellard, C. (2018). Without quality presence–absence data, discrimination metrics such as TSS can be misleading measures of model performance. *Journal of Biogeography*, *45*(9), 1994–2002. https://doi.org/10.1111/jbi.13402

Levsen, N. D., Tiffin, P., & Olson, M. S. (2012). Pleistocene Speciation in the Genus *Populus* (Salicaceae). *Systematic Biology*, *61*(3), 401–412. https://doi.org/10.1093/sysbio/syr120

Liang, L., Schwartz, M. D., & Fei, S. (2011). Validating satellite phenology through intensive ground observation and landscape scaling in a mixed seasonal forest. *Remote Sensing of Environment*, *115*(1), 143–157. https://doi.org/10.1016/j.rse.2010.08.013

Lichstein, J. W., Simons, T. R., Shriner, S. A., & Franzreb, K. E. (2002). Spatial autocorrelation and autoregressive models in ecology. *Ecological Monographs*, *72*(3), 445–463.

Lira-Noriega, A., & Manthey, J. D. (2014). Relationship of genetic diversity and niche centrality: a survey and analysis. *Evolution*, *68*(4), 1082–1093. https://doi.org/10.1111/evo.12343

Little, E. L. (1971). *Atlas of United States trees*. Washington, D.C., USA: U.S. Dept. of Agriculture, Forest Service.

Lobo, J. M., Jiménez-Valverde, A., & Real, R. (2008). AUC: a misleading measure of the performance of predictive distribution models. *Global Ecology and Biogeography*, *17*(2), 145–151. https://doi.org/10.1111/j.1466-8238.2007.00358.x

Lorenz, D. J., Nieto-Lugilde, D., Blois, J. L., Fitzpatrick, M. C., & Williams, J. W. (2016). Downscaled and debiased climate simulations for North America from 21,000 years ago to 2100AD. *Scientific Data*, *3*, 1–19. https://doi.org/10.1038/sdata.2016.48

Lumibao, C. Y., Hoban, S. M., & McLachlan, J. (2017). Ice ages leave genetic diversity 'hotspots' in Europe but not in Eastern North America. *Ecology Letters*, *20*(11), 1459–1468. https://doi.org/10.1111/ele.12853

MacDonald, G. M., & McLeod, T. K. (1996). The Holocene closing of the 'ice-free' corridor: A biogeographical perspective. *Quaternary International*, *32*, 87–95. https://doi.org/10.1016/1040-6182(95)00055-0

Maguire, K. C., Shinneman, D. J., Potter, K. M., & Hipkins, V. D. (2018). Intraspecific niche models for ponderosa pine (*Pinus ponderosa*) suggest potential variability in population-level response to climate change. *Systematic Biology*. https://doi.org/10.1093/sysbio/syy017

Manion, G., Lisk, M., Nieto-Lugilde, D., Mokany, K., & Fitzpatrick, M. (2017). gdm: Generalized Dissimilarity Modeling (Version 1.3.4). Retrieved from https://CRAN.R-project.org/package=gdm

Mann, D. H., Groves, P., Reanier, R. E., & Kunz, M. L. (2010). Floodplains, permafrost, cottonwood trees, and peat: What happened the last time climate warmed suddenly in arctic Alaska? *Quaternary Science Reviews*, *29*(27–28), 3812–3830. https://doi.org/10.1016/j.quascirev.2010.09.002

Marcer, A., Méndez-Vigo, B., Alonso-Blanco, C., & Picó, F. X. (2016). Tackling intraspecific genetic structure in distribution models better reflects species geographical range. *Ecology and Evolution*, *6*(7), 2084–2097. https://doi.org/10.1002/ece3.2010

McGuire, J. L., Lawler, J. J., McRae, B. H., Nuñez, T. A., & Theobald, D. M. (2016). Achieving climate connectivity in a fragmented landscape. *Proceedings of the National Academy of Sciences*, *113*(26), 7195–7200. https://doi.org/10.1073/pnas.1602817113

Meirmans, P. G., Godbout, J., Lamothe, M., Thompson, S. L., & Isabel, N. (2017). History rather than hybridization determines population structure and

adaptation in *Populus balsamifera*. *Journal of Evolutionary Biology*, *30*(11), 2044–2058. https://doi.org/10.1111/jeb.13174

Melaas, E. K., Friedl, M. A., & Zhu, Z. (2013). Detecting interannual variation in deciduous broadleaf forest phenology using Landsat TM/ETM+ data. *Remote Sensing of Environment*, *132*, 176–185. https://doi.org/10.1016/j.rse.2013.01.011

Memmott, J., Craze, P. G., Waser, N. M., & Price, M. V. (2007). Global warming and the disruption of plant–pollinator interactions. *Ecology Letters*, *10*(8), 710–717. https://doi.org/10.1111/j.1461-0248.2007.01061.x

Menzel, A., Sparks, T. H., Estrella, N., Koch, E., Aasa, A., Ahas, R., … Zust, A. (2006). European phenological response to climate change matches the warming pattern. *Global Change Biology*, *12*(10), 1969–1976. https://doi.org/10.1111/j.1365-2486.2006.01193.x

Montoya, J. M., & Raffaelli, D. (2010). Climate change, biotic interactions and ecosystem services. *Philosophical Transactions of the Royal Society of London B: Biological Sciences*, *365*(1549), 2013–2018. https://doi.org/10.1098/rstb.2010.0114

Morin, X., Roy, J., Sonié, L., & Chuine, I. (2010). Changes in leaf phenology of three European oak species in response to experimental climate change. *New Phytologist*, *186*(4), 900–910. https://doi.org/10.1111/j.1469-8137.2010.03252.x

Morin, X., Viner, D., & Chuine, I. (2008). Tree species range shifts at a continental scale: new predictive insights from a process-based model. *Journal of Ecology*, *96*(4), 784–794. https://doi.org/10.1111/j.1365-2745.2008.01369.x

Mulder, C. P. H., Iles, D. T., & Rockwell, R. F. (2017). Increased variance in temperature and lag effects alter phenological responses to rapid warming in a subarctic plant community. *Global Change Biology*, *23*(2), 801–814. https://doi.org/10.1111/gcb.13386

Murray, M. B., Cannell, M. G. R., & Smith, R. I. (1989). Date of Budburst of Fifteen Tree Species in Britain Following Climatic Warming. *Journal of Applied Ecology*, *26*(2), 693–700. https://doi.org/10.2307/2404093

Myking, T., & Heide, O. M. (1995). Dormancy release and chilling requirement of buds of latitudinal ecotypes of Betula pendula and B. pubescens. *Tree Physiology*, *15*(11), 697–704. https://doi.org/10.1093/treephys/15.11.697

Nielsen, R., Hubisz, M. J., & Clark, A. G. (2004). Reconstituting the Frequency Spectrum of Ascertained Single-Nucleotide Polymorphism Data. *Genetics*, *168*(4), 2373–2382. https://doi.org/10.1534/genetics.104.031039

Olson, M. S., Levsen, N., Soolanayakanahally, R. Y., Guy, R. D., Schroeder, W. R., Keller, S. R., & Tiffin, P. (2013). The adaptive potential of *Populus balsamifera* L. to phenology requirements in a warmer global climate. *Molecular Ecology*, *22*(5), 1214–1230. https://doi.org/10.1111/mec.12067

Oney, B., Reineking, B., O'Neill, G., & Kreyling, J. (2013). Intraspecific variation buffers projected climate change impacts on *Pinus contorta*. *Ecology and Evolution*, *3*(2), 437–449. https://doi.org/10.1002/ece3.426

Ortego, J., Gugger, P. F., & Sork, V. L. (2015). Climatically stable landscapes predict patterns of genetic structure and admixture in the Californian canyon live oak. *Journal of Biogeography*, *42*(2), 328–338. https://doi.org/10.1111/jbi.12419

Palacio-Lopez, K., Keller, S. R., & Molofsky, J. (2018). Genomic admixture between locally adapted populations of *Arabidopsis thaliana* (mouse ear cress): evidence of optimal genetic outcrossing distance. *Journal of Heredity*, *109*(1), 38–46. https://doi.org/10.1093/jhered/esx079

Parmesan, C. (2006). Ecological and evolutionary responses to recent climate change. *Annual Review of Ecology, Evolution, and Systematics*, *37*, 637–669.

Parmesan, C., & Yohe, G. (2003). A globally coherent fingerprint of climate change impacts across natural systems. *Nature*, *421*, 37–42.

Pau, S., Wolkovich, E. M., Cook, B. I., Davies, T. J., Kraft, N. J. B., Bolmgren, K., … Cleland, E. E. (2011). Predicting phenology by integrating ecology, evolution and climate science. *Global Change Biology*, *17*(12), 3633–3643. https://doi.org/10.1111/j.1365-2486.2011.02515.x

Pearman, P. B., D'Amen, M., Graham, C. H., Thuiller, W., & Zimmermann, N. E. (2010). Within-taxon niche structure: niche conservatism, divergence and predicted effects of climate change. *Ecography*, *33*(6), 990–1003. https://doi.org/10.1111/j.1600-0587.2010.06443.x

Pedersen, M. W., Ruter, A., Schweger, C., Friebe, H., Staff, R. A., Kjeldsen, K. K., … Willerslev, E. (2016). Postglacial viability and colonization in North America's ice-free corridor. *Nature*, *537*(7618), 45–49. https://doi.org/10.1038/nature19085

Peterson, M. L., Doak, D. F., & Morris, W. F. (2019). Incorporating local adaptation into forecasts of species' distribution and abundance under climate change. *Global Change Biology*, *25*(3), 775–793. https://doi.org/10.1111/gcb.14562

Petit, R. J., Aguinagalde, I., Beaulieu, J.-L. de, Bittkau, C., Brewer, S., Cheddadi, R., … Vendramin, G. G. (2003). Glacial refugia: hotspots but not melting pots of genetic diversity. *Science*, *300*(5625), 1563–1565. https://doi.org/10.1126/science.1083264

Petit, R. J., Bialozyt, R., Brewer, S., Cheddadi, R., & Comps, B. (2001). From spatial patterns of genetic diversity to postglacial migration processes in forest trees. *Special Publication-British Ecological Society*, *14*, 295–318.

Piao, S., Friedlingstein, P., Ciais, P., Viovy, N., & Demarty, J. (2007). Growing season extension and its impact on terrestrial carbon cycle in the Northern Hemisphere over the past 2 decades. *Global Biogeochemical Cycles*, *21*(3). https://doi.org/10.1029/2006GB002888

Pironon, S., Papuga, G., Villellas, J., Angert, A. L., García, M. B., & Thompson, J. D. (2017). Geographic variation in genetic and demographic performance: new insights from an old biogeographical paradigm. *Biological Reviews*, *92*(4), 1877–1909. https://doi.org/10.1111/brv.12313

Polgar, C. A., & Primack, R. B. (2011). Leaf-out phenology of temperate woody plants: from trees to ecosystems. *New Phytologist*, *191*(4), 926–941. https://doi.org/10.1111/j.1469-8137.2011.03803.x

Prasad, A. M., Iverson, L. R., Peters, M. P., & Matthews, S. N. (2014). Climate Change Atlas. Northern Research Station, U.S. Forest Services, Delaware, OH. Retrieved April 24, 2019, from https://www.fs.fed.us/nrs/atlas/

R Core Team. (2017). *R: A language and environment for statistical computing*. Retrieved from https://www.R-project.org/

Rafferty, N. E., & Ives, A. R. (2011). Effects of experimental shifts in flowering phenology on plant–pollinator interactions. *Ecology Letters*, *14*(1), 69–74. https://doi.org/10.1111/j.1461-0248.2010.01557.x

Richardson, A. D., Keenan, T. F., Migliavacca, M., Ryu, Y., Sonnentag, O., & Toomey, M. (2013). Climate change, phenology, and phenological control of vegetation feedbacks to the climate system. *Agricultural and Forest Meteorology*, *169*, 156–173. https://doi.org/10.1016/j.agrformet.2012.09.012

Roland, C. A., Stehn, S. E., Schmidt, J., & Houseman, B. (2016). Proliferating poplars: the leading edge of landscape change in an Alaskan subalpine chronosequence. *Ecosphere*, *7*(7), e01398. https://doi.org/10.1002/ecs2.1398

Romero-Lankao, P., Smith, J. B., Davidson, D. J., Diffenbaugh, N. S., Kinney, P. L., Kirshen, P., … Villers Ruiz, L. (2014). North America. In V. R. Barros, C. B. Field, D. J. Dokken, M. D. Mastrandrea, K. J. Mach, T. E. Bilir, … L. L. White (Eds.), *Climate Change 2014: Impacts, Adaptation, and Vulnerability.*

Part B: Regional Aspects. Contribution of Working Group II to the Fifth Assessment Report of the Intergovernmental Panel on Climate Change (pp. 1439–1498). Cambridge, United Kingdom and New York, NY, USA: Cambridge University Press.

Rull, V. (2009). Microrefugia. *Journal of Biogeography*, *36*(3), 481–484. https://doi.org/10.1111/j.1365-2699.2008.02023.x

Sagarin, R. D., & Gaines, S. D. (2002). The 'abundant centre' distribution: to what extent is it a biogeographical rule? *Ecology Letters*, *5*(1), 137–147. https://doi.org/10.1046/j.1461-0248.2002.00297.x

Savolainen, O., Lascoux, M., & Merilä, J. (2013). Ecological genomics of local adaptation. *Nature Reviews Genetics*, *14*(11), 807–820. https://doi.org/10.1038/nrg3522

Scheffers, B. R., Meester, L. D., Bridge, T. C. L., Hoffmann, A. A., Pandolfi, J. M., Corlett, R. T., … Watson, J. E. M. (2016). The broad footprint of climate change from genes to biomes to people. *Science*, *354*(6313), aaf7671. https://doi.org/10.1126/science.aaf7671

Schielzeth, H. (2010). Simple means to improve the interpretability of regression coefficients. *Methods in Ecology and Evolution*, *1*(2), 103–113. https://doi.org/10.1111/j.2041-210X.2010.00012.x

Schoville, S. D., Bonin, A., François, O., Lobreaux, S., Melodelima, C., & Manel, S. (2012). Adaptive Genetic Variation on the Landscape: Methods and Cases.

Annual Review of Ecology, Evolution, and Systematics, *43*(1), 23–43. https://doi.org/10.1146/annurev-ecolsys-110411-160248

Schwartz, M. D., Ahas, R., & Aasa, A. (2006). Onset of spring starting earlier across the Northern Hemisphere. *Global Change Biology*, *12*(2), 343–351. https://doi.org/10.1111/j.1365-2486.2005.01097.x

Schwartz, M. D., & Reiter, B. E. (2000). Changes in North American spring. *International Journal of Climatology*, *20*(8), 929–932. https://doi.org/10.1002/1097-0088(20000630)20:8<929::AID-JOC557>3.0.CO;2-5

Schweiger, O., Settele, J., Kudrna, O., Klotz, S., & Kühn, I. (2008). Climate Change Can Cause Spatial Mismatch of Trophically Interacting Species. *Ecology*, *89*(12), 3472–3479.

Shaw, R. G. (2018). From the Past to the Future: Considering the Value and Limits of Evolutionary Prediction. *The American Naturalist*, *193*(1), 1–10. https://doi.org/10.1086/700565

Smith, A. B., Godsoe, W., Rodríguez-Sánchez, F., Wang, H.-H., & Warren, D. (2019). Niche Estimation Above and Below the Species Level. *Trends in Ecology & Evolution*, *34*(3), 260–273. https://doi.org/10.1016/j.tree.2018.10.012

Soltis, D. E., Morris, A. B., McLachlan, J. S., Manos, P. S., & Soltis, P. S. (2006). Comparative phylogeography of unglaciated eastern North America:

Phylogeography of unglaciated eastern North America. *Molecular Ecology*, *15*(14), 4261–4293. https://doi.org/10.1111/j.1365-294X.2006.03061.x

Soolanayakanahally, R. Y., Guy, R. D., Silim, S. N., Drewes, E. C., & Schroeder, W. R. (2009). Enhanced assimilation rate and water use efficiency with latitude through increased photosynthetic capacity and internal conductance in balsam poplar (*Populus balsamifera* L.). *Plant, Cell & Environment*, *32*(12), 1821–1832. https://doi.org/10.1111/j.1365-3040.2009.02042.x

Sousa, M. B. e, Cuevas, J., Couto, E. G. de O., Pérez-Rodríguez, P., Jarquín, D., Fritsche-Neto, R., … Crossa, J. (2017). Genomic-enabled prediction in maize using kernel models with genotype × environment interaction. *G3: Genes, Genomes, Genetics*, *7*(6), 1995–2014. https://doi.org/10.1534/g3.117.042341

Stewart, L., Alsos, I. G., Bay, C., Breen, A. L., Brochmann, C., Boulanger-Lapointe, N., … Pellissier, L. (2016). The regional species richness and genetic diversity of Arctic vegetation reflect both past glaciations and current climate: Glaciation effect on arctic vegetation diversity. *Global Ecology and Biogeography*, *25*(4), 430–442. https://doi.org/10.1111/geb.12424

Syphard, A. D., & Franklin, J. (2010). Species traits affect the performance of species distribution models for plants in southern California. *Journal of Vegetation Science*, *21*(1), 177–189. https://doi.org/10.1111/j.1654-1103.2009.01133.x

Tang, J., Körner, C., Muraoka, H., Piao, S., Shen, M., Thackeray, S. J., & Yang, X. (2016). Emerging opportunities and challenges in phenology: a review. *Ecosphere*, *7*(8), e01436. https://doi.org/10.1002/ecs2.1436

Thomassen, H. A., Cheviron, Z. A., Freedman, A. H., Harrigan, R. J., Wayne, R. K., & Smith, T. B. (2010). Spatial modelling and landscape-level approaches for visualizing intra-specific variation. *Molecular Ecology*, *19*(17), 3532–3548. https://doi.org/10.1111/j.1365-294X.2010.04737.x

Thornton, P. E., Thornton, M. M., Mayer, B. W., Wei, Y., Devarakonda, R., Vose, R. S., & Cook, R. B. (2017). *Daymet: daily surface weather data on a 1-km grid for North America, Version 3*. Retrieved from https://doi.org/10.3334/ORNLDAAC/1328

Thuiller, W., Lafourcade, B., Engler, R., & Araújo, M. B. (2009). BIOMOD - a platform for ensemble forecasting of species distributions. *Ecography*, *32*(3), 369–373. https://doi.org/10.1111/j.1600-0587.2008.05742.x

Tuskan, G. A., DiFazio, S., Jansson, S., Bohlmann, J., Grigoriev, I., Hellsten, U., … Rokhsar, D. (2006). The Genome of Black Cottonwood, Populus trichocarpa (Torr. & Gray). *Science*, *313*(5793), 1596–1604. https://doi.org/10.1126/science.1128691

Vallejos, R., Osorio, F., & Bevilacqua, M. (2018). *Spatial Relationships Between Two Georeferenced Variables: with Applications in R*. Retrieved from http://srb2gv.mat.utfsm.cl

VanDerWal, J., Murphy, H. T., Kutt, A. S., Perkins, G. C., Bateman, B. L., Perry, J. J., & Reside, A. E. (2013). Focus on poleward shifts in species' distribution underestimates the fingerprint of climate change. *Nature Climate Change*, *3*(3), 239–243. https://doi.org/10.1038/nclimate1688

Varela, S., Anderson, R. P., García-Valdés, R., & Fernández-González, F. (2014). Environmental filters reduce the effects of sampling bias and improve predictions of ecological niche models. *Ecography*, *37*, 1084–1091. https://doi.org/10.1111/j.1600-0587.2013.00441.x

Vitasse, Y., Delzon, S., Dufrêne, E., Pontailler, J.-Y., Louvet, J.-M., Kremer, A., & Michalet, R. (2009). Leaf phenology sensitivity to temperature in European trees: Do within-species populations exhibit similar responses? *Agricultural and Forest Meteorology*, *149*(5), 735–744. https://doi.org/10.1016/j.agrformet.2008.10.019

Vucetich, J. A., & Waite, T. A. (2003). Spatial patterns of demography and genetic processes across the species' range: null hypotheses for landscape conservation genetics. *Conservation Genetics*, *4*(5), 639–645.

Wagenmakers, E.-J., & Farrell, S. (2004). AIC model selection using Akaike weights. *Psychonomic Bulletin & Review*, *11*(1), 192–196. https://doi.org/10.3758/BF03206482

Walter, R., & Epperson, B. K. (2005). Geographic pattern of genetic diversity in *Pinus resinosa*: contact zone between descendants of glacial refugia. *American Journal of Botany*, *92*(1), 92–100. https://doi.org/10.3732/ajb.92.1.92

Walther, G.-R. (2010). Community and ecosystem responses to recent climate change. *Philosophical Transactions of the Royal Society of London B:*

Biological Sciences, *365*(1549), 2019–2024. https://doi.org/10.1098/rstb.2010.0021

Walther, G.-R., Berger, S., & Sykes, M. T. (2005). An ecological "footprint" of climate change. *Proceedings of the Royal Society B: Biological Sciences*, *272*(1571), 1427–1432. https://doi.org/10.1098/rspb.2005.3119

Wiens, J. A., Stralberg, D., Jongsomjit, D., Howell, C. A., & Snyder, M. A. (2009). Niches, models, and climate change: Assessing the assumptions and uncertainties. *Proceedings of the National Academy of Sciences*, *106*(Supplement 2), 19729–19736. https://doi.org/10.1073/pnas.0901639106

Williams, J. W., & Jackson, S. T. (2007). Novel climates, no-analog communities, and ecological surprises. *Frontiers in Ecology and the Environment*, *5*(9), 475–482. https://doi.org/10.1890/070037

Williams, J. W., Jackson, S. T., & Kutzbach, J. E. (2007). Projected Distributions of Novel and Disappearing Climates by 2100 AD. *Proceedings of the National Academy of Sciences of the United States of America*, *104*(14), 5738–5742.

Williams, J. W., Shuman, B. N., Webb, T., Bartlein, P. J., & Leduc, P. L. (2004). Late-Quaternary Vegetation Dynamics in North America: Scaling from Taxa to Biomes. *Ecological Monographs*, *74*(2), 309–334. https://doi.org/10.1890/02-4045

Wolkovich, E. M., Cook, B. I., & Davies, T. J. (2014). Progress towards an interdisciplinary science of plant phenology: building predictions across

space, time and species diversity. *New Phytologist*, *201*(4), 1156–1162. https://doi.org/10.1111/nph.12599

Woudenberg, S. W., Conkling, B. L., O'Connell, B. M., LaPoint, E. B., Turner, J. A., & Waddell, K. L. (2010). The Forest Inventory and Analysis Database: Database description and users manual version 4.0 for Phase 2. *Gen. Tech. Rep. RMRS-GTR-245. Fort Collins, CO: U.S. Department of Agriculture, Forest Service, Rocky Mountain Research Station. 336 p.*, *245*. https://doi.org/10.2737/RMRS-GTR-245

Wright, M. N., & Ziegler, A. (2017). ranger: A fast implementation of Random Forests for high dimensional data in C++ and R. *Journal of Statistical Software*, *77*(1), 1–17. https://doi.org/10.18637/jss.v077.i01

Yannic, G., Pellissier, L., Ortego, J., Lecomte, N., Couturier, S., Cuyler, C., … Côté, S. D. (2013). Genetic diversity in caribou linked to past and future climate change. *Nature Climate Change*, *4*(2), 132–137. https://doi.org/10.1038/nclimate2074

Yun, J., Jeong, S.-J., Ho, C.-H., Park, C.-E., Park, H., & Kim, J. (2018). Influence of winter precipitation on spring phenology in boreal forests. *Global Change Biology*, *24*(11), 5176–5187. https://doi.org/10.1111/gcb.14414

Zasada, J. C., & Phipps, H. M. (1990). *Populus balsamifera* L. *Silvics of North America*, *2*, 518–529.

Zhang, X., Friedl, M. A., Schaaf, C. B., & Strahler, A. H. (2004). Climate controls on vegetation phenological patterns in northern mid- and high latitudes inferred

from MODIS data. *Global Change Biology*, *10*(7), 1133–1145. https://doi.org/10.1111/j.1529-8817.2003.00784.x

Zhou L., Bawa R., & Holliday J. A. (2014). Exome resequencing reveals signatures of demographic and adaptive processes across the genome and range of black cottonwood (*Populus trichocarpa*). *Molecular Ecology*, *23*(10), 2486–2499. https://doi.org/10.1111/mec.12752

Zohner, C. M., & Renner, S. S. (2014). Common garden comparison of the leaf-out phenology of woody species from different native climates, combined with herbarium records, forecasts long-term change. *Ecology Letters*, *17*(8), 1016–1025. https://doi.org/10.1111/ele.12308

Zohner, C. M., & Renner, S. S. (2015). Perception of photoperiod in individual buds of mature trees regulates leaf-out. *New Phytologist*, *208*(4), 1023–1030. https://doi.org/10.1111/nph.13510